UAlg
UNIVERSIDADE DO ALGARVE

UNIVERSIDADE DO ALGARVE

Study of the role of c*Ccbe1*, a novel gene coding for an EGF-like domain protein in the process of induction and organogenesis of the heart

João Francisco Venturinha Furtado

Tese para obtenção do grau de Doutor em Ciências Biomédicas

Trabalho efetuado sob a orientação de:
Professor Doutor José António Belo

2014

Study of the role of c*Ccbe1*, a novel gene coding for an EGF-like domain protein in the process of induction and organogenesis of the heart

Declaração de autoria de trabalho

Declaro ser o autor deste trabalho, que é original e inédito. Autores e trabalhos consultados estão devidamente citados no texto e constam da listagem de referências incluída.

ACKNOWLEDGEMENTS

I would like to express my gratitude and respect to my supervisor, Professor José A. Belo, who has given me the privilege to work in his lab for all these years. Thank you for believing I could carry out this project, for all the continuous guidance, support and enthusiasm throughout my PhD project and during the writing of the thesis.

I would like to thank my colleagues Ana Carolina, Ana Perestrelo, Elizabeth Correia, Fernando Cristo, Margaret Soares, Marta Burlacu, Sara Marques and Tiago Justo for their help, inspiration and friendship. Particularly, Elizabeth Correia and Margaret Soares for helping me in some experiments performed in this thesis.

I would like to express my gratitude to my great friend and colleague José Inácio, I can never thank you enough. Your generosity and enthusiasm is incredible. You are a true professional in every sense of the word.

To Paulo Pereira, thank you for your endless support and ability to always put things in perspective.

I would like to thank, Ricardo Cabrita, André Mozes, Filipe Figueiredo, Marco Inácio and Hugo Galvão for being there when I needed, for the lunches and coffee breaks, which help me to relax and remember that life, with friends like these beside me, it's easy.

I would also like to thank the "Fundação para a Ciência e Tecnologia" for financial support, the University of Algarve and the Biomedical Science department for enabling me to carry out my PhD studies and the "Centro de Biologia Molecular e Estrutural" for all the support and great conditions.

I would like to thanks all my friends and family for their support. Especially to my parents and brothers, thank you for everything you have done to get me here. I couldn't have done it without you.

Finally, I must acknowledge my girlfriend and best friend, Anastasia Matei, without her love, encouragement, comprehension and help, I would not have finished this thesis. Thanks for always being there.

RESUMO

A biologia do desenvolvimento é uma área que aborda os mecanismos envolvidos na formação progressiva de um animal a partir do ovo fertilizado, no qual abrange o crescimento, a diferenciação celular e a morfogénese que marcam as diversas fases do desenvolvimento dos seres vivos. Durante a embriogénese em vertebrados, o coração é o primeiro órgão a ser formado, tendo um papel vital na distribuição de nutrientes e oxigénio no embrião. Além disso, a cardiogénese é um processo muito sensível e consequentemente qualquer perturbação no desenvolvimento do coração leva a malformações cardíacas e, frequentemente, à morte embrionária. Realmente, a incidência de cardiopatias congénitas na população mundial é de 8 a 9 por 1000 nados vivos, sendo a segunda causa de morte no primeiro ano de vida, logo a seguir à prematuridade, segundo a Organização Mundial de Saúde.

Devido à sua conservação evolucionária, o nosso conhecimento sobre a formação do coração foi praticamente adquirido através de estudos em modelos de organismos vertebrados, nomeadamente, anfíbios, ratinho e galinha. No presente estudo, o modelo escolhido foi o da galinha (*Gallus gallus*), isto porque trata-se de um modelo animal utilizado já há bastante tempo em estudos sobre a biologia do desenvolvimento. O embrião de galinha é de fácil acesso, grande e translúcido, o que o torna ideal para manipulações cirúrgicas. O seu estádio de desenvolvimento é facilmente previsível, podem ser cultivados "*in vitro"* durante 3 a 4 dias e são perfeitos para análise de linhagem e destino celular assim como para as técnicas de microinjeção. Além disso, o desenvolvimento embrionário do humano e da galinha partilham mecanismos morfológicos idênticos, e defeitos cardíacos encontrados no embrião de galinha são similares aos que se encontram nos humanos. Posto isto, o embrião de galinha como modelo embrionário oferece múltiplas vantagens em relação ao embrião de mamífero, uma vez que permite cultivar o embrião "*ex ovo*", permitindo assim observar os movimentos celulares inerentes a formação do coração, algo que não e possível no embrião de mamífero.

Grande parte do conhecimento acerca da região formadora do coração provém de estudos que utilizam o embrião de galinha como modelo. As células

precursoras do coração são originárias do epiblasto, estas ingressam na linha primitiva e localizam-se na parte posterior da linha primitiva, (à exceção do nó de Hensen), migrando no sentido anterior-lateral e formando dois campos pré-cardíacos na placa mesodérmica anterior de cada lado da linha primitiva a estádio HH4-5 do desenvolvimento embrionário da galinha. Estas duas zonas cardíacas bilaterais, conhecidas como campo primário cardíaco, fundem-se a estádio HH9, aquando da diferenciação em cardiomiócitos, formando um único tubo cardíaco linear. Mais tarde no desenvolvimento cardíaco o campo secundário cardíaco é o responsável pela extensão do coração e consequente "looping" (HH11). Mesmo enquanto se forma, as regiões básicas do coração tornam-se aparentes, primeiro o "truncus" e ventrículos, depois o átrio e no final o "sinus-venosus". A circulação fica estabelecida por volta do estádio HH16 e a divisão do coração em lado esquerdo e direito ocorre durante os dias 3-5 do desenvolvimento embrionário da galinha.

No desenvolvimento cardíaco, a natureza do estabelecimento bioquímico e molecular é essencial para compreender a relação entre os aspetos genéticos e morfológicos da formação do coração. A necessidade de identificar genes que estão diferencialmente expressos entre populações de células dentro do embrião e do coração embrionário é um ponto crítico para a elucidação da complexidade que é a formação e o desenvolvimento do coração. Embora diversas linhas de evidência tenham determinado um certo número de genes como sendo cruciais para o desenvolvimento do coração, os indutores desses genes e os seus outros alvos permanecem desconhecidos. É por este motivo, que não é nada surpreendente descobrir que muito ainda permanece desconhecido em relação aos mecanismos que controlam a formação do coração. Para um melhor entendimento das moléculas e mecanismos envolvidos no desenvolvimento do coração foi efetuado no nosso laboratório um rastreio diferencial (Affymetrix GeneChip Chick system) para genes expressos nas células precursoras do coração/hemangioblasto. Este rastreio permitiu a identificação de novos genes com um aumento de expressão na região dos precursores cardiogénicos e entre eles estava o "Collagen and calcium-binding EGF-like domain 1" (c*Ccbe1*). Esta proteína é altamente conservada entre espécies durante os processos de desenvolvimento, possuindo uma elevada homologia 79%, 70% e 80% com os seus homólogos em ratinho, peixe zebra e humano, respetivamente.

Adicionalmente, c*Ccbe1* codifica para uma proteína de 396 aa e que contém um domínio, do inglês, Collagen and calcium binding EGF-like, normalmente presentes em grande número nas proteínas celulares e associadas às membranas. As moléculas pertencentes à família do EGF (do inglês *Epidermal Growth Factor*) possuem um papel importante no desenvolvimento e função do coração, e os seus domínios cálcio-EGF conservados, como aqueles detetados no *Ccbe1*, foram já associados à formação embrionária do coração.

Neste contexto, procedeu-se ao estudo e caracterização do padrão de expressão do c*Ccbe1* utilizando-se técnicas de hibridação *in situ* e histologia. De modo a obter um maior detalhe na exatidão da caracterização do padrão de expressão do c*Ccbe1* realizaram-se hibridações *in situ* em conjunto com outros genes, nomeadamente, o *Nkx2.5*, um dos marcadores iniciais das células percursoras cardíacas e expresso no coração ao longo do desenvolvimento, nomeadamente em células na região cardíaca primária e secundária, e *Islet-1*, que expressa em células altamente proliferativas e indiferenciadas, nomeadamente em células na região cardíaca secundária. Os dados apresentados neste estudo revelam que c*Ccbe1* é expresso inicialmente (estádios HH4 a HH8) nos dois campos cardiogénicos na placa mesodérmica anterior de cada lado da linha primitiva. Durante estádios HH9 a HH13, o transcrito de c*Ccbe1* é detetado na região sino-atrial. Nestas regiões, os níveis do transcrito não são apenas encontrados na mesoderme paraxial, mas também na placa mesodérmica lateral esplâncnica e somática. Estes níveis elevados de expressão nestes domínios refletem um papel potencial de c*Ccbe1* no desenvolvimento dos sómitos e na formação do coração. Ao longo do desenvolvimento embrionário, desde o estádio HH14 a HH18, o c*Ccbe1* é expresso na região dorsal do coração (dorsal e lateralmente ao coração), nomeadamente, na zona onde a formação do *conus arteriosus* ocorre e perto dos arcos faríngeos, mais especificamente na região do campo cardíaco secundário. c*Ccbe1* também é detetado nos sómitos e na região da cabeça, especificamente, na área acima do olho conhecida como *vena capitis* (veia da cabeça). Ao realizar as duplas hibridações *in situ* verificou-se que c*Ccbe1* é co-expresso com os dois genes (*Nkx2*.5 e *Islet1*) na região do campo cardíaco primário e secundário a estadios inicias e posteriormente somente no campo cardíaco secundário durante o desenvolvimento do coração em embrião de galinha. Adicionalmente, em experiências de perda e ganho de função do c*Ccbe1*

foi demonstrado que é necessário para a correta formação do coração. A injeção de oligonucleotido morpholino complementar ao gene c*Ccbe1*, provocou malformações cardíacas nos embriões de galinha, no qual a fusão das duas regiões bilaterais formadoras do coração estava incompleta ou deficiente. O mesmo aconteceu quando se efetuou o ganho de função do c*Ccbe1*, levando ao fenótipo de *cardia bífida* (as regiões formadoras do coração permaneceram na placa anterior da mesoderme sem que migrassem para a linha média do embrião de galinha e assim formassem um tubo cardíaco). Adicionalmente, verificou-se que o ganho e perda de função do c*Ccbe1* em embriões de galinha altera os níveis de proliferação cardíaca, e a alteração dos níveis de Hnk1 sugerem que a migração das células da crista neural cardíaca está afetada, levando a um desenvolvimento incorreto dos cardiomiócitos.

De um modo geral, os resultados apresentados nesta tese sugerem que o c*Ccbe1* em galinha é expresso nas zonas formadoras do coração e é necessário durante o desenvolvimento inicial do coração.

Palavras-Chave: Embrião de galinha, *Ccbe1*, região formadora do coração, mesoderme cardíaca, campo secundário cardíaco, proliferação, células da crista neural cardíaca.

ABSTRACT

The vertebrate heart is a complex organ composed of several cell types, being developed through cardiogenic regions that have different expressing specific genes involved in heart specification. Understanding heart development on a molecular level is a requirement for unravel the causes of congenital heart diseases since specific cardiac lineages have been associated with cardiovascular malformations. During the course of a differential screen to identify transcripts specific for chick heart/hemangioblast precursor cells, we have identified *Ccbe1* (*Collagen and calcium-binding EGF-like domain 1*). The current study intends to accomplish a detailed characterization of the expression pattern and functional analyses, by overexpression and knockdown approaches, of chick (c)*Ccbe1*. Whole-mount *in situ* hybridization analysis demonstrate that c*Ccbe1* is expressed in the early cardiac precursors of the heart forming regions at stage HH4 and at later stages is highly specific for the second heart field. Furthermore, functional analyses of c*Ccbe1* revealed an important role of c*Ccbe1* in early heart tube formation. In addition, the results presented in this thesis suggested that c*Ccbe1* is an important gene during heart development, is required for proper proliferation and migration of the heart precursors, and might be limited to multipotent and highly proliferative progenitors and downregulated upon cellular commitment into more specific cardiac phenotypes.

Keywords: Chick, c*Ccbe1*, heart forming regions, second heart field, heart development, proliferation

LIST OF CONTENTS

LIST OF FIGURES

LIST OF TABLES

LIST OF ABBREVIATIONS, ACRONYMS AND SYMBOLS

3’	3 prime
5’	5 prime
μg	Microgram
μl	Microliter
μm	Micra
°C	Degrees Celsius
aa	amino acid
AP	Alkaline phosphatase
AV	Atrioventricular canal
Bmp	Bone morphogenetic proteins
Ccbe1	Collagen and calcium-binding EGF-like domain 1
cCcbe1	Chick Collagen and calcium-binding EGF-like domain 1
cDNA	Copy deoxyribonucleic acid
CaMKs	Calmodulin-dependent protein kinases
CK1	Casein kinase 1
DEPC	Diethyl pyrocarbonate
DIG	Digoxigenin
DNA	Deoxyribonucleic acid
Dvl	Disheveled
EB	Elution buffer
ES	Embryonic stem
EGF	Epidermal growth factor
EST	Expressed sequence tag
Fgf	Fibroblast growth factor
Fgfr	Fibroblast growth factor receptor

FHF	First Heart Field
Fz	Frizzle
g	Gram
GFP	Green fluorescent protein
Gsk3β	Glycogen synthase kinase 3β
h	Hour
H/HPC	Heart/hemangioblast precursor cells
HFR	Heart forming region
HH	Hamburger and Hamilton
Hnk1	Human natural killer 1
JNK	Jun N-Terminal kinase
kb	Kilobase
LB	Luria broth
LRP	Low receptor protein
min	Minute
MF20	Sarcomeric myosin heavy chain
Mhc	Myosin heavy chain
ml	Milliliter
MO	Morpholino **o**ligonucleotides
mRNA	Messenger ribonucleic acid
NICD	Notch intracellular domain
OFT	Outflow tract
PCP	Planar cell polarity
PBS	Phosphate Buffered Saline
PBT	Phosphate Buffered Saline Tween
PCR	Polymerase chain reaction
PK	Proteinase K

PKC	Protein kinase C
RNA	Ribonucleic acid
ROCK	Rho-associated protein kinase
rpm	Revolutions per minute
RT	Room temperature
RT-PCR	Reverse transcriptase-PCR
s	Second
S.E.M.	Standard error of the mean
SHF	Second Heart Field
Shh	Sonic hedgehog
ON	Overnight
TAE	Tris-Acetate-EDTA
Tgf	Transforming growth factor
Tween-20	Polyoxyethylenesorbitan monolaurate
WISH	Whole-mount *in situ* hybridization
Wnt	Wingless/Integrated family members

CHAPTER 1 – GENERAL INTRODUCTION

GENERAL INTRODUCTION

Scientists have been fascinated with the developmental aspects of the heart for many centuries. While several model systems including zebrafish, mouse or Xenopus embryos are frequently studied to gain understanding into the convoluted processes of the vertebrate heart development, the avian embryo has positioned itself as the oldest model system used by scientists to elucidate the principles of basic vertebrate embryology and cardiovascular development, mainly because it is easy to acquire and possible to visualize the living embryo at early stages of development. Furthermore, development of the chick heart is quite similar to that of the human heart (Ruijtenbeek et al., 2002; Tutarel et al., 2005).

1.1 Chick (*gallus gallus*) as a model

The embryo of the domestic chicken (*Gallus gallus*) is the animal model with the longstanding history in developmental biology studies, covering more than 2 Millennia. Therefore, the chick, *Gallus gallus*, is one of the organisms of choice for developmental biologists. Detailed descriptions of avian development were published as early as the 16th century. This long history of descriptive analysis combined with the experimental embryology of recent times contributes to an enormous bibliography of avian system and organ development. Avian embryos offer a number of distinct advantages over other developmental systems: the embryos are large, translucent and easily accessible, which makes them ideal for performing delicate microsurgical manipulations. They can be cultured *in vitro* for 3-4 days and are perfect for microinjecting, cell fate and lineage analysis procedures. Most importantly, it is available all year-round and grows quickly (hatching in 21 days). Since the developmental stages of the chick have been well characterized, both prior to gastrulation (Eyal-Giladi et al., 1976) and following gastrulation (Hamburger and Hamilton, 1951) its developmental stage can be accurately predicted.

The chick embryo has become one of the most commonly used animal models for the study of heart formation and patterning, due to several techniques, such as, *in vitro* or *in ovo* electroporation (allowing gain-of-function and loss-of-function experiments in a time and space controlled way); culture of chick embryonic stem (ES) cells; novel methods for transgenesis; the completion of the chicken genome project and with the publication of a large-scale expressed sequence tag (EST) intended at avian gene discovery is a useful tool for chick developmental research (www.chick.umist.ac.uk). Also, using classical techniques such as grafting and lineage tracing, the chicken is one of the most resourceful experimental systems available (Stern, 2004). Thus, in the context of this thesis, the chick embryo offers a powerful system to reveal the mechanisms of cardiogenesis.

1.2 Early steps in chick development

1.2.1 Cleavage

All vertebrates go through similar steps in early developmental. Just immediately following fertilization, the ovum undergoes a series of mitotic divisions, giving rise to several smaller cells designates blastomeres. Further cleavages create a single-layered blastoderm (Figure 1.1) (Eyal-Giladi, 1997). This process is referred to as cleavage and takes place while the egg is still in the oviduct, before the albumen and the shell are secreted upon it. Between the blastoderm and the yolk there is an area termed the subgerminal cavity (Figure 1.2A). At this phase, several cells localized in the middle of the blastoderm dies, leaving behind a one cell thick layer, the area pellucida (gives rise mainly to embryonic tissues) and a surrounding area opaca (forms the extra-embryonic tissues). Between the area pellucida and the area opaca there is a thin layer of cells termed the marginal zone. Some of the marginal zone cells are important in the determination of cell fate during early chick development (Eyal-Giladi, 1997).

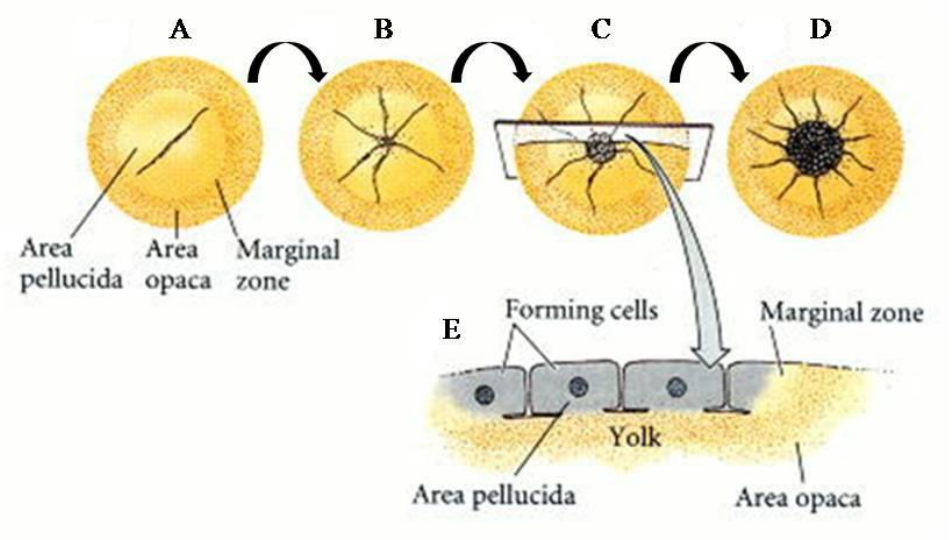

Figure 1.1 – The process of the discoidal meroblastic cleavage in a chick egg.
(A-D) Progressive stages viewed from the future dorsal side of the embryo (animal pole). **(E)** Schematic transversal section in an early-cleavage embryo (Adapted from(Gilbert, 2003).

1.2.2 Gastrulation

The term gastrulation is derived from the Greek word "*gaster*", meaning stomach or gut. It is an early phase in the development of animal embryos, in which the morphology of the embryo is dramatically restructured (shapes the internal and external features of developing animals). This is a key morphogenetic process that involves complex and highly coordinate cell movements and transforms the relatively unstructured early embryo into a gastrula with three germ layers: ectoderm, mesoderm and endoderm (Sanders et al., 1993).

1.2.2.1 Formation of epiblast and hypoblast

By the time a chicken has laid an egg, the blastoderm contains around 20000 cells. At this point, the majority of the cells of the area pellucida remain at the surface, forming the epiblast (Figure 1.2A). Then a small number of cells from the epiblast delaminate into the subgerminal cavity to form disconnected cell clusters known as the primary hypoblast (Figure 1.2B). Subsequently, a sheet of cells from the posterior margin of the blastoderm (Koller's sickle) migrates anteriorly to

join the primary hypoblast, thus forming the secondary hypoblast (Figure 1.2C) (Eyal-Giladi et al., 1992). At this moment the blastoderm is composed by the epiblast, the hypoblast and the space that separates them, the blastocoel.

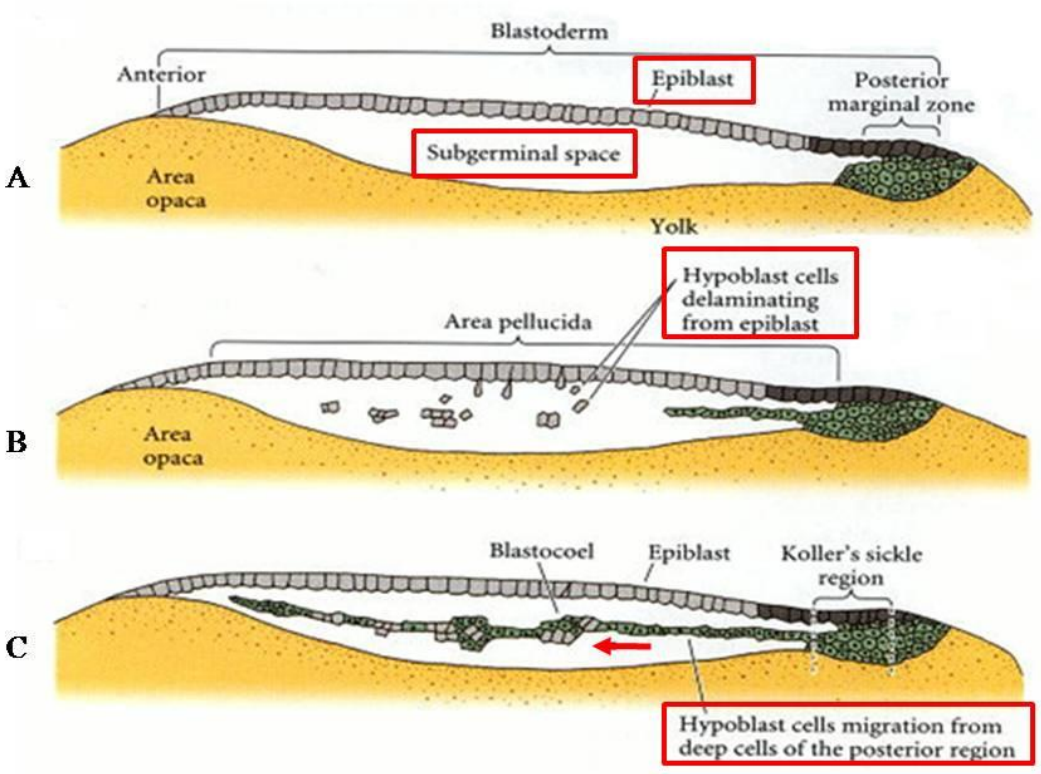

Figure 1.2 – Formation of the chick embryo two layered blastoderm
(A) The blastoderm is composed of a single layer of cells, the epiblast; **(B)** Cells delaminate from epiblast into the subgerminal cavity to form the primary hypoblast; **(C)** Cells from the posterior margin of the blastoderm (Koller's sickle and the posterior marginal cells behind, showed in green in the image) migrate and incorporate the primary hypoblast, thus forming the secondary hypoblast (Adapted from Eyal-Giladi et al. 1992).

The hypoblast cells does not contribute for any cells in the future embryo, instead it forms portions of the external membranes, especially the yolk sac and the stalk linking the yolk mass to the endodermal digestive tube, and also provide chemical signals that specify the migration of epiblast cell (Rosenquist, 1966). On the other hand, the epiblast gives rise to the embryo itself and to some of the extraembryonic structures (Rosenquist, 1966).

1.2.2.2 The primitive streak

The primitive streak development is the major structural characteristic of gastrulation in amniote (mammalian, avian and reptile) embryos. It is visible at about 6-7 h of incubation, stage HH2, (Hamburger and Hamilton, 1951) as cells accumulate in the middle layer, followed by a thickening of the epiblast at the posterior marginal zone, just anterior to Koller's sickle. The epiblast cells move in the direction of the midline of the extending primitive streak and ingress ventrally undergoing an epithelial to mesenchymal transition (Figure 1.3) (Eyal-Giladi et al., 1992).

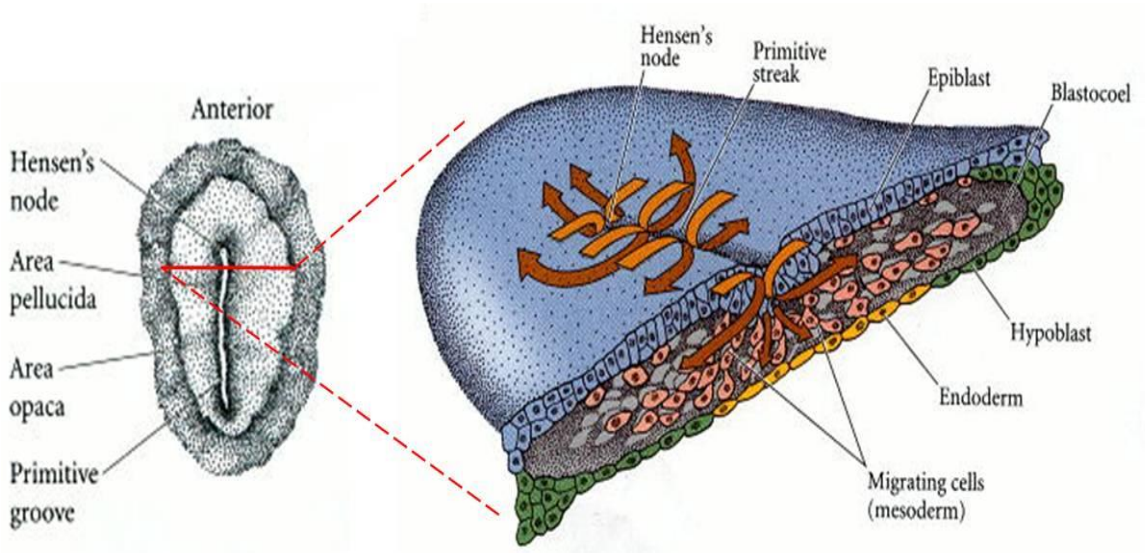

Figure 1.3 – Schematic diagram of a cross-section of a chick embryo undergoing gastrulation.
The migration of endodermal and mesodermal cells trough the primitive streak (Adapted from Gilbert, 2003)

The primitive streak elongates anteriorly as the cells ingress and reaches its maximum length at HH4 (Figure 1.4C). A depression called the primitive groove is formed as the cells converge and it is from this opening that the migrating cells pass into the blastocoel. Located at the anterior end of the primitive streak is a regional thickening of cells termed Hensen's node (Figure 1.4C), which constitutes the primary embryonic organizer of the chick embryo, and will guide the subsequent development of the embryo by ensuring the correct set up and

patterning of the main axes of the body plan (Boettger et al., 2001). The embryo axes are defined by the primitive streak that separates the left and right side of the embryo and extends from the posterior to the anterior side. The migrating cells enter through the dorsal side of the embryo and move to the ventral side.

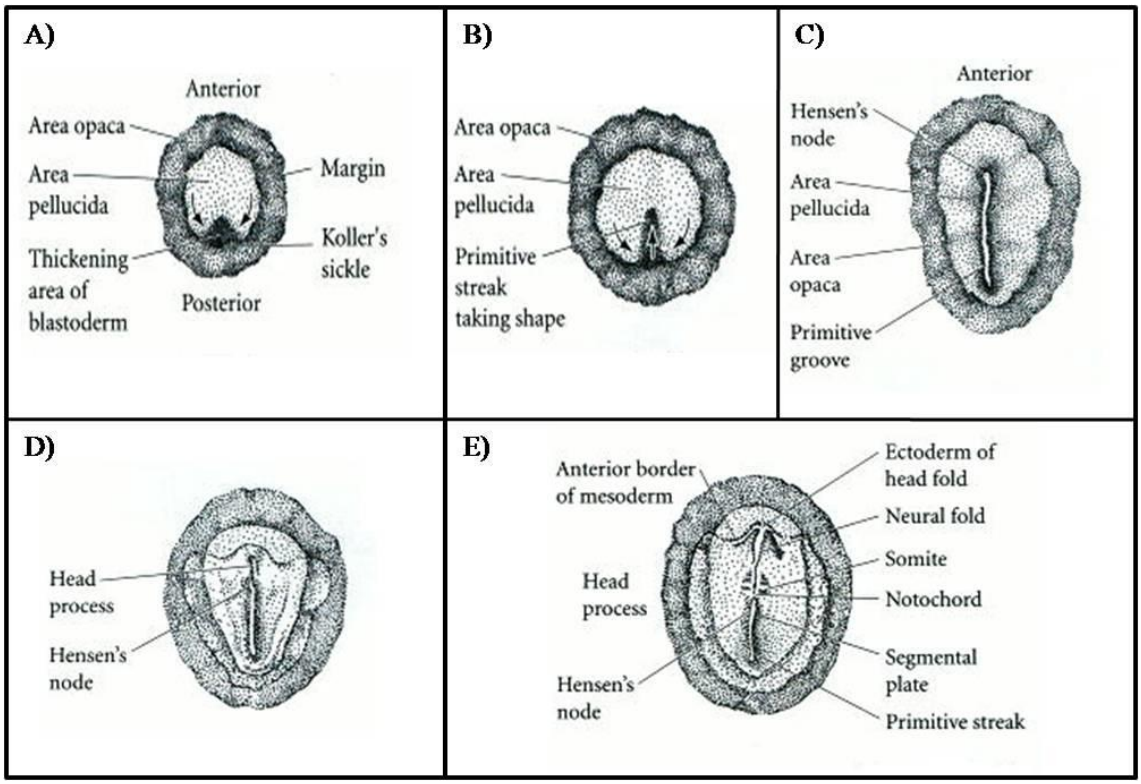

Figure 1.4 – Early steps in chick development.
(A-E) Images are representations of the dorsal surface of chick embryo. Gastrulation commences with the emergence of the primitive streak, in the posterior part of the embryo from Koller's sickle at stage HH3. As gastrulation proceeds the primitive streak gets to its full extension at stage HH4 and starts is regression along the midline, giving rise to different axial structures in the embryo (Adapted from Gilbert, 2003).

Following formation of the definitive primitive streak, epiblast cells migrate through the lateral portions of the primitive groove, leave the epithelium, and form the definitive mesoderm and definitive endoderm. Other cells instead, migrate through Hensen's node and pass down into the blastocoel and migrate anteriorly, forming foregut, head mesoderm, and notochord (Figure 1.4E) (Schoenwolf et al., 1992). This dynamic cellular movement implies that the cell populations in the primitive streak are in constant flux during gastrulation.

After the primitive streak formation, the embryo is composed of three germ layers: the ectoderm (surrounds the embryo and will give rise to skin and neural tissues), mesoderm (will give rise to several tissues including the heart, muscle, kidney, and blood) and endoderm (is the inner layer that forms the gut tube, liver, pancreas, gallbladder and lungs). The mesoderm, located between the endoderm and ectoderm, can be divided into four regions: 1) the chordamesoderm, will form the notochord; 2) the paraxial mesoderm forms the somites, which can become bone, cartilage and muscle; 3) the intermediate mesoderm that will form the kidneys and gonads; 4) the lateral plate mesoderm gives rise to the heart, blood vessel and blood cells of the circulatory system (Figure 1.5) (Gilbert, 2003).

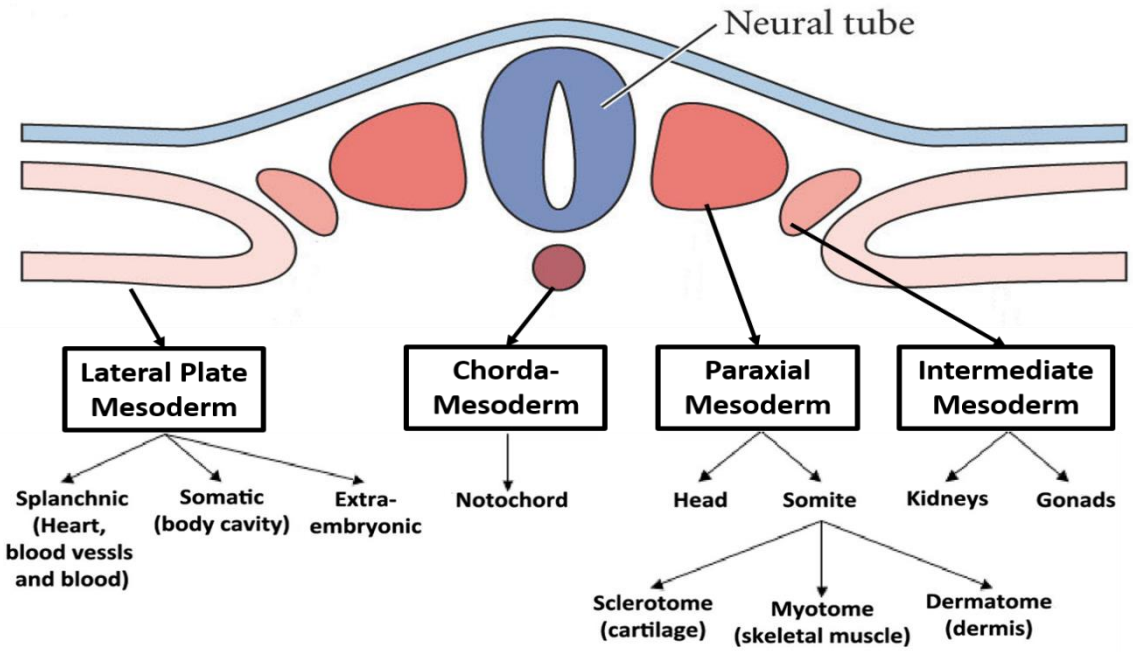

Figure 1.5 – Mesoderm organization during embryogenesis.
The mesoderm is divided in four regions: the lateral plate mesoderm, the chordamesoderm, the paraxial mesoderm and the intermediate mesoderm (Adapted from Gilbert, 2003).

During the later stages of gastrulation, the primitive streak gradually regresses along the midline and a series of daughter cells from the Hensen's node are arranged giving rise to the different axial structures in the embryo. The first cells that ingress through the node at stage HH4 give rise to prospective notochord,

prechordal mesendoderm, floor plate cells, prospective medial somites and endodermal precursors. Then, the mesodermal precursors migrate through the primitive streak giving rise to specific types of mesoderm according to their relative position in the axial midline (Solnica-Krezel, 2005). As the chick embryo develops and take form the anterior-to-posterior gradient becomes evident, that is, in the anterior part of the embryo organogenesis has started, while in its posterior end gastrulation is still taking place (Darnell et al., 1999).

1.3 Heart development in vertebrates

The vertebrate heart is an extraordinary and complex muscular vessel that works like a pump, providing a continuous circulation through the body. Its architecture and function depend on the correct development of numerous components, including chambers, conduction system, coronary circulation, valves and main vessels. The molecular and morphological events of the developing heart are sensitive to genetic perturbation, and congenital heart defects have been detected in 1% of live births (Harvey, 2002).

The heart is the first organ to form during embryogenesis and its circulatory function is critical for the viability of the developing embryo. Due to the evolutionary conservation, our understanding of vertebrate heart formation has been acquired from studies using vertebrate animal models, such as chick, mouse and amphibians (Srivastava, 2006). In fact, in all of these animal models, the heart arises from cardiac precursor cells in the anterior lateral plate mesoderm of the early embryo, where a single bilaterally heart field takes the shape of a crescent in mammals, while in the chick embryo they are arranged as bilateral fields on either side of the primitive streak (Brand, 2003). Signals from the surrounding tissues such as members of the transforming growth factor (Tgf) β, bone morphogenetic protein (Bmp) and fibroblast growth factor (Fgf) families promote the specification of myocardial fate (Sugi and Lough, 1995). The bilateral heart fields are formed in the splanchnic mesoderm as a result of the splitting of the lateral plate mesoderm into two layers.

The morphological changes are a result of a complex interaction of multiple transcription factors, such as *Nkx2.5*, *Gata4/6* and *Mef2c*, which confers commitment and determination of the heart field precursor cells to a myocardial fate (Abu-Issa and Kirby, 2007). Moreover, the heart fields reverse their position by a 125º rotation and then fuse medially as a continuous stream into the forming heart tube and simultaneously differentiate into a beating heart (Stalsberg and DeHaan, 1969). These morphogenetic movements require several cytoskeletal, adhesive and extracellular structural proteins and their regulators, such as *RhoA*, whereas differentiation requires the expression of another set of skeletal proteins, such as *cardiac troponin-I* and *sarcomeric myosin* (Abu-Issa and Kirby, 2007). In the chick embryo, the developing heart is initially assembled as a linear structure at stage HH10 and then gradually begins to loop, starting at stage HH11. During this phase, the basic regions of the heart become apparent, the truncus, ventricle, atrium and the sinus venosus (Stalsberg and DeHaan, 1969). The circulation is well established by about stage HH16 and the division into left and right sides takes place during days three to five of embryo development (Harvey and Rosenthal, 1999).

1.3.1 Origin, location and migration of cardiac precursors

Fate map and explant studies in the chick embryo showed that at stage HH3 the cardiac precursors are located in the epiblast and primitive streak (Figure 1.6 A). During early primitive streak stage, heart precursors cells within the epiblast, are bilaterally distributed on both sides of the primitive streak, caudal to the node (Lopez-Sanchez et al., 2001). Around stage HH3^{+}, the anterior half of the primitive streak, with the exception of the Hensen's node, contains the cardiac precursors (Figure 1.6 B), and these cells will contribute to all layers of the heart tube, including endocardium, myocardium and epicardium (Garcia-Martinez and Schoenwolf, 1993).

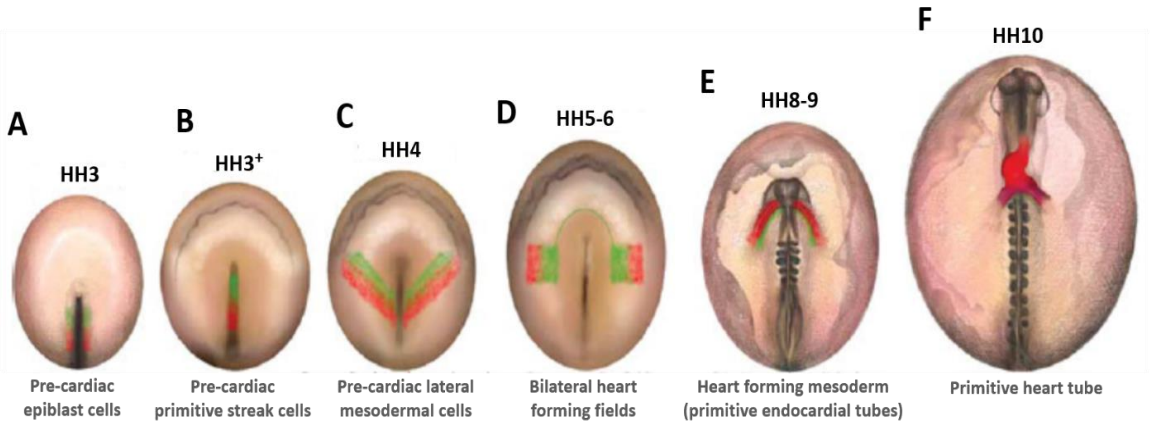

Figure 1.6 – Localization of the two sources of cardiac precursors cells, from stage HH3 to stage HH10, during chick heart development.
Cardiac precursors are located: **(A)** in the epiblast and primitive streak (green and red area), **(B)** In the anterior primitive streak in an anterior–posterior sequence (green and red area); **(C-D)** cardiac precursors migrate to the anterior lateral plate mesoderm, the heart forming region: the cells occupying a more lateral position will give rise to the left ventricle (red area), whereas the medial region forms the outflow tract (OFT) and most of the right ventricle (green area); **(E)** The heart forming regions migrate to the midline to fuse; **(F)** The primitive heart tube is formed from the lateral-most part of the heart forming mesoderm (red area). The visceral mesoderm behind the primitive heart tube (green area) contains the cells that will populate the heart to form the OFT, the right ventricle, the atrioventricular canal and the atria. A-D, dorsal view; E and F, ventral view. (Adapted from(López-Sánchez and García-Martínez, 2011).

The cardiac precursor cells in the primitive streak presents an anterior-posterior sequence, meaning that the cells that will give rise to the outflow tract (OFT) and right ventricle are located in the anterior region of the anterior half of the primitive streak (Figure 1.6B, green area), while the left ventricle, the atria, and the sinus venosus forming cells are in the posterior region of the anterior half of the primitive streak (Figure 1.6B, red dots) (Garcia-Martinez and Schoenwolf, 1993).

At stage HH4, cardiac precursor cells from the epiblast migrate through the primitive streak (anterior-laterally) to form the bilateral cardiogenic mesoderm (Figure 1.6C-D) known as the heart forming region (HFR) (Münsterberg and Yue, 2008; Yang et al., 2002). At this moment, the epiblast progenitor cells of the pharyngeal and foregut endoderm migrate through the primitive streak to incorporate the endoderm. In addition, the cardiogenic mesoderm is adjacent to the endoderm that plays a crucial role during cardiac specification (Lopez-Sanchez et al., 2009). After the cardiac precursor cells take up residence in the lateral plate mesoderm as the HFR, it remains as progenitors for an extended

period of time without showing any signs of differentiation until their migration towards the midline (Colas et al., 2000). In the chick embryo, there was a misconception, about the fusion of the heart fields occurring at stage HH6, in which supposedly a cardiac crescent was to be formed (as in happens in humans and mouse embryos) (DeHaan, 1963). That was strengthened when the expression of *Nkx2.5* showed up as a crescent in stages HH5 to HH8 (Schultheiss et al., 1995). The expression of *Nkx2.5* in the midline was exclusively present in the endoderm and ectoderm, meaning, there was no splanchnic mesoderm established at the midline (Colas et al., 2000). Therefore, a single bilaterally symmetrical heart field takes the shape of a crescent in mammals but remains as separate bilateral heart fields in the chick embryo until stage HH9 (Figure 1.6D-E).

1.3.2 Formation of the early heart tube

From stage HH7 begins the organization of the HFR in the anterior lateral plate mesoderm, which splits into somatic and splanchnic mesoderm (originates the pericardial cavity), being the cardiac precursor cells restricted to the splanchnic mesoderm, with two distinct cell populations: one localized in the lateral-most side of the splanchnic mesoderm and other in the mediocaudal region of the splanchnic mesoderm (Linask, 1992). With the formation of the foregut pocket the bilateral heart fields invert along the anterior-posterior axis of the coelom, twist ventral and fuse at the midline (stage HH9) to form a linear heart tube (Figure 1.7), composed by an outer myocardial layer and an inner endocardial layer (Abu-Issa and Kirby, 2007; Hurle et al., 1980; Kirby, 2002). Later, the margins of the tube fuse and closes dorsally attached to the ventral pharynx to form the roof of the linear heart tube, which is suspended between the dorsal and ventral mesocardium. The rupture of both mesocardium generate a heart tube that is attached only at its anterior (arterial pole) and posterior (venous pole) limits (Noden, 1991).

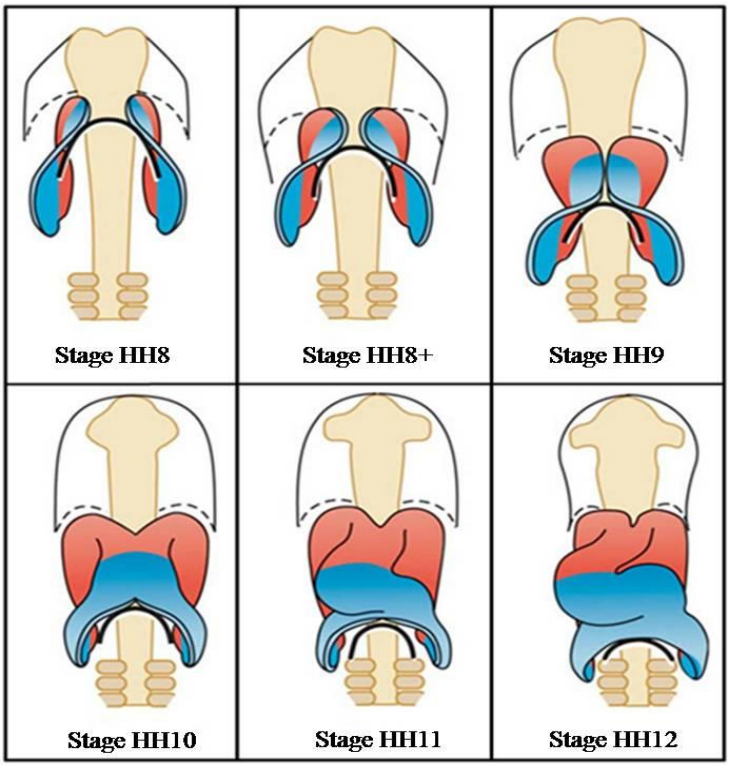

Figure 1.7 – Schematic representation of early heart tube development in chick.
Formation of the ventral midline heart tube from the cardiogenic mesenchyme in chick embryo from stage HH8 to HH12. The stage HH8 shows separate bilateral heart fields until stage HH9. At stage HH10 the linear heart tube is formed and starts the looping process. The stage HH11 shows an elongated heart tube that is slightly looped, being more prominent at stage HH12 (adapted from(Abu-Issa and Kirby, 2007).

The newly formed heart tube comprises cells from the lateral-most region of the HFR contributing to the entire left ventricle and most of the atria, whereas the medial region forms the outflow tract (OFT) and the majority of the right ventricle (Figure 1.7, blue area and red area, respectively) (Abu-Issa and Kirby, 2007). The looping process of the linear heart tube begins around stage HH11, whereby the ventricular region of the heart adopts a pronounced rightward curvature (Figure 1.8C) thus establishing the fundamental pattern of the four-chambered heart. It is also during the early stages of looping that primitive segments become evident in the heart tube, namely the OFT, future right and left ventricle, atrioventricular canal, and future atria (Figure 1.8) (Harvey and Rosenthal, 1999). With the increasing thickness of the ventricular walls, the cardiac jelly is rapidly replaced by a network of myocardial trabeculae allowing blood to flow to the myocardium. Septa then forms between the atria and ventricles, endocardial cushions and

valves develop, conduction tissue becomes specialized, and the epicardial layer is formed. It is at this point that the heart resembles its mature form (Figure 1.8D) (Nakajima, 2010; Taber, 1998).

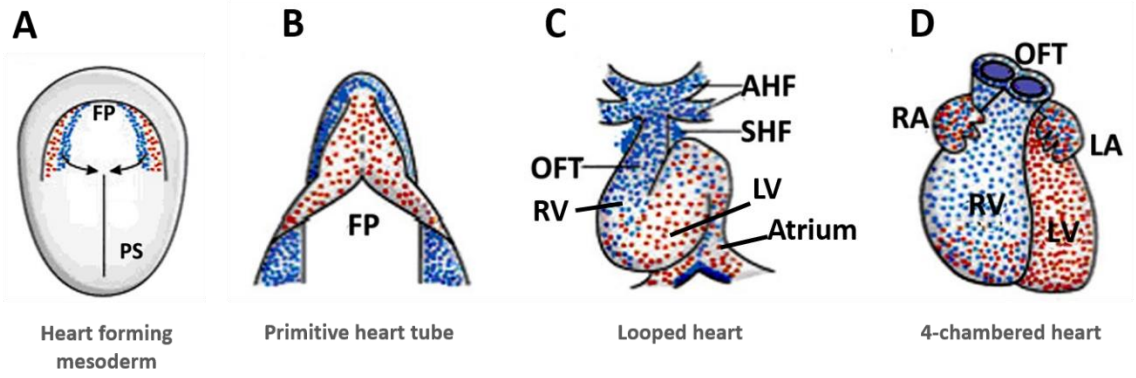

Figure 1.8 – Schematic diagram of vertebrate cardiogenesis
Bilaterally symmetrical cardiac progenitor cells **(A)** are specified to form distinct regions of the linear heart tube **(B)**. The heart undergoes rightward looping **(C)** and begins to establish the orientation of the four-chambered mature heart **(D)**. A-D, ventral view. AHF, anterior heart field; FP, foregut pocket (anterior intestinal portal); LA, left atrium; LV, left ventricle; OFT, outflow tract; PS, primitive streak; RA, right atrium; RV, right ventricle; SHF, posterior second heart field (Adapted from(Nakajima, 2010).

1.3.3 Second heart field elongates the heart tube

Studies carried out more than 30 years ago suggested that elongation of the heart tube results from the addition of an extra cardiac cell population to the outflow and inflow tract (Virágh and Challice, 1973). Marking experiments *in ovo* of chick cardiogenesis showed that the outflow tract is added during the looping process of the heart tube (between stages HH11-22), in which its derived mainly from cells that reside in the pharyngeal and splanchnic mesoderm rather than cell expansion of the primitive heart tube (de la Cruz et al., 1977).

In 2001, several studies about the exact spatial fate map of the heart field were conducted by three different groups, using experimental manipulation of chick embryos and transgenic approaches in mice, in which they rediscovered that a population of cells in pharyngeal and splanchnic mesoderm give rise to the myocardium of the OFT and right ventricle (Kelly et al., 2001; Mjaatvedt et al.,

2001; Waldo et al., 2001). In the study performed by Waldo et al. (2001) it was showed, using marking experiments and quail-chick chimeras, that during chick cardiogenesis, the OFT is secondarily added to the linear heart tube from a secondary heart field situated at the splanchnic mesoderm beneath the floor of the foregut just caudal to the OFT. These myocardial precursor cells express the heart-specific transcription factor *Nkx2.5* and *Gata4*, but not the *Myosin heavy chain* (Mhc). When precursor cells move to the OFT, they begin to express human natural killer (Hnk) 1 and then Mhc. This cell population was described as the second source of the heart, therefore named the "secondary heart field" which is located in the splanchnic mesoderm behind the heart (Figure 1.9E). Mjaatvedt et al. (2001) showed, using fate-mapping, ablation and explantation experiments in chick embryos, that the OFT is not derived from expansion from the primitive heart tube, rather originates from the mesoderm surrounding the aortic sac. This population was defined as the anterior heart field (Figure 1.9D). So, Waldo et al. (2001) and Mjaatvedt et al. (2001) showed that some of the myocardium originates from a distinct heart field and called it the secondary heart field and anterior heart field, respectively. Moreover, a field of the same name (anterior heart field) was identified in mice by Kelly et al. (2001), who reported a LacZ transgenic insertion into the mouse Fgf10 locus, in which LacZ activity reporting *Fgf10* expression was found in the myocardium of the OFT and right ventricle of the looped heart, and in the mesodermal core of the pharyngeal arches (pharyngeal and splanchnic mesoderm), a similar location to that propose by Mjaatvedt et al, 2001 (Figure 1.9C). Altogether, these studies demonstrated that cells comprising the earliest fusing heart tube, originated from the first heart field (FHF) progenitors, are not responsible for the totality of the OFT and right ventricle progenitors, and that these structures derive completely or in part, from the precursors of the SHF, which are later added to the linear heart tube.

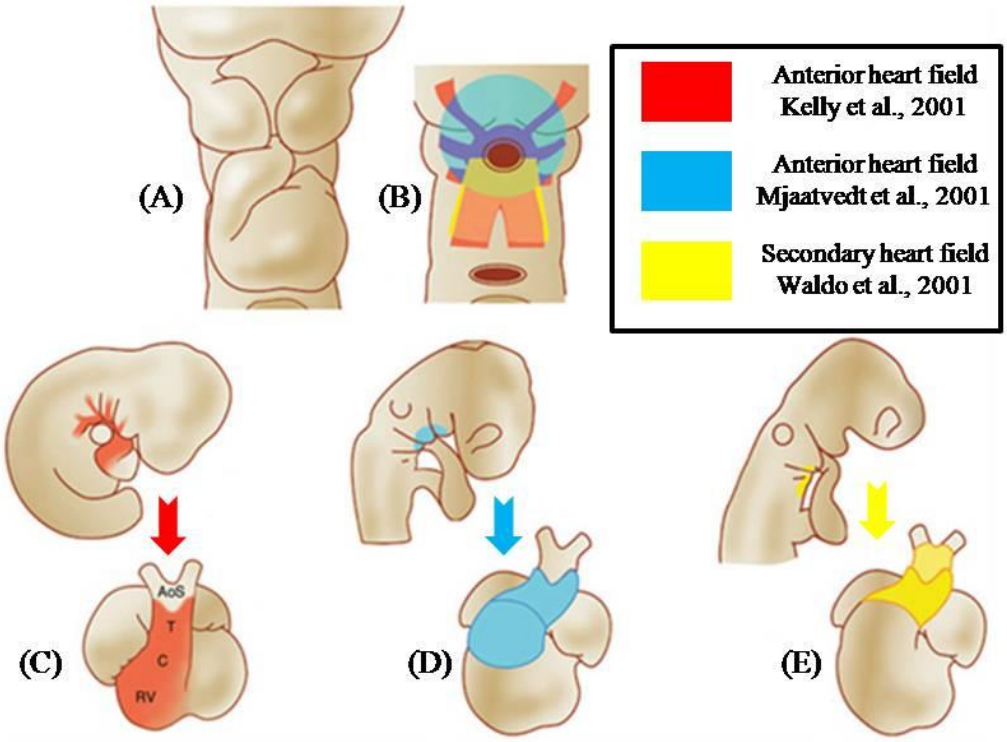

Figure 1.9 – Schematic representation of the location and contribution of the anterior and secondary heart field into the primitive heart tube.
This figure shows the location and contribution of cells that are added into the heart after the formation of the heart tube. **(A)** Ventral view of the looped heart of an E9.5 mouse embryo (stage HH12 in chick embryo). **(B)** Ventral view of the anterior and secondary heart fields overlapping on each other. **(C)** The red area as proposed by Kelly et al. (2001): mouse embryo at E9.5 and developed until E11.5. **(D)** The blue area as proposed by Mjaatvedt et al. (2001): chick embryo at stage HH16 and developed until stage HH22. **(E)** The yellow area as proposed by Waldo et al. (2001): chick embryo at stage HH14 and developed until stage HH22. Note that the outflow is divided from anterior to posterior into aortic sac (AoS), truncus (T), conus (C), and right ventricle (RV) (adapted from(Abu-Issa et al., 2004).

If all the cells in the heart fields described originate in the bilateral heart forming regions, these differences reveals a complex patterning of the cardiogenic mesoderm, indicating that the cardiac progenitors go through all of the early steps in commitment and then are inhibited from differentiating when the heart tube is assembled. Only later, these inhibited cardiogenic cells are added to the poles of the heart tube development. However, the data from the *Islet-1* null mouse indicated a more complex cardiogenic model than a simple model of the cardiogenic field being divided into prospective regions; instead the heart is constructed from several populations in the bilateral cardiogenic fields that assemble in a coordinated fashion from different locations and at different times

(Cai et al., 2003). At the gastrula stage *Islet-1* is expressed in the mediocaudal region of the heart forming mesoderm (Figure 1.8A, blue dots), but not in the lateral region of the HFR. Later, *Islet-1* is expressed in the pharyngeal and splanchnic mesoderm, that are connected to the OFT, and in the caudal splanchnic mesoderm, which is connected with the inflow tract (extracardiac blue dots in figure 1.8B). Indeed, Cai et al. (2003) report that an LIM homeodomain transcription factor *Islet-1* null mutant showed severe heart defects involving the OFT, the right ventricle and the atria, which are added to the heart tube during the looping process. *Islet-1* seems to be required for the proliferation, survival and migration of these cells into the heart tube, and is downregulated when the cardiac precursor cells differentiate (Cai et al., 2003). This idea is supported by a lineage tracing study based on the use of a lacZ reporter gene targeted to the *α-cardiac actin* locus, demonstrating that the left ventricle and the OFT are derived exclusively from a single lineage (the FHF and the SHF, respectively), and all other regions of the heart tube possess both lineages (Meilhac et al., 2004).

Taken together, all of this studies revealed a population of cardiac progenitor cells in the pharyngeal mesoderm that gives rise to a major part of the amniote heart. These undifferentiated and highly proliferative cells, known as SHF, contribute progressively to the poles of the elongating heart tube during looping morphogenesis being essential for correct alignment of the aorta with the left ventricle. The SHF deployment when perturbed it causes anomalies in OFT formation that underlie 30% of human congenital heart defects (like tetralogy of Fallot, double outlet right ventricle) (Srivastava and Olson, 2000).

1.4 Heart forming regions

The transformation of an epithelial sheet of cells into a functional heart is one of the most fascinating morphogenetic processes of embryonic development. The heart forming regions, FHF and SHF, with a common origin appear to contribute with different cells to the developing heart in a temporally and spatially specific fashion (Figure 1.10). While, some cardiac precursors differentiate earlier (FHF),

others (SHF) remain undifferentiated, indicating a control in the timing of differentiation. Moreover, the cardiac cells that differentiate later are more sensitive to genetic perturbation of several genes than the cardiac precursors that differentiate earlier (Buckingham et al., 2005).

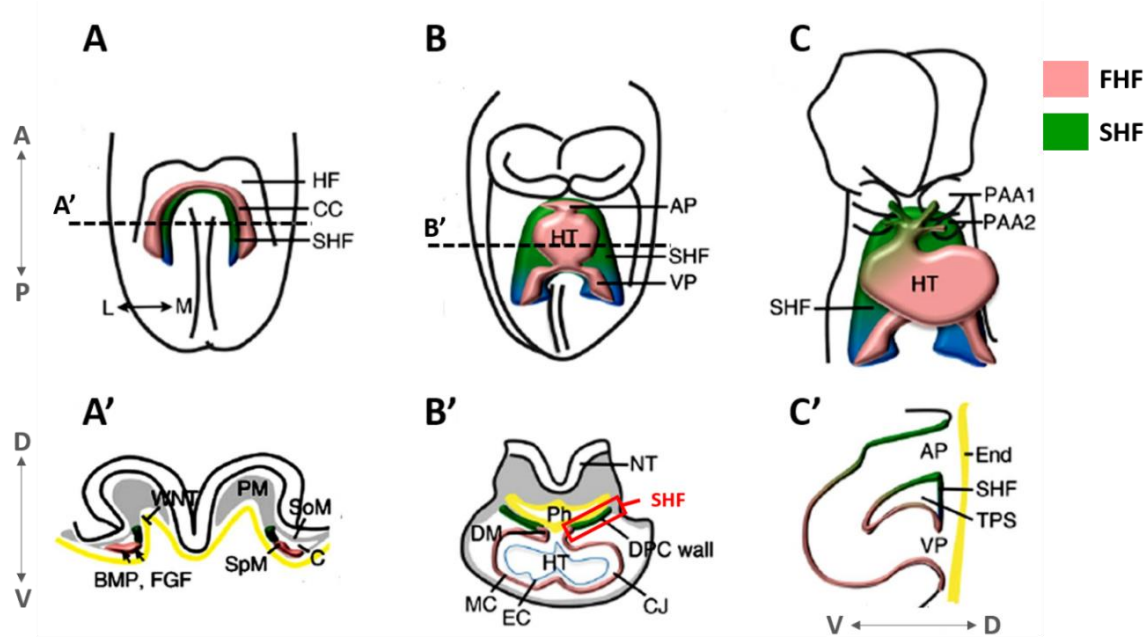

Figure 1.10 – Development of the vertebrate early heart tube.
(A) The cardiac progenitors are located in the anterior lateral mesoderm. The cardiac crescent (CC) in mouse and cardiogenic fields in the chick embryo are located in the anterior splanchnic mesoderm underlying the head fold (HF). Late differentiating SHF cells are localized medially. **(A')** Transverse section in A demonstrating positive signals from underlying endoderm FGF and BMP, and negative signals from the midline β-catenin/WNT. **(B)** The linear heart tube (HT) is attached at the arterial pole (AP) and venous pole (VP). **(B')** Transverse section in B showing the ventral HT attached to the dorsal mesocardium (DM) and comprised of an outer myocardial layer (MC) and inner endocardial tube (EC) separated by cardiac jelly (CJ). SHF cells are situated in medial splanchnic mesoderm in the dorsal pericardial wall (DPC wall) (red box) underlying the pharynx (Ph). **(C)** During looping the AP of the HT is attached to the first (PAA1) and second (PAA2) pharyngeal arch arteries. **(C')** Sagittal section showing the transverse pericardial sinus (TPS) after breakdown of the DM, and location of SHF cells in the DPC wall. A, anterior; C, coelom; D, dorsal; End, endoderm; L, lateral; M, medial; N, node; NT, neural tube; P, posterior; PM, paraxial mesoderm; SoM, somatic mesoderm; SpM, splanchnic mesoderm; V, ventral. Color code: pink, FHF and derivatives; green, SHF and derivatives; blue, posterior SHF; yellow, endoderm. (Adapted from(Kelly, 2012).

The FHF contributes to the myocardial cells of the primitive heart tube, which contributes exclusively to the left ventricle. Regarding to the SHF, it lies anterior and posterior, and dorsal to the linear heart tube and is derived from the pharyngeal mesoderm medial to the heart forming regions (Figure 1.10A-C),

contributing exclusively to the OFT region (Buckingham et al., 2005). The cells of the SHF localized in the dorsal pericardial wall become separated from the heart tube when the dorsal mesocardium breaks down, being attached only at the arterial and venous poles of the heart tube (Figure 1.10C-C'). The other structures, such as, the right ventricle, the atrioventricular canal, and the atria have contribution from both lineages.

The SHF can be divided in two regions, the anterior and posterior SHF (Figure 1.11A'), which contributes with cardiac progenitor cells to the arterial (give rise to right ventricular and OFT myocardium and smooth muscle at the base of the great arteries) and venous poles (give rise to atria, atrial septum and inflow tract myocardium) of the heart tube (Figure 1.11 A-B), respectively (Galli et al., 2008; Hoffmann et al., 2009; Kelly et al., 2001; Sun et al., 2007; Waldo et al., 2005). Furthermore, the development of the arterial pole is a result of a coordinated and tight crosstalk between heart field, cardiac neural crest cells and the pharyngeal endoderm (Figure 1.11B'-B''). The addition of proliferative cells to the heart tube is a balance between the induction of proliferation from the canonical Wnt and Fgf signaling, and the differentiation induction by the Bmp pathway (Buckingham et al., 2005; Hutson et al., 2010; Tirosh-Finkel et al., 2010). In addition, the incursion of the neural crest cells into the pharyngeal region have a role in this balance by reducing Fgf signal reception in the SHF cells (Hutson et al., 2006).

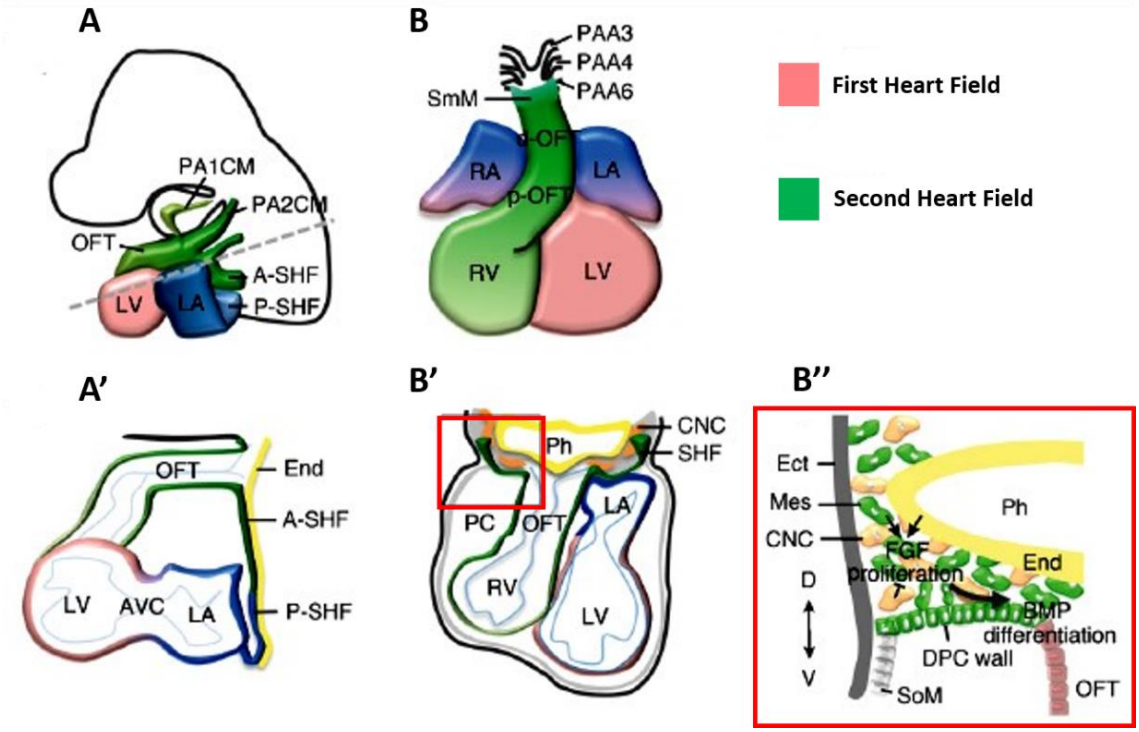

Figure 1.11 – Contribution of the second heart field to the developing heart.
(A) Lateral view of the SHF contribution to the heart at E9.5, showing anterior (green) and posterior regions (blue). Core pharyngeal arch mesoderm of arches 1 (PA1CM) and 2 (PA2CM). **(A')** Sagittal section of A, demonstrating the different contributions of the FHF and SHF. **(B)** Embryonic heart at E10.5 showing parts of the heart derived from the anterior SHF (green), linear heart tube (pink), and posterior SHF (blue). The anterior SHF also contributes with smooth muscle (SmM) at the arterial pole of the heart tube, which is attached to pharyngeal arch arteries (PAA) 3, 4, and 6. **(B')** Transverse section in B showing juxtaposition between anterior SHF cells (green) and neural crest-derived mesenchyme (CNC, orange) lateral to and underlying the pharynx (Ph). **(B'')** Zoom of the red boxed area in B' showing mixed CNC and mesodermal (Mes) mesenchymal cells and the balance between FGF and BMP signals regulating proliferation and differentiation during the elongation of the OFT. A-SHF, anterior second heart field; AVC, atrioventricular canal; D, dorsal; d-OFT, distal outflow tract; DPC wall, dorsal pericardial wall; End, endoderm; LA, left atrium; LV, left ventricle; OFT, outflow tract; p-OFT, proximal outflow tract; P-SHF, posterior second heart field; RA, right atrium; SoM, somatic mesoderm; V, ventral. Color code: pink, FHF and derivatives; green, SHF and derivatives; blue, posterior SHF; yellow, endoderm (Adapted from(Kelly, 2012).

1.4.1 Signaling pathways regulating the HFR

The signaling molecules and tissue interactions that recruit multipotent progenitor populations to the cardiac lineage are not yet fully defined, indeed, it appears to take place via multiple signals and interactions that are regulated precisely in time and space (McGrew et al., 1999). A vast array of genes and signaling pathways, have been reported to be crucial in all steps of cardiogenesis, from migration of

primitive-streak progenitor cells, formation of the HFR, cardiac looping, to later morphogenetic mechanisms. The major signaling pathways controlling heart development are the Wnt proteins, Fgf, Notch, Bmp, Nodal and Activin (Figure 1.12) (Noseda et al., 2011). While the architecture of the heart is different between species, the inductive paths are ancestral and conserved, as is the transcription machinery that controls the cardiomyogenesis fate. Such information is crucial to comprehend the formation of the heart and to transform the knowledge into quantitative network models that provides for uncountable translational applications.

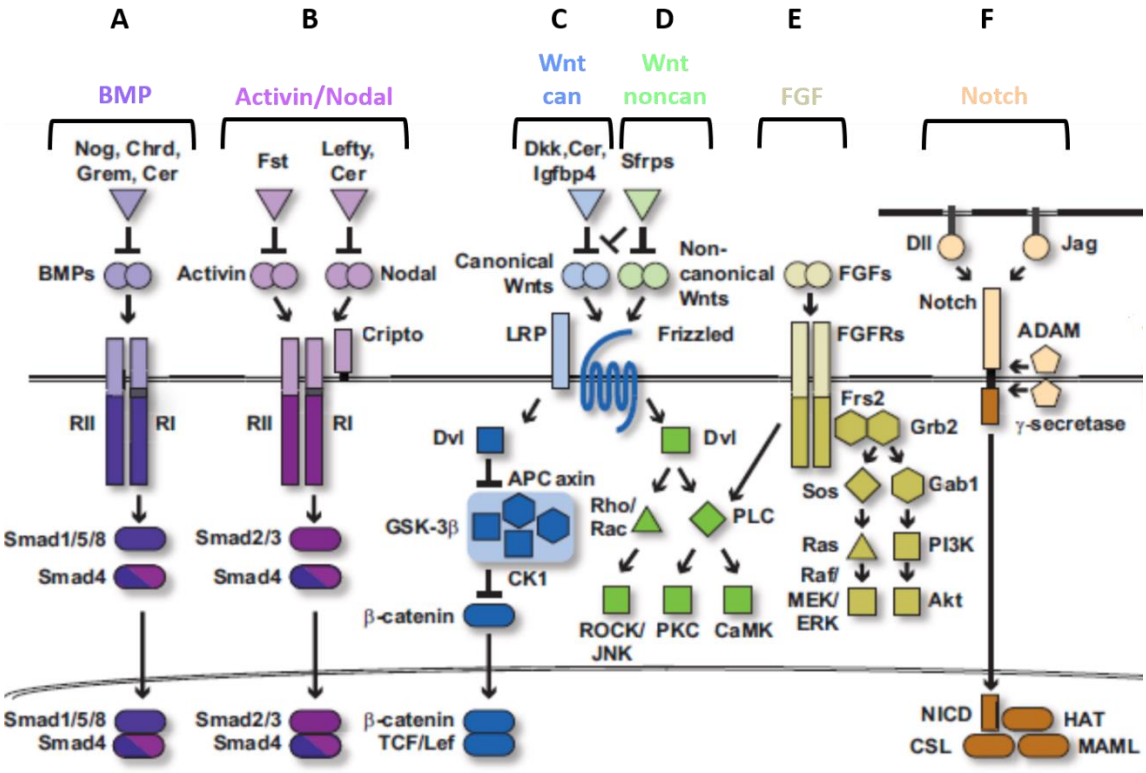

Figure 1.12 – Summary of major signaling pathways controlling heart development. Schematic representation of the major signaling pathways from left to right: **A)** BMP, **B)** Activin/Nodal, **C)** canonical Wnt **D)** non-canonical Wnt, **E)** FGF and **F)** notch pathways. For details of each, see the text. **Circle** indicates ligand; **inverted triangle**, ligand antagonist; **rectangle**, receptor ligand-binding and signaling domains (light and dark, respectively); **square**, protein kinase; **triangle**, G-protein; **hexagon**, scaffold protein; **pentagon**, protease; **oval**, transcription factor (Adapted from (Noseda et al., 2011).

1.4.1.1 Bone Morphogenetic Protein (Bmp)

The Bmp are multifunctional regulators that play a panoply of roles in development by regulating cell proliferation, differentiation and apoptosis in different tissues (Massagué and Chen, 2000). In the chick embryo, Bmp are necessary for the cardiogenic activity of anterior endoderm, inducing the specification of the cardiogenic mesodermal cells, shown by the ability of inhibitors like Chordin and Noggin to suppress cardiac differentiation (Andree et al., 1998; Schultheiss et al., 1997). Activation of BMP signaling pathway starts when Bmp ligand binds to Bmp receptor I and II (Kishigami and Mishina, 2005). The receptor II activates the receptor I by phosphorylation of the serine/theronine residue, thus, the activated receptor I can now phosphorylate the Smad transcription factors, triggering the intracellular signal cascade. Moreover, Bmp activity is regulated by a large number of extracellular antagonists, such as, Cerberus, Chordin and Noggin. These molecules bind directly to Bmp ligands and block their interaction with signaling receptors, thus inhibiting the Bmp signaling (Figure 1.12A) (Rodríguez Esteban et al., 1999).

1.4.1.2 Activin and Nodal

Activin and Nodal share receptors I and II and have the same Smad signaling pathway (Figure 1.12B) (Kitisin et al., 2007). In addition, they signal via Smad2/3, and the R-Smad/Smad4 complexes promote cooperative DNA binding by the forkhead winged-helix protein FoxH1, which mediates many effects of the pathway. The majority of Nodal effects requires a co-receptor of the EGF-CFC family, whose members are defined by an epidermal growth factor-like domain and include mammalian Cripto and Cryptic, Xenopus FRL-1, and zebrafish one-eyed pinhead (Chu and Shen, 2010). The Nodal and Activin activity are regulated by the extracellular antagonists, Lefty, and Cerberus, and follistatin (Fst), respectively. Moreover, Nodal is vital for establishing the anterior-posterior and left-right axes, gastrulation, primitive streak development, and thus the formation of mesoderm and endoderm, germ layer specification being a requirement for later cardiac tissue formation (Schier, 2003).

1.4.1.3 Wingless-type MMTV integration site (Wnt)

Signaling by the Wnt family of secreted glycoproteins is one of the fundamental mechanisms that direct/regulate cell differentiation, proliferation, survival, polarity and migration during embryogenesis (Logan and Nusse, 2004). The signaling pathways involve 19 Wnt secreted proteins, 10 Frizzle (Fz) receptors and the co-receptors LRP5 and LRP6 (lipoprotein low-density-lipoprotein receptor-related protein) in mammals, suggesting a vast complexity of this signaling pathway (Figure 1.12C-D) (Bejsovec, 2005). Wnt signaling pathways are divided in canonical (β-catenin) and noncanonical (β-catenin-independent), which have two branches, the planar cell polarity pathway and the calcium pathway (Nusse, 2005; Nusse and Varmus, 2012; Nusse and Varmus, 1992).

The canonical Wnt pathway (Figure 1.12C) plays a role in the regulation of the amount of transcriptional co-activator β-catenin, which controls crucial developmental gene expression programs. It starts when Wnt proteins (Wnt1, 2a, 3a and 8) bind to Fz and LRP family members, either on the producing or adjacent cells (MacDonald et al., 2009). Upon receptor binding disheveled protein (Dvl) is activated, which in turn inhibits a protein complex that includes the constitutively glycogen synthase kinase 3β (Gsk3β) and CK1 (casein kinase 1), as well as the scaffolding proteins axin and adenomatous polyposis coli (APC). This complex normally phosphorylates β-catenin and targets it for degradation. These events lead to decreased phosphorylation of β-catenin, allowing stabilization, cytoplasmic accumulation and consequent nuclear translocation of the protein (MacDonald et al., 2009). The inhibition of the degradation complex allows high levels of β-catenin to accumulate in the nucleus, where it interacts with TCF/LEF family DNA binding proteins to activate the transcription of Wnt target genes (Mosimann et al., 2009). In the chick embryo, experiments showed that the levels of Wnt canonical (Wnt3a and 8c) signaling are lower in the anterior mesoderm (cardiogenic) and higher in the posterior mesoderm (blood-forming), thus Wnt β-catenin signals inhibits cardiac tissue formation in chick embryo and therefore needs to be inhibited itself for proper heart development (Marvin et al., 2001; Tzahor and Lassar, 2001).

The noncanonical Wnts (Figure 1.12D) such as Wnt4, 5a and 11 activate two main signaling pathways. In the planar cell polarity (PCP) pathway, Wnt proteins bind to Fz receptors, that recruit Dvl and activate Rho-family small GTPases (Rho and Rac) and their downstream effectors such as Rho-associated protein kinase (ROCK) and Jun N-Terminal kinase (JNK) (Tada et al., 2002). On the other side, the Wnt/Calcium signaling pathway, through the G-protein-dependent activity of Frizzled receptors, induce the release of $Ca2^{+}$ intracellular by phospholipase C, which activate the $Ca2^{+}$ - dependent protein kinases Protein Kinase C (PKC) and CaMKs (calmodulin-dependent protein kinases) (Kohn and Moon, 2005; Sheldahl et al., 2003). In the chick embryo, experiments demonstrated that Wnt noncanonical, like *Wnt11*, is present in the precardiac mesoderm suggesting a role in myogenesis (Eisenberg and Eisenberg, 1999; Eisenberg et al., 1997). In addition, noncanonical Wnt signaling inhibits the canonical Wnt signaling promoting myocardial differentiation and have a role in cardiac morphogenesis by regulating cadherin-mediated cell adhesion and cell polarity (Brade et al., 2006).

1.4.1.4 Fibroblast Growth Factors (Fgf)

Fibroblast growth factors (Fgf) (Figure 1.12E) and their receptors control a panoply of cellular processes, regulating cellular proliferation, survival, apoptosis, migration and differentiation (Böttcher and Niehrs, 2005). Fgf contain a large family of growth factors, with twenty two ligands and four transmembrane receptor tyrosine kinases (Fgfr) (Itoh and Ornitz, 2004; Turner and Grose, 2010). Fgf proteins are characterized by their high affinity with heparin, a molecule that facilitates their binding to cell surface Fgfr. Binding of the Fgf ligands to the extracellular domain of the Fgfr in combination with heparan sulfate leads to the dimerization of the receptor resulting in the transphosphorylation of specific intracellular tyrosine residues in the receptor (Turner and Grose, 2010). Consequently, activate cytoplasmic signal transduction pathways, such as the Ras/ERK pathway that is associated with differentiation and proliferation, the Akt

pathway, which is associated with cell survival or the PKC pathways that have a role in cell morphology and migration) (Dailey et al., 2005; Schlessinger, 2000).

In the chick embryo, experiments demonstrated that Fgf have several functions in early cardiogenesis (Parlow et al., 1991; Sugi et al., 1993), such as, the loss of function of *Fgf2* causes loss of cardiac precursor proliferation (Sugi et al., 1995; Sugi et al., 1993). On the other hand, *Fgf2* gain of function induce cardiac actin (Sugi and Lough, 1995). Ectopic delivery of *Fgf8*, that is expressed in the endoderm adjacent to precardiac mesoderm, promotes lateral expansion of the heart field and ectopic expression of *Nkx2.5* and *Mef2c*, but not *Gata4* (Alsan and Schultheiss, 2002). Fgf and Bmp signaling have an interesting relationship in the development of the SHF, such as, the role of *Bmp4* in the differentiation of cardiac precursors and at the same time inhibits Fgf (like Fgf8), keeping the cardiac precursor cells in a proliferative undifferentiated state (Tirosh-Finkel et al., 2010).

1.4.1.5 Notch

Notch signaling (Figure 1.12F) has been shown to be involved in a wide range of developmental processes, such as, cell fate decisions, cellular development, differentiation, proliferation, apoptosis, adhesion and epithelial-to-mesenchymal transition (Miazga and McLaughlin, 2009; Watanabe et al., 2006). The Notch encodes for a transmembrane protein receptor (Notch 1 to 4), that functions at the cell surface to bind transmembrane ligands (Delta 1 to 4 or Jagged 1 and 2) on adjacent cells (Bray, 2006). Upon ligand binding, a series of proteolytic cleavages (y-secretase complex and a disintegrin and metalloproteinase) releases the intracellular domain of Notch (NICD) allowing for translocation of the NICD into the nucleus. This cleavage product mediates the function of Notch in the nucleus by interacting with CSL proteins (CBF1/recombination signal binding protein for immunoglobulin kappa J region [Rbpj], suppressor of hairless, Lag1) to activate downstream target genes (Bray, 2006). The primary downstream effectors of Notch signaling have been identified as members of the Hairy/Enhancer of split and Hey families of repressive basic helix–loop–helix transcription factors that are important to chamber specification and demarcating

the AV canal from surrounding myocardium (Davis and Turner, 2001; Iso et al., 2003; Niessen and Karsan, 2008). Since the NICD interacts with Smad and Dvl proteins, there is also a crosstalk with the TGF and Wnt cascades (Blokzijl et al., 2003). In the chick embryo, experiments demonstrated that Notch while blocks cardiac muscle differentiation, it enhances the expression of conduction system markers (Chau et al., 2006). Notch signal pathway plays a key role in the processes of AV canal, myocardial and OFT development and regulation of endothelial-mesenchymal transition during heart valves formation (Niessen and Karsan, 2008; Rutenberg et al., 2006).

1.4.2 Regulation of Second Heart Field

The SHF, that is located at caudal pharyngeal region, contains undifferentiated and highly proliferative cell population that can give rise to myocardial, endocardial and smooth muscle cells (Laugwitz et al., 2005; Moretti et al., 2006), which is regulated by a complex network of intercellular signals. These signals control and are controlled by transcription factors in the pharyngeal mesoderm and adjacent cells types, like neural crest-derived cells (Figure 1.13) (Dyer and Kirby, 2009; Vincent and Buckingham, 2010). The SHF is characterized by the expression of transcription factors *Islet-1* and *Tbx1* and the growth factors *Fgf8* and *Fgf10* (Cai et al., 2003; Ilagan et al., 2006; Kelly et al., 2001; Xu et al., 2004).

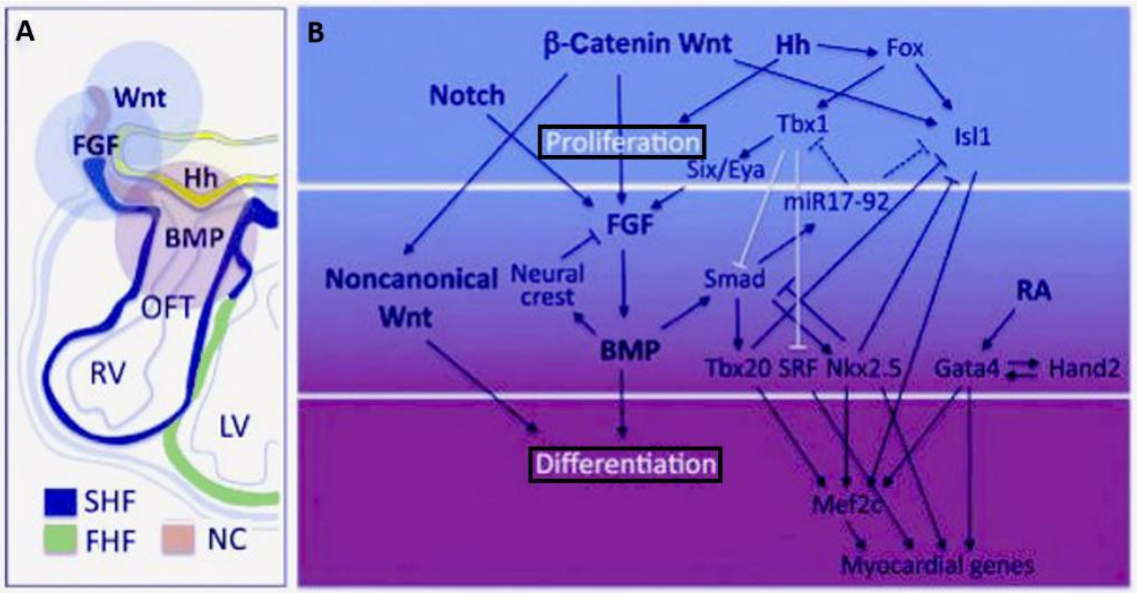

Figure 1.13 – Signaling pathways regulating the second heart field.
(A) Signaling at the arterial pole of the heart tube displaying zones of Wnt, FGF, Hedgehog (Hh), and BMP. **(B)** Schematic network representation of the major signaling pathways and regulatory genes involved in SHF development during the transition from proliferating progenitor cell (top) to differentiated cardiomyocyte (bottom). Isl1 and Tbx1 have a central position in controlling the proliferative progenitor cell state (top), FGF/BMP antagonism with a pivotal position in regulating the balance between proliferation and differentiation (middle), and the activation of the cardiomyogenic program by a network of interacting transcription factors (bottom). Gray lines, direct protein interactions; dotted lines, microRNA silencing. LV, left ventricle; RV, right ventricle; OFT, outflow tract; SHF, second heart field; NC, neural crest-derived cells (Adapted from(Kelly, 2012).

1.4.2.1 Regulation of proliferation in Second Heart Field

The activation of the cardiac transcriptional program in the cardiogenic mesoderm (anterior lateral splanchnic mesoderm) is regulated by signals from adjacent tissues, including Wnt, Fgf and Bmp signals (Figure 1.14) (Evans et al., 2010). Progressive control of mesodermal precursor cells to a myocardial fate begins with the induction of *Mesp1* in the anterior mesoderm precursor cells, followed by activation of cardiac transcription factors and epigenetic regulators, including *Isl1*, *Tbx5*, *Nkx2-5*, *Mef2c*, *Gata4* and *Baf60c* that together drive cardiomyogenesis (Miquerol and Kelly, 2013). As the linear heart tube form, SHF cells (expressing *Isl1*) in medial splanchnic mesoderm remain in contact with the pharyngeal endoderm and their continued proliferation, delayed differentiation and contribution to growth of the myocardium is regulated by canonical Wnt, Fgf and

Hedgehog signalling pathways (Figure 1.13) (Cai et al., 2003). During heart development the SHF cells contributes to the elongation of the heart tube through the dorsal mesocardium. After its rupture and consequent dorsal closure of the heart tube, cardiac precursors cells in pharyngeal mesoderm are isolated in a highly proliferation region (dorsal pericardial wall) contributing to the heart tube extension by addition at both poles (van den Berg et al., 2009). In the chick embryo, the proliferative center is localized caudally in the dorsal pericardial wall, moving from this region towards the poles of the heart tube at a high rate (van den Berg et al., 2009). As cells differentiate at the poles of the heart tube, cell proliferation dramatically drop, to be restarted during the development of the cardiac chamber (de Boer et al., 2012).

In the dorsal pericardial wall, the proliferation of the cardiac precursors appears to be controlled by Fgf signaling (Figure 1.14), namely *Fgf3*, *8* and *10*, which are expressed in the pharyngeal mesoderm and adjacent pharyngeal epithelia. *Fgf8*, within pharyngeal mesoderm, appears to be the main controller of heart tube extension with important contributions from *Fgf10* and *Fgf3* revealed by analysis of mutant embryos (Park et al., 2008; Urness et al., 2011; Watanabe et al., 2010). These Fgfs, expressed in the pharyngeal region, are regulated by Wnt/β-catenin and Notch signaling (Cohen et al., 2007; Klaus et al., 2012). The conditional loss-of-function analysis of these signaling pathways in the SHF results in OFT defects leading to subsequent arterial pole septation defects (Klaus et al., 2012; Park et al., 2008). Additionally, the migration of neural crest cells into the caudal pharyngeal regions regulates local Fgf signaling and leads to a reduction in cell proliferation in the SHF, acting as a proliferative brake during the terminal stages of heart tube extension (OFT septation) (Hutson et al., 2006). Recently it was shown, that canonical Wnt signaling (β-catenin) operate downstream of Notch in the regulation of cardiac precursors cell differentiation and OFT morphogenesis (Klaus et al., 2012). Hedgehog (Hh), expressed in the pharyngeal endoderm, is required for maximal proliferation in the SHF and to maintain progenitor cell properties of SHF cells in the dorsal pericardial wall (Dyer and Kirby, 2009). In addition, Hh signaling has been shown to control progenitor cell proliferation in the posterior SHF via the transcription factor *Tbx5*, in a pathway vital for atrial septation (Xie et al., 2012).

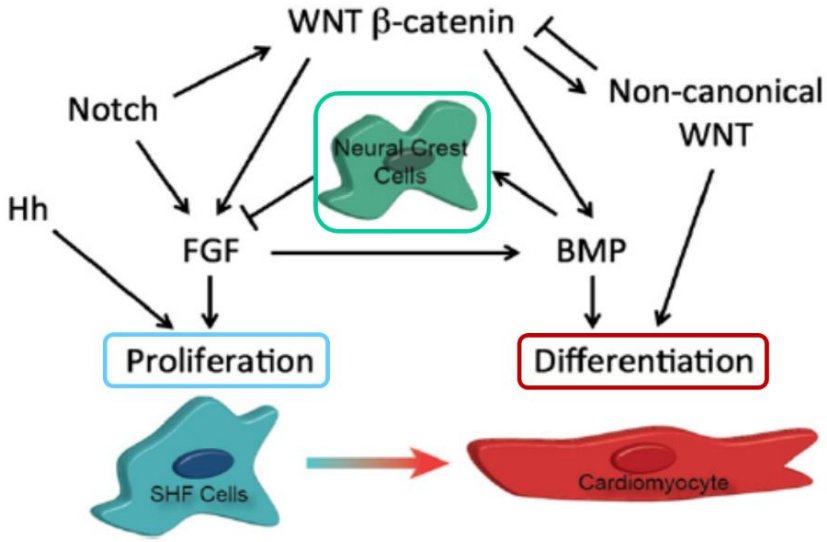

Figure 1.14 – Second heart field major signaling pathways.
Image shows the major signaling pathways known to control proliferation and progressive differentiation of second heart field cardiac progenitor cells in the early embryo (Adapted from(Rochais et al., 2009b).

In all animal models, LIM homeodomain transcription factor *Islet-1* (Figure 1.13) marks proliferating undifferentiated cardiac precursors. *Islet-1* is essential for proliferation and survival of the SHF progenitors, and might be required for their migration into the heart (Cai et al., 2003), indeed, analysis of *Islet-1* mutants demonstrated defects in the arterial and venous poles of the heart tube (Park et al., 2006). Initial expression of *Islet-1* is dependent of Wnt/β-catenin and Fgf signaling, both of which are required for proliferation of early cardiac precursors (Cohen et al., 2007). β-catenin can directly activate transcription from *Islet-1* and *Fgf10* promoters and when canonical Wnt signaling is increased *Islet-1* positive cells shows up-regulation of Fgf, promoting proliferation (Kwon et al., 2009). Moreover, *Islet-1* controls the T-box transcription factor 1 (*Tbx1*) (Figure 1.13), that regulates Fgf signaling (Cai et al., 2003; Vitelli et al., 2002). Loss of *Tbx1* in mouse embryos demonstrated a reduction of cardiac progenitor cells proliferation resulting in a hypoplastic dorsal pericardial wall and in a short narrow OFT (Zhang et al., 2006). This transcription factor is the major candidate gene for DiGeorge syndrome in man, associated with craniofacial and cardiovascular anomalies including OFT congenital heart defects (Baldini, 2005).

Hes1, a target gene of the Notch signalling pathway, is present in the dorsal pericardial wall and is required for proper cardiac precursors cells proliferation, preventing precocious differentiation (Rochais et al., 2009a). In SHF development proliferation is a crucial regulatory step, however cell survival also as an important role in the SHF that was demonstrated with the transcription factor *Hand2* (Tsuchihashi et al., 2011).

1.4.2.2 Control of gradual differentiation during heart tube elongation

The transition from proliferative cardiac precursors to differentiated cardiomyocytes requires both downregulation of expansion pathways and upregulation of differentiation pathways (Figure 1.14). The SHF cells during heart tube elongation migrates to the ventral region of the embryo and as these cells approach both poles of the heart tube, they are exposed to Bmp and noncanonical Wnt signals that drive differentiation and at the same time cell proliferation decreases (Figure 1.13 and Figure 1.14). Thus, the balance and transition between undifferentiated cardiac precursors to differentiated cardiomyocytes is important to regulate the gradual addition of SHF cells to the heart tube. At the distal OFT (arterial pole) the differentiation is regulated by Bmp signaling, antagonizing Fgf signals through neural crest-derived cells (*Msx1* or *Msx2*) promoting cardiac differentiation (Figure 1.14) (Hutson et al., 2010; Tirosh-Finkel et al., 2010). Indeed, the balance between these pathways is influenced by neural crest cell influx into the pharyngeal region, playing a crucial role in slowing the proliferative effect of Fgf in the SHF region (Hutson et al., 2006). Furthermore, Bmp signaling is capable of the activation of transcription microRNAs that targets SHF regulatory genes, like *Islet-1* and *Tbx1* (Wang et al., 2010). When cardiac progenitor cells are near to the heart tube, they initiate expression of genes encoding crucial cardiac transcription factors, such as *Nkx2.5*, *Tbx20*, *Mef2c*, *Gata4* and *Hand2*, that are required to activate the cardiac tissue formation (Waldo et al., 2001). Specification of cardiac precursor cells in pharyngeal mesoderm is increased after *Nkx2.5* ablation through upregulation of Jarid2 and Bmp ligand gene expression (Barth et al., 2010). On the other hand,

Nkx2.5 is capable of repressing *Bmp2* activated Smad1 signaling to inhibit differentiation (Prall et al., 2007).

In embryos lacking *Tbx2* and *Tbx3*, the Bmp signal is downregulated resulting in increased Fgf signaling proximal to the OFT (Mesbah et al., 2012). In addition, Tbx1, 2 and 3 regulates positively the proliferation and negatively the differentiation in the caudal pharyngeal region maintaining the cardiac progenitor cells homeostasis in the SHF. It can inhibit BMP signaling by direct binding to the mediator Smad1 and suppressing BMP4/Smad1 pathway. While, in *Tbx1* knockout mice occurs premature differentiation of the SHF progenitors due to abnormal induction of differentiation, in gain of function approaches it leads to reduction of differentiation in the OFT (Chen et al., 2009; Liao et al., 2008). Moreover, *Tbx1* has been shown to interact with *Mef2c* and serum response factor, thus preventing cardiomyocyte differentiation (Chen et al., 2009; Pane et al., 2012). Therefore, loss of function of any two of these three genes results in severely altered Bmp and Fgf signaling, pharyngeal hypoplasia and heart tube expansion defects (Mesbah et al., 2012). Different from *Tbx1*, *Islet-1* seems to be maintained in the distal part of the OFT and through Mef2c it contributes to cardiac progenitor differentiation (Dodou et al., 2004).

Studies in which β-catenin was constitutively activated in cardiac progenitors, caused lack of differentiation to myocardial cells. Loss of Wnt signaling reduces the number of *Islet-1* expressing cells, causing OFT and right ventricle defects, while overexpression of Wnt signaling expands *Islet-1* positive population (Cohen et al., 2007). Therefore, the canonical Wnt/β-catenin signaling inhibits cardiac induction, promoting proliferation and sustaining the SHF in an undifferentiated state. Its repression is essential for myocardial differentiation, which induces both Bmp and noncanonical Wnt (*Wnt11* and *Wnt5a*) expression in the SHF region (Cohen et al., 2012; Klaus et al., 2007).

1.4.2.3 Patterning of cardiac precursor cells in the dorsal pericardial wall

In the dorsal pericardial wall the cardiac precursors are regulated by complex interactions of signals, which promotes proliferation and gradually regulates differentiation (Figure 1.14). During heart tube elongation the SHF cells become patterned, being distinguished in two populations of cells, the anterior SHF adjacent to the arterial pole and the posterior SHF adjacent to the venous pole, in which they are responsible for the formation of the right ventricular, OFT and atrial myocytes. Among the genetic markers that distinguish these populations of precursor cells and provide the information of anterior-posterior patterning in the pharyngeal mesoderm, are the *Fgf10* and a *Mef2c* expressed in the anterior SHF, and *Tbx5* and *Osr1* present in the posterior SHF (Kelly, 2012). *Hox* genes are key controllers of anterior–posterior information in the developing embryo, contributing to the atrial myocardium, inferior wall of the OFT and to the myocardium at the base of the outlet of the right ventricle (sub-pulmonary myocardium) (Bertrand et al., 2011). Moreover, the future subpulmonary myocardium appears to be mainly dependent on *Tbx1* function, which is known to have contributions to the inferior wall of the developing OFT (Théveniau-Ruissy et al., 2008). Interestingly, in the *Tbx1* null embryos, the failure of subpulmonary myocardial development is associated with abnormal expression of *Fgf10* transgene in myocardium at the venous pole of the heart (Kelly and Papaioannou, 2007). This suggests that *Tbx1* plays a role not only in regulating proliferation and differentiation delay, but also in patterning of cardiac precursors cells in the dorsal pericardial wall.

1.5 Aim of this thesis

Previously in our lab, a differential screening to search for novel genes differentially expressed in the heart/hemangioblast precursor cells of chick embryos was performed. From this screening, several genes were identified. Among others, Collagen and calcium-binding EGF-like domain 1 (c*Ccbe1)*, a novel protein containing signal peptide for secretion, collagen domains and a calcium binding EGF-like domain, was found to be upregulated in the cardiac progenitors in comparison to the embryonic control cells. The overall aim of this thesis is to study and characterize the role of c*Ccbe1* during early heart development in the chick.

In particular, the specific aims of this thesis are:

First, to generate a fine and detailed characterization of the expression pattern of c*Ccbe1* during early heart development, employing double whole-mount *in situ* hybridization with well-known cardiac markers and histology techniques to determine in which structures this gene might be playing a role.

Second, by employing overexpression and knockdown approaches, to address the functional role of c*Ccbe1* in chick early heart development.

CHAPTER 2 – MATERIALS AND METHODS

2.1 Chick embryo collection and culture

Fertilized chicken eggs (Sociedade Agrícola Quinta da Freiria, SA, Torres Vedras, Portugal) were incubated for 1-3 days maintained at 38 °C in a humidified incubator. Embryos were staged according to Hamburger and Hamilton (Hamburger and Hamilton, 1951) (Appendix 1). For the culture, embryos were explanted at HH3^{+}/HH4 together with the vitelline membrane and anchored to a metacrilate ring following the protocol of New (New, 1955).

2.2 Embryo dissection and fixation

Fertilized chick eggs were removed from the incubator after the suitable time of incubation, in order to obtain the appropriated developmental stages, and broken into a sterile petri dish. Embryos were dissected (suitable and sterilized surgery material) from the egg and placed in ice-cold RNase-free phosphate buffer saline (PBS 1X plus diethyl pyrocarbonate (DEPC) treated water) for further manipulations. Extraembryonic membranes were removed and for embryos older than stage 12, a small hole was placed in the head and heart with a glass-pulled pipette. Embryos were fixed overnight at 4ºC in 4% paraformaldehyde (4%PFA plus PBS1X DEPC), in order to preserve all the embryo structures and to reduce RNA degradation, and dehydrated the following day. Following removal of the fixative from the embryos, two 5 min washes were carried out with ice-cold PBT (PBS 1X + 0.1% Tween-20). The embryos were then dehydrated for 10 min in each of 25% methanol (in PBT), 50% methanol (in PBT), 75% methanol (in PBT) and twice in 100% methanol and subsequently stored at –20°C until required. The embryos must be stored in 100% methanol to prevent the formation of water crystals, in order to protect the integrity of the cells (List of solutions and their composition in appendix 2).

2.3 Synthesis of antisense mRNA probe

The chick Ccbe1 (1191-bp) was generated by RT-PCR cloning (clone was obtained from the BBSRC chick EST database: ChEST963b3 for cCcbe1; seq. identifier 603865952F1).

In order to study a particular gene it is necessary to generate a probe that will mark its domains of expression, meaning, an antisense RNA strand for the mRNA of interest must be synthesized and the following steps must be taken.

2.3.1 Transforming of competent E. coli cells

To generate the probes used in whole-mount *in situ* hybridization (WISH), chemically competent *Escherichia coli* cells were transformed with a plasmid that contains the coding sequence of the gene of interest. The transforming DNA was added (no more than 50ng in a volume of 10µl or less) to 100µl of competent cells (DH5α Max efficiency) in a polypropylene tube, under a flame of a Bunsen burner. The tube was swirl gently in order to mix their content, and stored on ice for 20 min. The tube was placed in a preheated 37ºC water bath for 60 seconds, without shaking, and rapidly transferred to an ice bath, allowing the cells to cool for 2 min. After this period, 400µl of Luria Broth (LB) medium was added and the tube was transferred to a shaking incubator at 37ºC for 45 min to allow the bacteria to recover and to express the antibiotic resistance marker encoded by the plasmid. Appropriated volume (up to 200µl per 90-nm plate) of the transformed competent cells was transferred onto an agar plate with ampicillin. The plate was stored at room temperature until the liquid has been absorbed, and then inverted and incubated at 37ºC for 12-16 hours.

2.3.2 Plasmid amplification

Individual bacterial colonies were inoculated into 3ml of LB media containing the appropriate selective antibiotic (100µg/ml of ampicillin). The tube containing the

suspension of cells with the plasmid of interest was incubated at 37ºC in a shaking incubator overnight (225rpm).

2.3.3 Plasmid DNA Isolation

Plasmid DNA extraction was carried out using a miniprep kit (QIAprep Spin miniprep kit, Qiagen), according to the protocol provided by the manufacturer: 1.5ml of cell suspension was pelleted by centrifuging 1 min at 9000 rpm in a microcentrifuge and the supernatant discarded; then 250µl of a resuspension buffer (Solution I)) was added and the tube vortexed until the cells were in suspension, then another 250µl of lyses buffer (Solution II) was added and the tube mixed thoroughly by inverting several times, to obtain a clear lysate. The cells were left incubating up to 5 min in this buffer. In order to stop the lyses reaction, 350µl of neutralization buffer (Solution III) was added and the tube was gently mixed by inverting several times until a flocculent white precipitate forms. The tube was centrifuged for 10 min at maximum speed (13000rpm) and a compact white pellet was observed. Then the supernatant, by pipetting, were transferred to the QIAprep spin column, following centrifugation for 60s and the discard of the flow-through. The QIAprep spin column was washed by adding 500µl of washing buffer I (HB) and centrifuging for 60s. The flow-through was discarded and 700µl of washing buffer II was added to the column, and was centrifuged for an additional 1 min to remove the residual wash buffer. To elute the DNA, the column was placed in a clean 1.5ml microcentrifuge tube and 50 µl to 100µl of elution buffer (EB) (10mM Tris-HCl, pH 8.5) was added to each QIAprep spin column, let stand for 1 min, centrifuged for another 1 min and after that the DNA was collected.

2.3.4 Plasmid Linearization and Purification

In order to make antisense probes it‘s necessary to use restriction enzymes and RNA polymerases to synthesized antisense RNA probes for the genes of interest,

namely, c*Ccbe1*, *Nkx2.5*, *Tbx-5*, *Mhc* and *Islet-1* (Table 1). The reaction mixture was prepared in a 1.5ml microtube: 10µl (2µg) of plasmid DNA was digested using the appropriated restriction enzyme, the adequate volume of the supplied reaction buffer (Roche) and sterile deionized water to a total volume of 30µl; and then was incubated at 37ºC for 3h or overnight. The digestion product was checked on a 1% agarose gel (SeaKem LE Agarose), using 1/30 of the digestion reaction volume, to confirm the completion of the digestion.

Table 2.1 – List of restriction enzymes and RNA polymerases used for antisense RNA probe preparation

Clone	Restriction enzyme	RNA polymerase
cCcbe1 **(in pGem-TEasy)**	NcoI	SP6
Tbx5 **(in pBlueScriptIIKS(+/-))**	XbaI	T7
Nkx2.5 **(in pGem-TEasy)**	NcoI	SP6
Islet-1 **(in pBlueScriptIIKS(+/-))**	NotI	T7
Mhc **(in pBlueScriptIIKS(+/-))**	NdeI	T7

The linearized DNA was purified using spin columns from the QIAprep Spin Miniprep Kit. To do this, 5x the volume of the digestion reaction mixture volume (30µl) was added with washing buffer I (150µl), thoroughly mixed, transferred to the column and centrifuged for 1min at maximum speed (13000rpm). The flow-through was discarded; the spin column was washed with 700µl of ETOH buffer (buffer II) and centrifuged at maximum speed for 1min. Again, the flow-through was discarded and the spin column centrifuged at maximum speed (13000rpm) for 1min, to get rid of residual ethanol from buffer II. The column was placed into a clean 1.5ml microcentrifuge tube; the nuclease-free water (Promega) was added to the center of the QIAquick membrane for 5 min, to elute the DNA, and then centrifuged for 1 min at maximum speed. The spin column was discarded and the linearized DNA in the microtube was now purified.

2.3.5 Antisense RNA probe synthesis by *in vitro* transcription

The RNA probes were generate by *in vitro* transcription from a linearized DNA template using the appropriated SP6 or T7 (Roche) RNA polymerase, which synthesizes RNA complementary to the DNA template. Transcription reaction components were added in the following order to a 1.5ml RNase-free tube at room temperature: nuclease-free water up to a final of 20µl, 10µl linearized and purified DNA template, 2µl 10X transcription buffer (Roche), 2µl 10X DIG (Roche) or 2µl Fluo (Roche) RNA labelling mix, 1µl of RNase inhibitor (RNAsin; Promega) and 1µl of T7 or SP6 RNA polymerase. The reaction mix was then incubated at 37°C for 2 h.

2.3.6 Antisense RNA probe purification

Mini Quick Spin RNA columns were used to remove unincorporated nucleotides from the prepared labelled RNA. During centrifugation mini Quick spin columns allow larger molecules (DNA, RNA or oligonucleotides) to pass through quickly, while retaining smaller molecules (such as unincorporated oligonucleotides). The matrix of the mini Quick Spin RNA columns (Roche) was initially resuspended in the buffer by gentle inverting. The top cap of the column was removed, the bottom tip snapped off and it was placed in a sterile microcentrifuge tube. To pack the column matrix and remove residual buffer the column was centrifuged (at 4ºC) for 1min at 1000g. The antisense RNA probe was then applied to the center of the column bed, followed by the centrifugation (at 4ºC) of the column for 4 min at 1000g, the sample was collected in a microcentrifuge tube and stored at -20ºC.

2.3.7 Agarose gel electrophoresis of DNA

Electrophoreses through agarose gels is commonly used for separating and analyzing DNA, since the DNA fragments are separated according to the molecular weight. This technique was used to check the completion of a

restriction enzyme digestion or to determine the yield of the plasmid DNA purification.

DNA size determination and semi-quantification were achieved by agarose gel electrophoresis. The size of the DNA fragment to be resolved determined the percentage of agarose in the gel. Gels ranging from 1% to 2% (w/v) agarose were routinely used. Agarose gels were prepared by adding an appropriate amount of DNA grade agarose to 1x TAE (40mM Tris.acetate, 2mM EDTA pH8) buffer and boiling until dissolved. Upon cooling to approximately 50°C, Ethidium bromide (EtBr) was added to a final concentration of 0.05%. The agarose solution was then poured into a suitable mold to set and following this, placed in an electrophoresis apparatus with 1x TAE running buffer. DNA samples were mixed with Orange G loading buffer (15% Ficoll, 0.2% Orange G) and then loaded alongside a 1 kb Plus DNA ladder (Invitrogen). The DNA was electrophoresed at 90-120V. The EtBr is a fluorescent dye that intercalates between the bases of the DNA, allowing the gel to be visualized by ultraviolet (UV) illumination. The gel was then observed with a UVP® white/UV transilluminator (AGP Technologies), Gene Flash BioImaging System

2.4 Morpholinos and DNA constructs

The pCAGGS-GFP vector (Momose et al., 1999), carrying the cDNA of the green fluorescence protein under the control of the CAGGS promoter, was used to control the extent and efficiency of electroporation. Chick Ccbe1 overexpression plasmids were based on a modified pCAGGS-MCS-IRES-GFP vector (gift from I. Palmeirin, CBME, UALG). The coding sequence of c*Ccbe1* was amplified by PCR. The c*Ccbe1* coding sequence was isolated by reverse transcriptase (RT)-PCR according to the published sequence (GeneBank accession no. XM_001233357) and subcloned into the *EcoRI* site of pCAGGS-MCS-IRES-GFP. Fluorescein-tagged antisense morpholinos oligonucleotides cCcbe1MO: 5'-CGCGGCTCTGCGCTCACCTGAAGCA-3' and CoMO: 5'-CCTCTTACCTCAGTTACAATTTATA-3' were designed and produced by Gene Tools.

2.5 Early chick embryo electroporation

Embryos were microinjected and electroporated as described previously (Tavares et al., 2007) at HH3^{+}/HH4 stage with DNA solution (0.5–3 mg/ml; 0.1% Fast Green; Sigma) in the region fated to form the heart. For the knockdown experiments, control morpholino (CoMO) or cCcbe1 morpholino (cCcbe1 MO) (Gene Tools LLC) were electroporated. For the gain-of-function experiments the control (pCAGGS-IRES-GFP) or cCcbe1 overexpression (pCAGGS-cCcbe1-IRES-GFP) vectors were electroporated. The embryos were then incubated at 38 °C for the appropriate period of time (10–30 h), at end of the cultured fixed with 4% paraformaldehyde (PFA) and processed for WISH and immunofluorescence. The embryos were observed under a fluorescence stereomicroscope (Leica MZ16FA).

2.6 Whole-mount *in situ* hybridization

It's a technique that allows specific nucleic acid sequences (mRNAs) to be detected and studied their expression patterns in embryonic tissues or sections. The constant improvements in the protocol allow us to detect and visualize two, or even three, mRNAs in the same embryo. This allows a finer characterization of the spatial and temporal relationships between the expressions of genes, even to the level of being able to show simultaneous expression of two genes within one cell. In this study, WISH was carried out in order to detect mRNA transcripts within wild-type chick embryos.

2.6.1 Embryo pre-treatments

Embryos were rehydrated by washing through the methanol series in reverse, 100% - 75% - 50% - 25% (for periods of 5 to 10 min). Embryos were washed two times for 5 min in PBT and then incubated (in the dark) in a solution of 6% hydrogen peroxide in PBT during 1 h at room temperature. After this, embryos

were washed three times for 5 min in PBT and then treated with 10µg/ml proteinase K (Roche) in PBT at room temperature and the period of treatment depended on the HH developmental stage of the chick embryo (Table 2). After that, the embryos were washed for 5min in a freshly prepared glycine solution (2mg/ml in PBT), subsequently two washes were performed with PBT and refixed with 0.2% glutaraldehyde/4% paraformaldehyde in PBT for 20 min. Embryos were then washed twice in PBT for 5 min.

Table 2.2 – Embryo's Proteinase K time.

Embryonic stage	Proteinase K time (minutes)
HH3 – 5	1'
HH6 - 8	6'
HH9 - 12	10'
HH13 - 16	12'
HH17 - 20	15'
HH21 - 27	20'

2.6.2 Hybridization

Hybridization comprises two steps. First the embryos (on vials) must be incubated in 1ml prehybridization solution (Appendix 2) for 3 hours at 70ºC, period in which the solution can penetrate into the cells and the optimal temperature to the hybridization is achieved. Then the hybridization buffer was removed and new hybridization buffer with the previously prepared antisense RNA probe was added. Then it was performed overnight at 70ºC.

2.6.3 Antibody incubation

After the hybridization steps, the solution was removed and replaced with solution I (pre-heated to 70ºC) (Appendix 2) and incubated at 70ºC for 1 h (this step was performed twice). Subsequently the solution I, was removed and replaced with solution III (pre-heated to 70ºC) (Appendix 2) and incubated at 65ºC for 30 min

(this step was performed twice). Afterwards, the embryos were rinsed 2 times with MABT solution (Appendix 2) for 5 minutes each, at room temperature with rocking. In order to block unspecific antibody binding sites, the embryos were incubated with blocking solution (MABT/10% Sheep Serum/2% Blocking Reagent) for 2 to 3 h at room temperature in a rocker. The previously solution was removed and replaced by the same solution but containing a dilution 1/2000 of anti-DIG-AP antibody (anti-Digoxigenin Fab fragments antibody, AP conjugated, Roche) or 1/4000 anti-Fluo-AP antibody (anti-Fluorescein Fab fragments antibody, AP conjugated, Roche) being incubated overnight at 4ºC with smooth agitation.

2.6.4 Immunological detection

The antibody solution was removed and the embryos were washed in MABT three times for 5 min and three times for 1 h at room temperature. The embryos were then washed with NTMT solution (Appendix 2) three times for 10 min. The detection buffer contains a precipitating substrate of alkaline phosphatase (AP), is added to the embryos which by the previous treatments, have antibodies attached with this enzyme in the place where the antisense RNA probe is connected to the mRNA of the gene, which provides where the gene of interest is being expressed. So, the embryos were incubated in the detection buffer (BM Purple or BCIP, Roche) in the dark, at room temperature, for the appropriated time. Once achieved the desired staining, the embryos were washed with NTMT solution (it's used when it's needed to take some photographs and continue to a Double WISH) or several times in PBT in order to stop completely the reaction. Embryos were photographed, post-fixed, dehydrated and subsequently stored at -20°C.

2.6.5 Double whole-mount *in situ* hybridization

The double (two-color) WISH method is used to determine both spatial and temporal patterns of gene expression, using two genes of interest. The procedure was the same as describe above except that the embryos were hybridized with two different probes, one attached to DIG and the other attached to Fluo. Color reaction for anti-Fluo/AP substrate (BCIP) was performed and a light blue color appeared. Then the embryos were washed once with PBT for 5 min, twice with MABT for 5 min, twice with MABT for 10 min and then incubated in MABT at 70ºC for 1 h. After inactivating the AP attached to the anti-Fluo antibody in this last incubation step, the embryos were washed twice with MABT for 10 min, and incubated with blocking solution for 2 to 3 h; afterwards the blocking solution was removed and replaced by the same solution but containing anti-DIG/AP antibody being incubated overnight at 4ºC with smooth agitation. Subsequently, the immunological detection step (2.6.4) was repeated, but the detection buffer used was the BM Purple, that yields a purple staining.

All the embryos used for the whole mount *in situ* hybridization and the double WISH were photographed in PBT or NTMT using a Leica DC 200 camera coupled to a Leica MZ16FA stereomicroscope. Images were processed using Adobe Photoshop software.

2.7 Histological sections

The embryos were processed for histological analysis by sectioning after re-fixation and dehydration by methanol series. Subsequently, they were washed in isopropanol for 15 min at 65ºC, after that, the embryos were transferred to the molds and incubated with a 1:1 of isopropanol and paraffin solution during 30 min at 65ºC. The next step is embedding the embryos in paraffin by washing for 1 h at 65ºC and a second time overnight at 65ºC. The embryos were oriented, the paraffin solidified and the blocks were stored at 4ºC. The sectioning was performed using microtome Leica RM2125RT, first it's was performed a trim at 40µm to remove the excess of paraffin, and then sections at 8µm, both sagittal

and transversal sections of the embryo were collected to microscope slides (Menzel-Glaser, Superfrost), subsequently the slides with the sections of the embryos were placed in a hot chamber at 37ºC overnight, in order to the sections adhere to the slides.

After the sections, the next step is to remove the paraffin from the tissue's sections by washing twice with xylene during 15 min to remove the paraffin. The final step is to mount with DPX (mountant for histology, Fluka) and microscope cover glasses of 24x60mm and let stand them overnight.

Histological sections of the embryos were photographed using an Olympus DP11 camera attached to an optic microscope (Olympus). Images were processed using Adobe Photoshop software.

2.8 Immunohistochemistry analyses

Fixed untreated, CoMO, cCcbe1MO, pCAGGS-IRES-GFP (control) and pCAGGS-Ccbe1-IRES-GFP injected embryos were washed with PBS, dehydrated in methanol series and paraffin embedded. Serial 8 μm sections were taken (microtome Leica-RM 2135), dewaxed and rehydrated. After tissue rehydration, antigen retrieval was performed in 10 mM TrisBase/1mM EDTA solution/0.05% Tween20 pH 9.0. Immunostaining was performed using primary antibodies against avian MF20 (1:200; MF 20-c; DSHB), Phospho-Histone H3 (Ser10) (1:400; Cell Signaling), Hnk1 (1:200; 1C10; DSHB) and fluorescently coupled secondary antibodies Alexa Fluor 594 goat anti-mouse (1:800; #A11005; Molecular Probes) or Alexa Fluor 488 goat anti-rabbit (1:800; #A11008; Molecular Probes). Cell nuclei were labeled with 4', 6-diamidino-2-phenylindole (1ug/ml; DAPI; Sigma). Sections were mounted with Mowiol and analyzed with Zeiss Axioimager Z2 microscope (Carl Zeiss Group). For quantitation of the Hnk1 signal, fluorescence images of the heart region were processed using ImageJ software. The level of background fluorescence was estimated by averaging background values at four points of each image and was subtracted from the fluorescence. Then areas of fluorescence were marked manually, and

fluorescence values were calculated automatically as described elsewhere (Nakamura et al., 2012).

2.9 Western blotting

The area pellucida of four cCcbe1 MO injected embryos and respective control MO at stage HH11 embryos was microdissected and suspended in ice-cold lysis buffer consisting of 20 mM HEPES, pH 7.5, 50 mM β-glycerophosphate, 10% glycerol, 2 mM EGTA, 1% Triton X-100, 1 mM sodium vanadate, and the Complete protease inhibitor cocktail (Roche, Indianapolis, IN). The explants were homogenized on ice, centrifuged and transferred to a fresh tube. Upon quantification of the total protein concentrations by the method of Bradford, 10 µg of protein extracts from control and c*Ccbe1* knockdown embryos were loaded on a 12% SDS-PAGE polyacrilamide gel, subjected to electrophoresis and transferred to Hybond-C extra membrane (Amersham Pharmacia Biotech). Blots were probed with the antibody against Ccbe1 (Ccbe1 ab 101967; 1:500; Abcam, UK) followed by 1 hour at RT with a rabbit polyclonal secondary antibody (Dako, Denmark), developed using a chemiluminescent substrate (Pierce) and analysed using Chemidoc (Bio-Rad).

2.10 Statistical Analysis

Results were expressed as mean ± standard error of the mean (S.E.M.), and experiments were performed at least in triplicate. Significant differences were assessed by *t*-test using SigmaStat vs 3.5 software. Differences at p-value <0.05 were considered to be significant.

CHAPTER 3 – RESULTS

Expression and function of *Ccbe1* in the chick early cardiogenic regions are required for correct heart development

João Furtado [a,b], Margaret Bento [a,b], Elizabeth Correia [a,b], José Inácio [a,b] and José A. Belo [a,b,c]

[a] Regenerative Medicine Program, Departamento de Ciências Biomédicas e Medicina, Universidade do Algarve, Portugal.

[b] IBB–Institute for Biotechnology and Bioengineering, Centro de Biomedicina Molecular e Estrutural, Universidade do Algarve, Campus de Gambelas, Faro, Portugal.

[c] Faculdade de Ciências Médicas, Universidade Nova de Lisboa, Campo Mártires da Pátria 130, Lisboa, Portugal

Manuscript submitted to PLOS ONE

Author's contribution:

The majority of the experimental work was performed by J. Furtado with the exception of the generation of pCAGGS-cCcbe1-IRES-GFP vector which was generated by M. Bento; and some of the gain-of-function experiments were performed by both.

3.1 Abstract

During the course of a differential screen to identify transcripts specific for chick heart/hemangioblast precursor cells, we have identified *Ccbe1* (*Collagen and calcium-binding EGF-like domain 1*). While the importance of Ccbe1 for the development of the lymphatic system is now well demonstrated, its role in cardiac formation remained unknown. Here we shown by whole-mount *in situ* hybridization analysis that c*Ccbe1* mRNA is initially detected in early cardiac progenitors of the two bilateral cardiogenic fields (HH4) and in the cardiogenic mesoderm, and at later stages on the second heart field (HH9-18). Furthermore, we characterized the role of c*Ccbe1* during early cardiogenesis by performing gain and loss-of-function experiments. Upon morpholino-induced c*Ccbe1* knockdown, the chick embryos displayed heart malformations, which include incomplete or aberrant fusion of the heart fields. c*Ccbe1* overexpression also resulted in severe heart tube malformations, including strong *cardia bifida.* Absence of c*Ccbe1* leads to reduced levels of cardiac neural crest cells, of the conduction system marker Hnk1 and of the proliferation marker PHH3, in the early heart tube. Conversely, c*Ccbe1* overexpression leads to increased Hnk1 and PHH3 levels. Altered Hnk1 levels caused by gain and loss-of-function of c*Ccbe1*, indicates that the migration of cardiac neural crest cells is affected, leading to an incorrect development of cardiomyocytes. Altogether, our data suggest that c*Ccbe1* is required for proper proliferation and migration of the heart precursors, some aspects of terminal differentiation and in the migration of the cardiac neural crest cells.

Keywords: c*Ccbe1*, cardiogenic mesoderm, second heart field, cardiogenesis, proliferation, cardiac neural crest cells.

3.2 Introduction

The vertebrate heart develops from distinct cardiogenic pools located in separate regions and exposed to specific signals during development. These pools of cardiac progenitors are temporally segregated in the developing embryo and give rise to distinct cardiac structures (Harvey, 2002; Laugwitz et al., 2008). In the chick embryo, the cardiac precursors are located in the cardiogenic mesoderm (heart forming region) at stage HH4-5, and consist of two different populations of heart progenitors, namely the first heart field (FHF) and the second heart field (SHF). The FHF precursors clearly differentiate earlier than the precursors of the SHF, indicating differential control on loss of precursor state and timing of differentiation. Furthermore, the SHF precursors are much more sensitive to genetic perturbation than the FHF precursors (Buckingham et al., 2005). The FHF is derived from the anterior splanchnic mesoderm and contributes to the myocardial cells of the primitive heart tube, which ultimately contributes to the left ventricular region. On the other hand, the SHF lies anterior and dorsal to the linear heart tube and is derived from the pharyngeal mesoderm medial to the heart fields, which will contribute to the outflow tract region (Laugwitz et al., 2008; Vincent and Buckingham, 2010). The cells of the SHF localized in the dorsal pericardial wall become separated from the heart tube when the dorsal mesocardium breaks down, maintaining continuity with the heart only at the arterial and venous poles. The remaining structures, namely, the right ventricle, the atrioventricular canal and the atria, have contribution from both heart forming regions (HFR). Understanding the molecular control of heart organogenesis, including the characterization and functional analysis of novel genes involved in cardiogenesis, has major implications for treating congenital and adult heart diseases since specific heart lineages have been associated with particular human cardiovascular malformations.

We have recently reported a differential screening using Affimetrix GeneChip® Chicken Genome arrays aiming to identify novel genes required for the development and differentiation of the vertebrate heart and hemangioblast precursor cell lineages (Bento et al., 2011). A construct containing EGFP expression under the control of a 2.5 kb promoter fragment upstream the ATG of

chick *Cerberus* (c*Cer*; Tavares *et al*., 2007) was used to electroporate chick embryos and isolate early cardiac progenitors. The genetic profiling provided relevant data about the identity of the chick heart/hemangioblast precursors and led to the detection of more than 700 transcripts expressed in the heart forming regions (HFR), which included hundreds of uncharacterized genes enriched in the heart/hemangioblast precursors in comparison to embryonic control cells (Bento *et al*., 2011). Among the uncharacterized genes was the chick collagen and calcium-binding EGF-like domain 1 (c*Ccbe1*; gene ID: 770043), a protein containing signal peptide for secretion, collagen domains and a calcium binding EGF-like domain. The gene has 11 exons, and is localized in the *Gallus gallus* chromosome Z, oriented in the reverse strand at the genomic region between 9,158,827K - 9,247,702K. Furthermore, c*Ccbe1* encodes a predicted protein with 396 amino acids with a molecular weight of 42.9kDA, highly conserved across vertebrates. The c*Ccbe1* protein sequence is 79%, 70% and 80% identical to the mouse, zebrafish and human Ccbe1 protein, respectively.

While the importance of mouse (m)*Ccbe1* for the development of the lymphatic system is indisputable (Bos et al., 2011; Hogan et al., 2009) , its role in cardiac development remains unknown, despite the increasing evidence of a potential function in cardiogenesis. Indeed, expression analysis has shown that m*Ccbe1* is expressed in heart precursors of the FHF, SHF and proepicardium in mouse embryos from embryonic day (E)7.0 to E9.5 (Facucho-Oliveira et al., 2011). Furthermore, analyses of m*Ccbe1* heterozygous knockout embryos have shown X-Gal staining at the mesothelium of the heart at E12.5 (Bos et al., 2011). In humans, mutations in *CCBE1* are associated with Hennekam syndrome, a disorder characterized by abnormal lymphatic system development where some patients present as well congenital heart defects, including hypertrophic cardiomyopathy (Alders et al., 2009; Connell et al., 2010).

Here, we show that during early chick development c*Ccbe1* is expressed in the early cardiac progenitors that emerge from the primitive streak to form the two bilateral cardiogenic fields at HH4 and in the cardiogenic mesoderm of the FHF and SHF between HH5 to HH8. As development proceeds c*Ccbe1* localizes predominantly in the region of the SHF (HH9 to HH18). In addition, we address

the functional role of cCcbe1 in chick early heart development by employing overexpression and knockdown approaches. Through c*Ccbe1* knockdown, the embryos displayed heart abnormalities, which the phenotype included aberrant or incomplete fusion of the heart forming regions. Furthermore, c*Ccbe1* morphants embryos demonstrated reduced levels of the proliferation of cells in cardiac regions and in the Hnk1 signal in the region of the heart tube. On the other hand, c*Ccbe1* overexpression resulted in severe heart tube abnormalities, being *cardia bifida* the most common phenotype, seen in half of the treated embryos. Moreover, overexpressed-c*Ccbe1* embryos demonstrated increased proliferation of cells in cardiac regions and Hnk1 levels in the cardiac neural crest cells and heart tube region. Taken together, the gain and loss-of-function of c*Ccbe1* affects the proliferation of the cardiac cells, and the alteration in the Hnk1 levels, suggests that the migration of cardiac neural crest cells is affected, leading to an incorrect development of cardiomyocytes. These data support that c*Ccbe1* plays a crucial role during early heart development.

3.3 Results

3.3.1 c*Ccbe1* expression during early heart development

Whole-mount in situ hybridization demonstrated that c*Ccbe1* mRNA is first detected at stage HH4-4^{+} as two patches on each side of the primitive streak corresponding to the bilateral cardiogenic mesoderm (Figure 3.1A, black arrow). From stage HH5 to stage HH8, c*Ccbe1* expression expands along the lateral plate mesoderm (Figure 3.1B-E, black arrow). c*Ccbe1* is also expressed in the first somite and it can be observed since the formation of the somite at stage HH7 until HH11^{+} (Figure 3.1D-H). Transverse sections of whole mount stained embryos at stage HH6 (Figure 3.1C') revealed that c*Ccbe1* is expressed in the paraxial mesoderm (orange arrows), splanchnic lateral plate mesoderm (black arrows) and in the somatic lateral plate mesoderm (yellow arrow). At stage HH9 to HH11, c*Ccbe1* transcripts were observed near the posterior part of the heart, namely, in the sino-atrial region, splanchnic mesoderm, somatic mesoderm and

ectoderm lateral to the pharynx. The expression along the lateral plate mesoderm comprises the area between the sino-atrial region down to the level of the last formed somites (Figure 3.1F-G, black arrow). More cranially the expression is seen in the in the pericardial region: in the endoderm, in the splanchnic mesoderm, in the somatic mesoderm and in the ectoderm and mesoderm lateral to the pharynx (Figure 3.1F-G, green arrow). The pericardial region comprises the area between the sinu-atrial region and the stomodaeum. Transverse sections were performed of whole mount stained embryos at stage HH 9^{+} (F) and HH10 (G). In figure 3.1F' expression of c*Ccbe1* can be observed at the level of the somatic lateral plate mesoderm (yellow arrows) and also some expression is labelled in the endoderm (white arrow); in figure 3.1F'' the somatic and splanchnic lateral plate mesoderm (yellow arrow and black arrow) are labelled with c*Ccbe1*, and continues partially into the paraxial mesoderm (orange arrow). In addition, c*Ccbe1* expression is seen in the splanchnic mesoderm of the ventral pharyngeal mesoderm (Figure 3.1G'; black arrow), which is known to represent the SHF. At stage HH13-14, c*Ccbe1* mRNA was found in the anterior part of the embryo that surrounds the pharynx, the SHF region (red arrow; Figure 3.1I-J). At these developmental stages staining can also be observed in the most posterior part of the embryo, the tail bud (Figure 3.1I-J, black arrow). Furthermore, c*Ccbe1* is highly expressed in the region of the SHF and *conus arteriosus* (Figure 3.1K, HH16, red and orange arrow, respectively). Later on, at stage HH18 (Figure 3.1L-M), c*Ccbe1* was detected above the eye, particularly, in the region of the head vein or *vena capitis* (blue arrow), in the region of the SHF (red arrow), and around the somites (purple arrow). Sagittal section of whole mount stained embryos at stage HH18 (Figure 3.1M') confirms c*Ccbe1* expression in the region of the SHF (red arrow). Taken together, these data indicate that c*Ccbe1* is expressed in cardiogenic regions since their very early formation during avian heart development

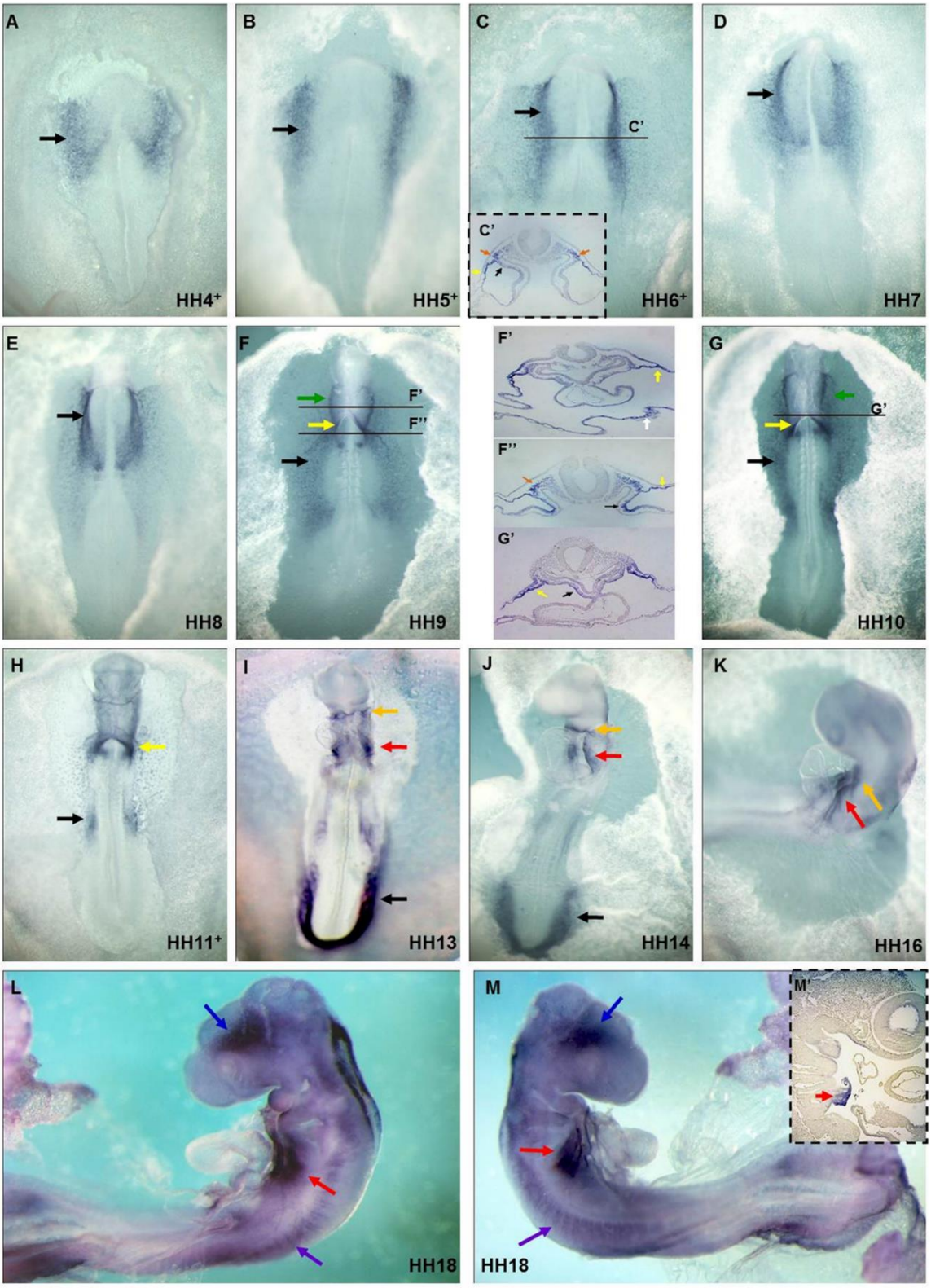

Figure 3.1 – c*Ccbe1* expression in developing chick embryos.
(A) Expression of c*Ccbe1* is present at HH4+ in the cardiogenic mesoderm (black arrow); **(B–E)** the expression is present in the anterior lateral plate mesoderm as two patches on either side of the head process (black arrows point to the heart-forming fields); **C´**: Transverse paraffin sections (8µm) of whole mount stained embryos at stage HH6, c*Ccbe1* is expressed in the paraxial mesoderm (orange arrow), splanchnic lateral plate mesoderm (black arrow) and in the somatic

lateral plate mesoderm (yellow arrow). **(F–H)** Green arrow point to the lines of expression in the lateral pharynx region; bilateral expression can be observed in the sino-atrial region (yellow arrow), and in the lateral plate mesoderm (black arrow); **(I–K)** Expression can be seen in the tail bud (black arrow); in a specific region behind the heart, known as the SHF (red arrow) and near the anterior part of the heart (orange arrow, *conus arteriosus* region); **F'-F''** and **G'**: Transverse paraffin sections (8µm) of whole mount stained embryos at stage HH9 (F) and HH10 (G) respectively (from anterior to posterior). The sections are oriented with dorsal up and ventral down. **(F')** Expression of c*Ccbe1* can be observed at the level of the somatic lateral plate mesoderm (yellow arrow) and also some expression is labelled in the endoderm (white arrow); **(F'')** Somatic and splanchnic lateral plate mesoderm (yellow arrow and black arrow) are labelled with c*Ccbe1*, and continues partially into the paraxial mesoderm (orange arrow); **(G')** c*Ccbe1* expression is seen in the somatic lateral plate mesoderm (yellow arrow) and in the splanchnic mesoderm of the ventral pharyngeal mesoderm (black arrow); **(L–M)** Lateral view of the embryo with expression above de eye (blue arrow), in the SHF region (red arrow) and also some expression is seen around the somites (purple arrow); **M'**: Sagittal paraffin section (8µm) of whole mount stained embryos at stage HH18, c*Ccbe1* is expressed in the region of the SHF (red arrow).

3.3.2 c*Ccbe1* is expressed in the second heart field

To evaluate in greater detail whether c*Ccbe1* expression is correlated with the first, second or both heart field populations, we performed double WISH for c*Ccbe1* and the cardiac markers *Nkx2.5* or *Islet-1*. The homeobox transcription factor *Nkx2.5* is one of the earliest markers of the cardiac precursor cells and in heart muscle through life (Schultheiss et al., 1995), and it is found in both FHF and SHF (Gessert and Kühl, 2010; Lints et al., 1993; Waldo et al., 2001). The LIM homeodomain transcription factor Islet-1 has become a popular molecular marker demarcating the SHF (Cai et al., 2003; Laugwitz et al., 2008).

Double WISH with c*Ccbe1* and *Nkx2.5* showed the co-localization in the cardiogenic mesoderm at stage HH7 (Figure 3.2F, black arrow), and also in the region of sino-venosus by stage HH10 (Figure 3.2H, yellow arrow). In transverse sections it is possible to observe c*Ccbe1* and *Nkx2.5* co-expressed in the cardiogenic mesoderm of the heart forming fields (F' and F''; black arrow), some co-labelling in the ventrolateral aspect of the splanchnic mesoderm (G' and G''; black arrow) and in the dorsomedially region of the splanchnic mesoderm extending towards the cranial paraxial mesoderm (G' and G''; red arrow), namely the SHF. At stage HH12 we found co-labelling in the most anterior part of the heart, the region of the *conus arteriosus* (blue arrow) and in the ventral pharyngeal mesoderm between the attachments of the cardiac outflow and inflow tracts (red arrow). However, unlike *Nkx2.5*, c*Ccbe1* expression is absent from the

heart tube (Figure 3.2I). Transverse sections showed overlapping expression of c*Ccbe1* and *Nkx2.5* in endoderm (Figure 3.2I'; black arrow), in the *conus arteriosus* (Figure 3.2I'; blue arrow) and a pale co-expression in splanchnic mesoderm (SHF region; red arrow; Figure 3.2I''). At stage HH18, the expression of both genes coincides in the SHF and in the *conus arteriosus* (Figure 3.2J; red and blue arrow). Sagittal (J') and transverse (J'' and J''') sections of double stained embryos showed that c*Ccbe1* and *Nkx2.5* are co-expressed in the SHF (red arrow).

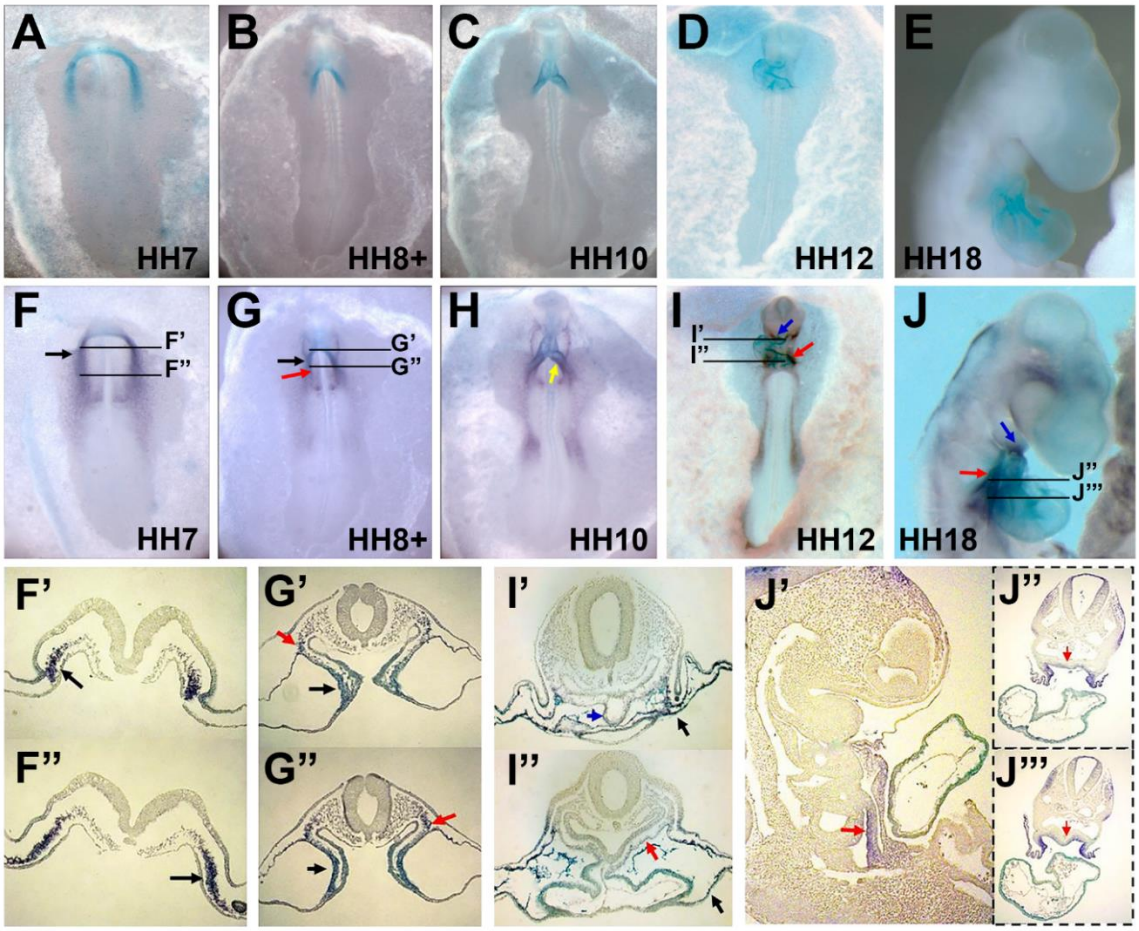

Figure 3.2 – Double WISH analysis of c*Ccbe1* and *Nkx2.5* expression.
(A-E) *Nkx2.5* expression in developing chick embryos. **(F-J)** Comparative expression of c*Ccbe1* and *Nkx2.5* during early heart development. All are ventral views (anterior to top) except for E that is lateral view. **(F-H)** c*Ccbe1* and *Nkx2.5* have overlapping patterns of expression in the heart fields (F and G; black arrow) and in the sino-venosus (H; yellow arrow); **F'** and **F'':** Transverse paraffin sections (8µm) of double stained embryos at stage HH7, c*Ccbe1* and *Nkx2.5* are co-expressed in the cardiogenic mesoderm of the heart forming fields (black arrow); **G'** and **G'':** Transverse paraffin sections (8µm) of double stained embryos at stage HH8^{+}, c*Ccbe1* and *Nkx2.5* are co-labeled in the ventrolateral aspect of the splanchnic mesoderm (black arrow) and in the dorsomedially region of the splanchnic mesoderm (red arrow). **(I)** Co-expression in the region of the *conus arteriosus* (blue arrow) and in the ventral pharyngeal mesoderm (red arrow, SHF); **I'**

and **I'':** Transverse paraffin sections (8µm) shows, an overlapping expression in the endoderm (black arrow), in the region of the *conus arteriosus* (blue arrow) and a pale co-expression in the splanchnic mesoderm (SHF; red arrow). **(J)** c*Ccbe1* and *Nkx2.5* have overlapping patterns of expression in the SHF (red arrow) and in the *conus arteriosus* region (blue arrow); **J'-J''':** Sagittal (J') and transverse (J'' and J''') paraffin sections (8µm) at stage HH18 shows c*Ccbe1* and *Nkx2.5* co-expressed in the region of the SHF (red arrow).

To confirm that *cCcbe1* is indeed expressed in the SHF region, we performed double WISH of c*Ccbe1* with the SHF marker *Islet-1*. At early stages of development, c*Ccbe1* and *Islet-1* expression overlap in the anterior lateral plate mesoderm (Figure 3.3F-G, black arrow).

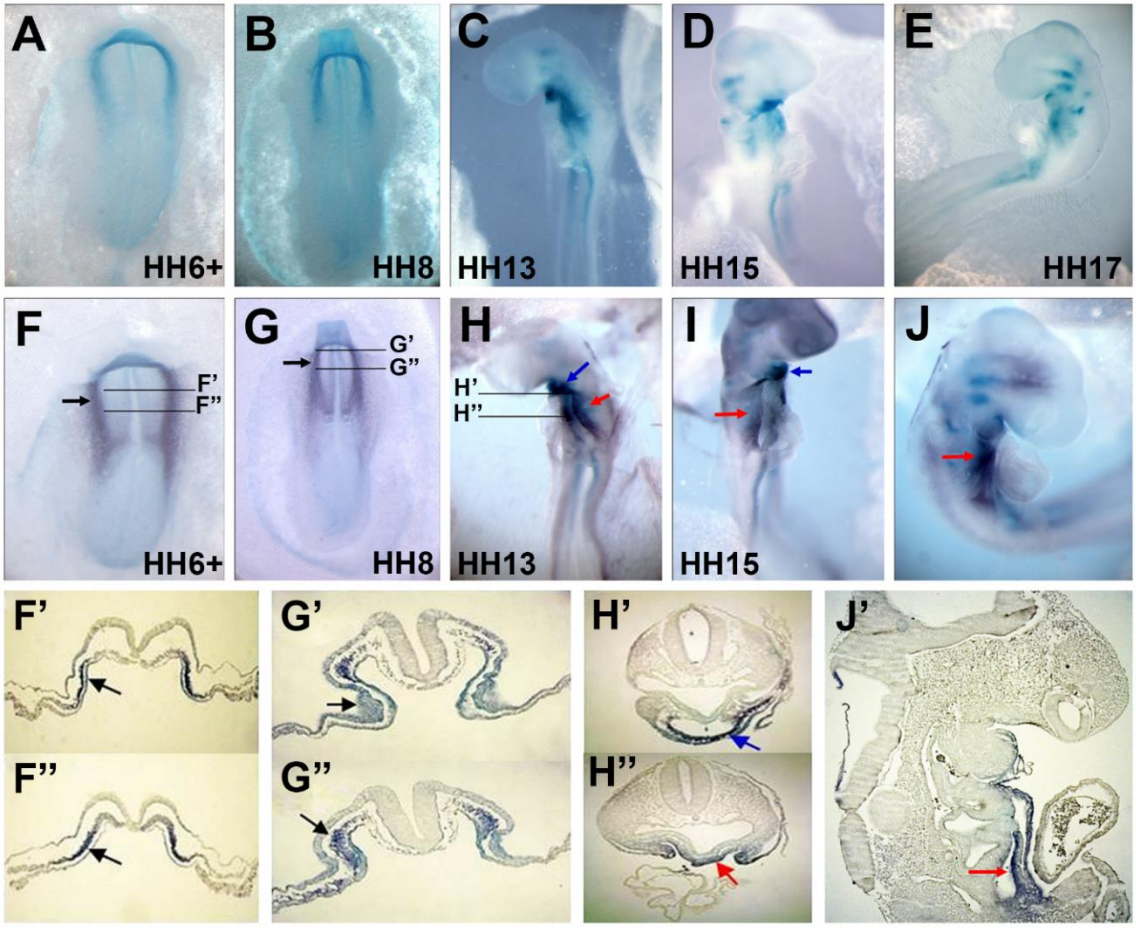

Figure 3.3 – Double WISH analysis of c*Ccbe1* and *Islet-1* expression.
(A-E) *Islet-1* expression in developing chick embryos. **(F-J)** Comparative expression of c*Ccbe1* and *Islet-1* during early heart development. A and B: ventral views (anterior to top); C-E: lateral views. **(F-G)** c*Ccbe1* and *Islet-1* have overlapping patterns of expression in the anterior lateral plate mesoderm (black arrows); **F'** and **F'':** Transverse paraffin sections (8µm) of double stained embryos at stage HH6^{+}, shows an overlapping expression in the cardiogenic mesoderm of the heart forming fields (black arrow); **G'** and **G'':** Transverse sections of double stained embryos at

stage HH8, both are co-labeled in the dorsomedially region of the splanchnic mesoderm (black arrow). (H-J) co-expression of cCcbe1 and Islet-1 is observed in the caudal part of the distal outflow tract of the heart (*conus arteriosus*, blue arrow) and in the ventral pharyngeal mesoderm (SHF; red arrow); **H'-J':** Transverse sections shows, a co-expression in the region of the *conus arteriosus* (H'; blue arrow) and in the splanchnic mesoderm of the SHF (H''; red arrow); **J':** Sagittal paraffin section (8µm) of double stained embryos at stage HH18, c*Ccbe1* and *Islet-1* are co-expressed in the region of the SHF (red arrow).

Transverse sections at stage HH6^{+} (F) and HH8 (G) showed that c*Ccbe1* and *Islet-1* are co-expressed in the cardiogenic mesoderm of the heart forming fields (F'-F'', black arrow) and in the dorsomedially region of the splanchnic mesoderm (G'-G''). Later during development they are co-expressed in the anterior part of the embryo that surrounds the pharynx, the SHF (Figure 3.3H-J; red arrow; pharyngeal mesoderm) and in the region of the *conus arteriosus* (Figure 3.3H and I, blue arrow). Transverse and sagittal sections showed that c*Ccbe1* and *Islet-1* are co-labelled in the caudal part of the distal outflow tract of the heart (H'; blue arrow; *conus arteriosus*) and in the splanchnic mesoderm of the pharyngeal floor, which corresponds to the SHF (H''-J'; red arrow). Our data, demonstrates that c*Ccbe1* expression is present early in the FHF and SHF and later is highly specific of the SHF region.

3.3.3 c*Ccbe1* knockdown leads to aberrant heart formation

To dissect the role of c*Ccbe1* during early chick development, we used morpholino technology to knockdown c*Ccbe1*. A splicing inhibitory morpholino oligonucleotide was designed (Gene Tolls, LLC) by targeting the splice donor site of E2 (cCcbe1MO). A standard morpholino was used as control (CoMO). Embryos at HH3^{+} were injected with each MOs (1mM) into the right and left sides of the primitive streak, followed by *in vivo* electroporation. Both morpholinos were fluorescein tagged at the 3' end to assess injection efficiency and stability of the morpholino over time. Furthermore, western blot analysis of injected embryos was performed to confirm that the cCcbe1 MO was causing the knockdown of c*Ccbe1* and leading to decreased amount of protein. Indeed, injection with the

morpholino cCcbe1 resulted in a reduction of cCcbe1 protein when compared with CoMO injected embryos (Figure 3.4G).

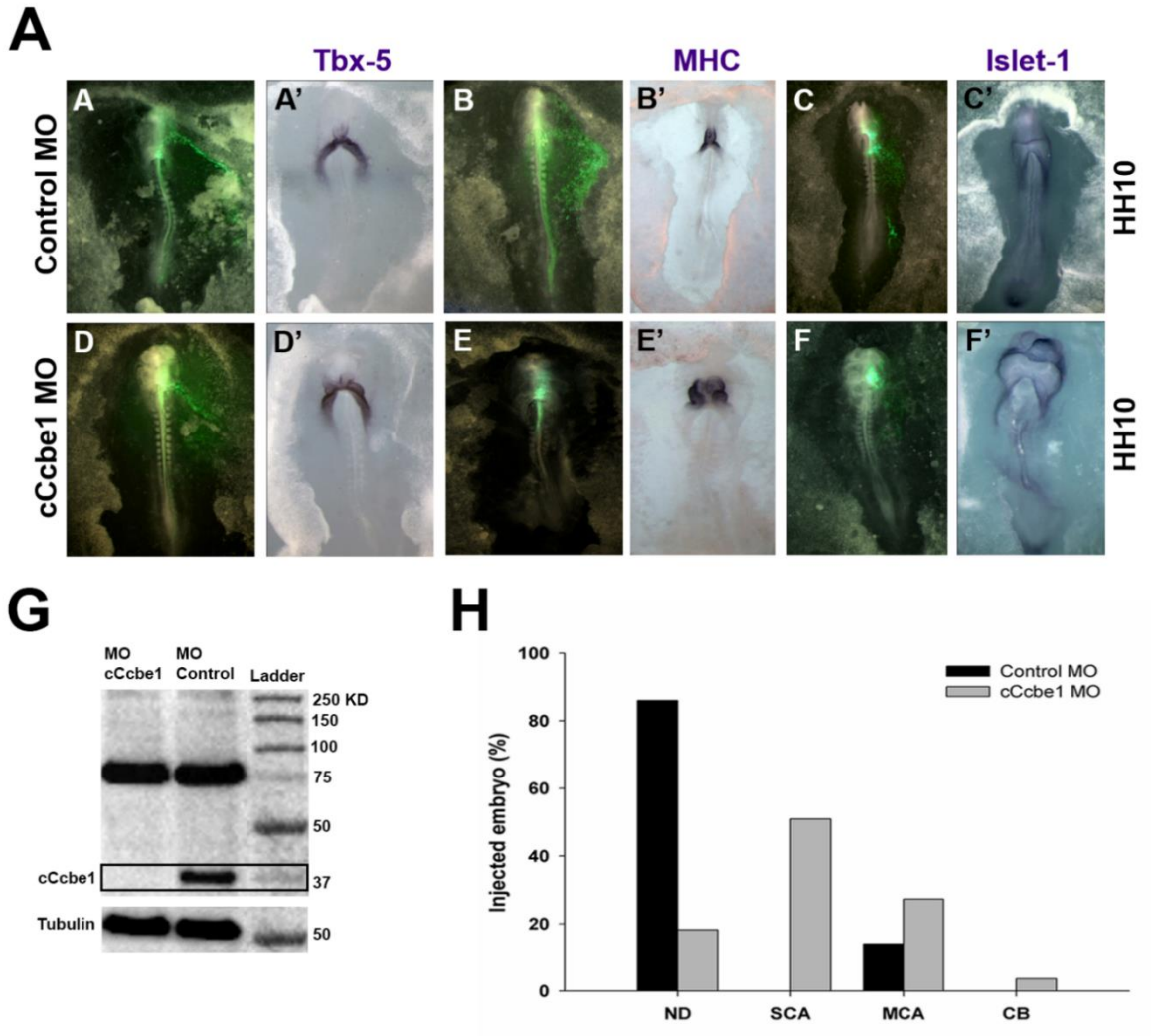

Figure 3.4 – c*Ccbe1* loss-of-function leads to heart malformations.
The embryos were first targeted at stage HH3⁺/HH4 with the designed morpholino and were collected later in development between stage HH9⁺ and HH10. **(A-C')** Embryos injected with the control morpholino. **(D-F')** Embryos injected with the cCcbe1 MO. **(A-F)** Localization and efficiency of the MO injection by detection of fluorescein expression. **(A'-F')** Detection of *Tbx5*, *Mhc* and *Islet-1* expression by WISH of the injected embryos with CoMO and cCcbe1 MO, respectively. All embryos are ventral. **(G)** Western blot analysis of the cCcbe1 MO and Control MO embryos. It was possible to see a loss in cCcbe1 protein levels observed in the c*Ccbe1* knockdown in comparison to morpholino control embryos. **(H)** Analysis of the phenotypes caused by electroporated embryos with cCcbe1 MO and Control MO. Bar charts showing the percentage of chick embryos presenting cardiac alterations after injection with Control or cCcbe1 MO. Only embryos at stage HH9 and later were considered to this analysis. The total of samples analyzed (n): 100 Control MO and 110 cCcbe1 MO embryos. The y-axis represents the percentage of embryos. The x-axis represents the defects: normal development (ND), severe cardiac alterations (SCA), moderate cardiac alterations (MCA) and *cardia bifida* (CB).

According to our data after 18h to 24h of incubation the cCcbe1 MO injected embryos displayed severe heart tube malformations (Figure 3.4D-F') absent in CoMO injected embryos (Figure 3.4A-C'). Cardiac precursor cells normally migrate anteriorly towards the midline and fuse into a single heart tube. However, in many cCcbe1 MO injected embryos the cardiac fields failed to form a linear heart tube, displaying an aberrant cardiac tube (Figures 3.4D-F' and 3.5D-F). Analysis of the distribution of the phenotypes showed that almost all the CoMO embryos developed normally (86%) (Figure 3.4H). The remaining 14% had some cardiac alterations, but none of them displayed severe abnormalities. In contrast, 81.8% of the cCcbe1 MO embryos showed significant cardiac alterations (Figure 3.4H). Among these, 50.9% displayed severe cardiac abnormalities, 27.2% moderate cardiac abnormalities and 3.7% *cardia bifida*. The cardiac defects were classified as severe when the heart tube failed to form the regular tube shaped heart, forming instead a deformed heart (Figure 3.4E'). The moderate phenotype encompasses embryos with a nearly normal heart tube, although presenting different morphology. Gene expression analysis trough whole-mount *in situ* hybridization of well-characterized heart-specific markers *Nkx2.5*, *Islet-1*, *Fgf8, Mhc* and *Tbx5* demonstrated that, even though c*Ccbe1* knockdown causes severe heart dystrophy, the spatiotemporal expression of these markers was not altered in c*Ccbe1* knockdown embryos up to stage HH11. This suggests that c*Ccbe1* may not be required for the specification and determination of the heart fields, but instead for the morphogenetic patterning of the cardiogenic mesoderm. In addition, this suggests that c*Ccbe1* is perhaps downstream of these cardiac genes or that it plays role in a different pathway.

Next, we performed immunofluorescence staining against MF20 (sarcomeric myosin heavy chain) a marker expressed in terminally differentiated cardiomyocytes, to follow the fusion of bi-lateral cardiac fields to form the heart tube. At stage HH9^{-}, we observed that the heart fields in the cCcbe1 Mo injected embryos were further appart than the control embryos (Figure 3.5A and D). This suggests that de heart fields are somewhat delayed in the absence of c*Ccbe1*. Later at stage HH10-12, the heart fields fail to fuse properly at the ventral midline (Figure 3.5B, C and E, F).

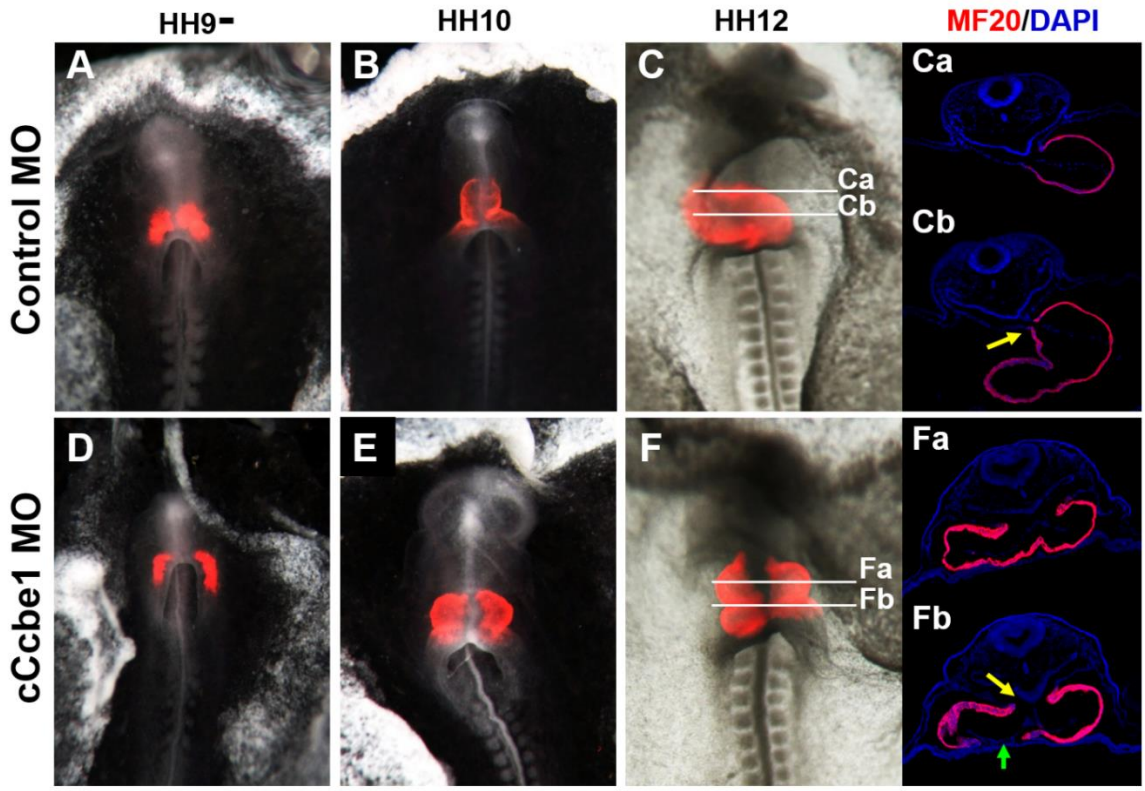

Figure 3.5 – Immunofluorescence analysis of cCcbe1 and Control MO in chick embryos. Embryos were target at HH3+/HH4 with cCcbe1 (cCcbe1 MO) and Control (CoMO) morpholino and allowed to develop until stage HH12. Some embryos were subsequently analyzed by whole mount (A-F) or in sections (Ca, Cb, Fa and Fb) immunofluorescence staining for MF20 (myocardium: red; Dapi: blue). **(A-C)** Embryos injected with CoMO showed no cardiac malformations. **(D-F)** embryos injected with cCcbe1 MO showed alterations in cardiac tube fusion: a delay in the fusion (D), fusion failure (E) and incomplete fusion (F). **(Ca-Cb)** Transverse sections (8µm) of embryos electroporated with CoMO at the level of the heart. **(Fa-Fb)** Transverse sections (8µm) of embryos electroporated with cCcbe1 MO at the level of the heart: these images highlight the malformations at the ventral midline (yellow arrowhead) and the lack of cell expressing myosin heavy chain (green arrowhead) caused by a failure on initiation of cardiac differentiation at the ventral midline.

Indeed, in transverse sections we confirmed that the cardiac fields do not properly fuse at the ventral midline, and that the spece between the cardiac fields is replaced by that do not express the cardiomyocyte marker MF20 (Figure 3.5Fa and Fb, greem arrow). In addition, the closure of the dorsal mesocardium was also affected in cCcbe1 MO injected embryos (Figure 3.5Cb and Fb; yellow arrow). The dorsal mesocardium is a transient structure formed when the splanchnic mesoderm (SHF) of opposite sides of the embryo come together from dorsal and ventral to the heart, forming double layered supporting membranes.

After the rupture of the dorsal mesocardium the heart tube closes dorsally and the dorsal pericardial walls fuse, something that in the c*Ccbe1* morphant embryos seems also to fail to happen. Taken together, these data indicates that the bilateral fields fail to properly fuse at the midline in the absence of c*Ccbe1,* leading to the development of an aberrant heart tube.

3.3.4 c*Ccbe1* knockdown affects the proliferation of the cardiac cells

Cell proliferation, while not the only mechanism, is an important process that contributes for the formation of the heart, which relies greatly on the rapid proliferation of cardiomyocytes at specific stages during early development (Sissman, 1966; Stalsberg and DeHaan, 1969). It is known that the initially formed myocardial tube continues to grow by recruitment of cells that originate from flanking mesoderm, dubbed the SHF (Cai et al., 2003; Mjaatvedt et al., 2001; Waldo et al., 2001). Additionally, the newly formed heart tube is non-proliferating, implying that growth of the primary heart tube can only occur by differentiation of precursor cells. During the looping of the heart cells are added from the splanchnic and pharyngeal mesoderm. Usually, if something interfers with the ability of these cells to replicate at this stage heart defects will became apparent. To determine if c*Ccbe1* is involved in the proliferation of heart precursor cells, we analysed cell proliferation through immunostaing for phospho-Histone 3 (PHH3), which marks only cells in mitosis, on transverse sections of c*Ccbe1* knokdown and control embryos.

Comparative analysis of proliferation in c*Ccbe1* knockdown embryos and control embryos revealed that the proliferation decreases in both pharyngeal and splanchnic mesoderm of the c*Ccbe1* morphant embryos (Figure 3.6A-B). Quantification of the cell proliferation in the cardiac region (splanchnic mesoderm and pharyngeal endoderm regions) and overall (cardiac plus non-cardiac regions) was consistent with decreased proliferation on those regions.

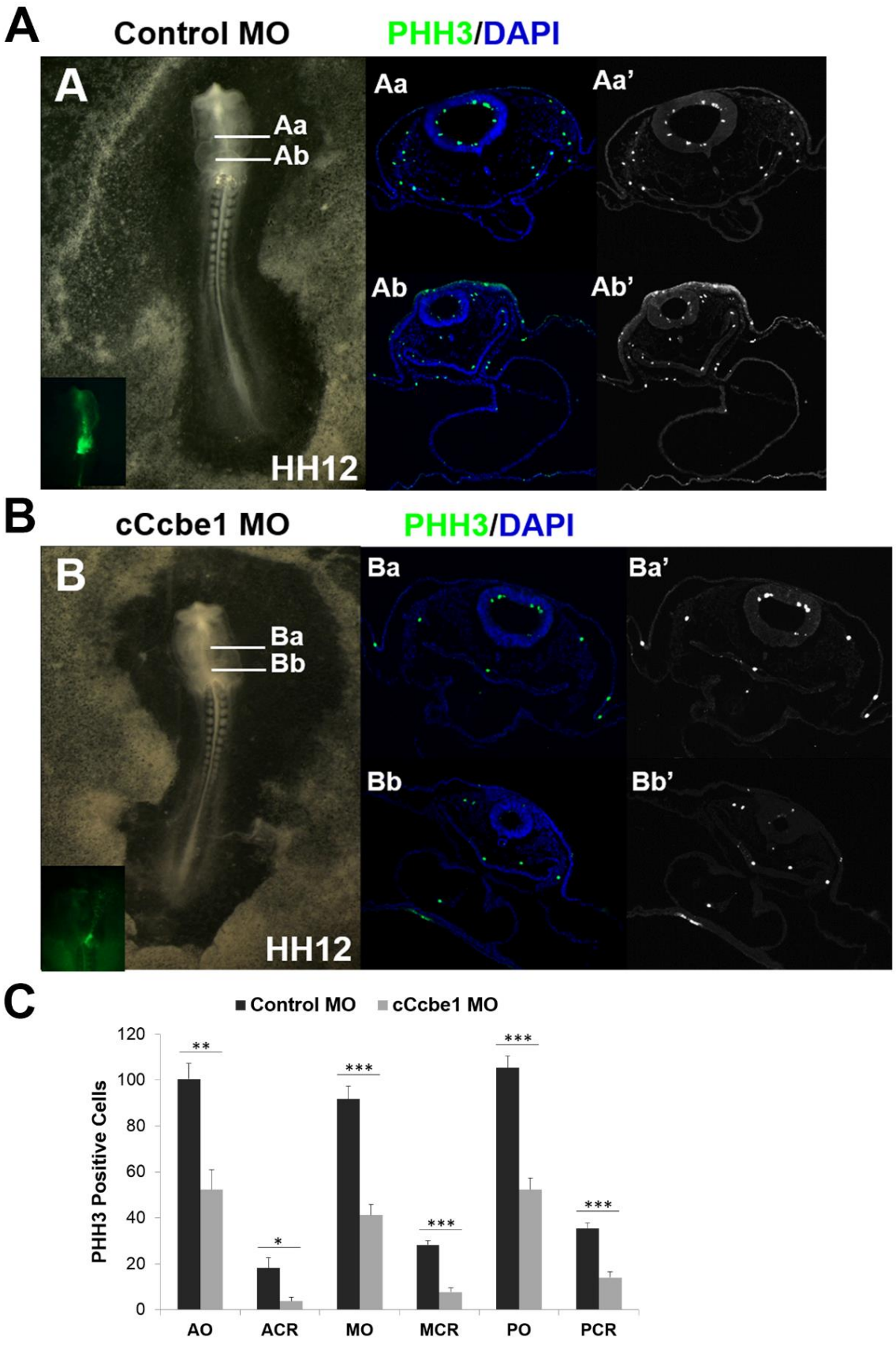

Figure 3.6 – c*Ccbe1* knockdown reduce cell proliferation in chick embryos.
Embryos at stage HH3⁺/HH4 were target with the cCcbe1 MO (B) and CoMO (A), and developed until HH12. Embryos were transverse sectioned and then immunohistochemistry staining was

performed for PHH3 (green; Aa-Bb'). **(B-Bb')** c*Ccbe1* treated embryos showing heart alterations and a decrease in proliferating cells; **(A-Ab')** Control morpholino treated embryos showing normal heart development and proliferation. Note that at this stage the heart is not proliferative, therefore the region of the pharyngeal and splanchnic mesoderm was taken in consideration (SHF contribution). Dapi: blue; PHH3: green. **(C)** Analysis of the cCcbe1 knockdown in cardiac cells proliferation. Embryos were subsequently analyzed in transverse sections by immunohistochemistry staining for PHH3. Proliferating cells were counted in 2 distinct regions: cardiac region (pharyngeal and splanchnic mesoderm) and overall (all the regions in the embryo: cardiac and non-cardiac). The total of embryos analyzed (n): 4 control MO and 4 cCcbe1 MO. The y-axis represents the PHH3 positive cells. The x-axis represents the regions of the counted PHH3 positive cells: anterior overall (AO), anterior cardiac region (ACR), medial overall (MO), medial cardiac region (MCR), posterior overall (PO) and posterior cardiac region (PCR). Error bars represent the S.E.M. from four replicates. *p<0.05; **p<0.01; ***p<0.001.

We selected sections at the anterior, medial and posterior levels of the heart tube region to count the number of proliferating cells. cCcbe1 MO embryos showed an overall decrease (ratio 2:1) in proliferating cells, but in the cardiac cells this difference in proliferation was even higher (ratio 3:1) when compared with the control MO embryos (Figure 3.6C). These data are similar to those found in *Islet-1* null mutants in which, absence of *Islet-1* leads to a decrease in cell proliferation and cell survival (Cai et al., 2003). Since like *Islet-1*, c*Ccbe1* is expressed in those regions, our data suggests that c*Ccbe1* is required for proper proliferation of SHF progenitors

3.3.5 c*Ccbe1* overexpression leads to *cardia bifida*

In the chick embryo, cardiac precursor cells migrate anteriorly towards the midline and fuse into a single heart tube. If this migration event is blocked, the two heart primordia remain separated and *cardia bifida* occurs. Interestingly, it has been reported that overexpression of CCBE1 inhibits cell migration in breast cancer cells (Barton et al., 2010). To dissect the role of c*Ccbe1* during early chick development, we used gain-of-function approaches to overexpress c*Ccbe1*. A vector with constitutive promoter (CAGGS) was used to clone the c*Ccbe1* transcript (pCAGGS-cCcbe1-IRES-GFP). An empty pCAGGS-IRES-GFP vector was used as control. Embryos at $HH3^{+}$/HH4 were injected with each vector into the right and left sides of the primitive streak, followed by *in vivo* electroporation. Furthermore, WISH of injected embryos was performed to confirm that pCAGGS-

cCcbe1-IRES-GFP was causing overexpression of c*Ccbe1*. Indeed, injection with the pCAGGS-cCcbe1 resulted in a co-localized c*Ccbe1* expression with GFP, including in places where c*Ccbe1* is normally absent (Figure 3.7C-C').

According to our data, upon 18h to 24h of incubation the injected embryos with c*Ccbe1* overexpression displayed severe heart tube malformations (Figure 3.7B-B') that were absent in control vector injected embryos (Figure 3.7A-A'). Normally, cardiac precursor cells migrate anteriorly towards the midline and fuse into a single heart tube. In many c*Ccbe1* overexpression vector injected embryos both heart fields failed to migrate properly towards the midline remaining in the lateral plate mesoderm, i.e. *cardia bifida* (Figure 3.7B and F).

Analysis of the distribution of the phenotypes showed that almost all the control vector injected embryos developed normally (86.8%) (Figure 3.7D). The remaining 13.2% had some cardiac alterations, but none of them displayed *cardia bifida*. In contrast, 89.5% of the c*Ccbe1* overexpression embryos showed significant cardiac alterations (Figure 3.7D). Among these, 52.6% displayed *cardia bifida* and 36.9% milder cardiac alterations, i.e. the heart fields were able to migrate to the midline but they failed to fuse properly and the hearts consistently failed to undergo looping of the heart tube (Figure 3.7D).

The *cardia bifida* phenotype that was observed in the c*Ccbe1* overexpression embryos were strikingly similar to those seen in embryos lacking the cardiac transcription factor *Gata4*. In these embryos, two separate heart tubes develop in the majority of mutants (Kuo et al., 1997; Molkentin et al., 1997). Immunofluorescence analysis of MF20 showed that the cardiac fields of c*Ccbe1* overexpression embryos remain close to the lateral plate mesoderm and consequently the embryos showed a bifid heart phenotype (Figure 3.7E-Fc'). This observation is consistent with failure of the migration of the cardiac fields towards the midline. In light with the similarities with the Gata4 mutants, we examined as well the expression pattern of *Gata4* in the c*Ccbe1* overexpression vector injected embryos.

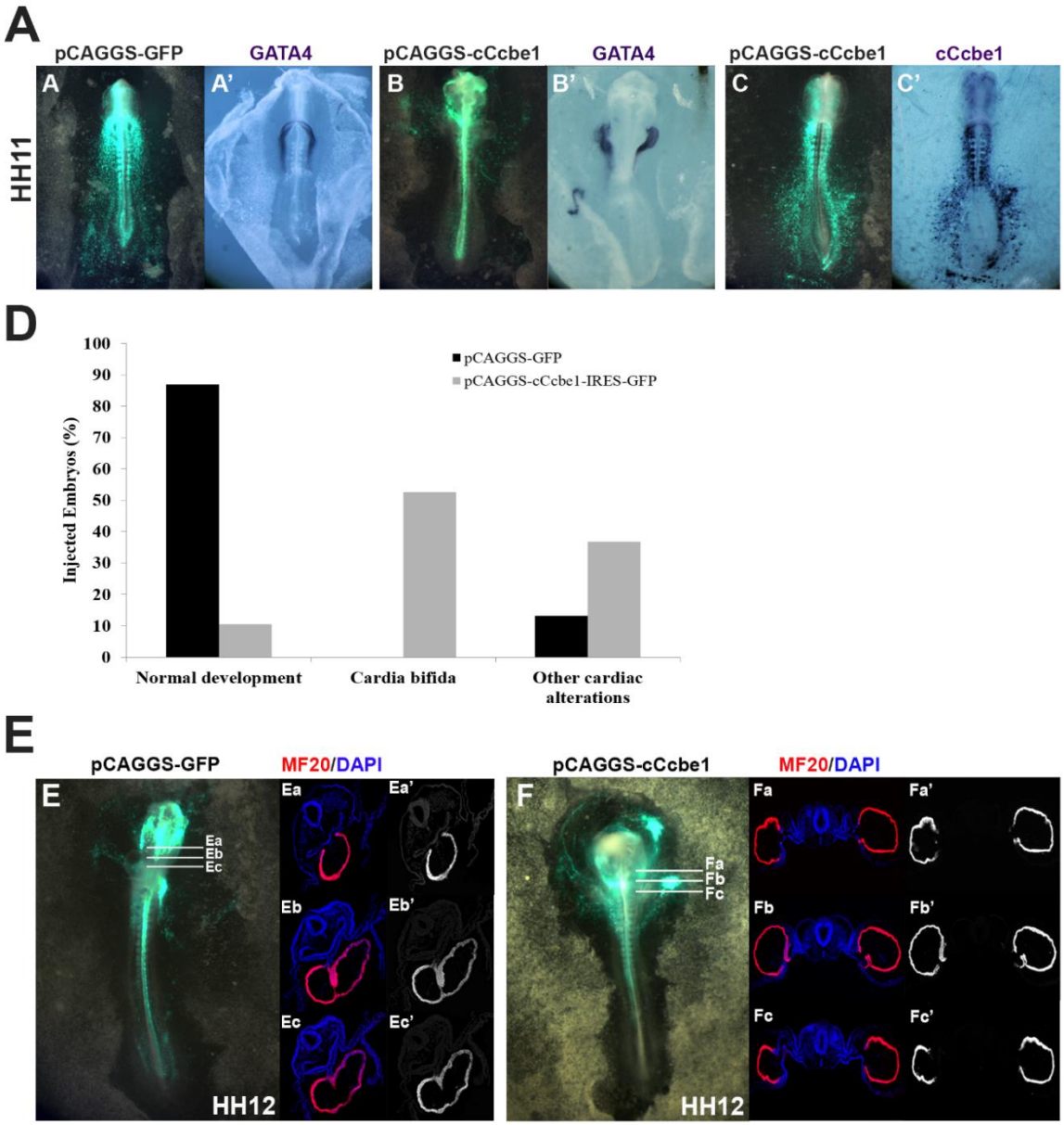

Figure 3.7 – c*Ccbe1* gain-of-function in chick embryos.
Embryos were targeted at stage HH3^{+}/HH4 with the control vector pCAGGS-IRES-GFP (A) or with the overexpression vector pCAGGS-cCcbe1-IRES-GFP (B-C) and collected at stage HH11. **(A)** Localization and efficiency of the control vector pCAGGS-GFP injection by detection of fluorescein expression. **(A')** Embryos injected with control vector showed no cardiac malformations detected with *Gata4* by WISH. **(B-C)** Localization and efficiency of the overexpression vector pCAGGS-cCcbe1-IRES-GFP injection by detection of fluorescein expression. **(B')** Embryos injected with pCAGGS-cCcbe1-IRES-GFP showed alterations in cardiac tubes fusion detected with *Gata4* by WISH, namely, bifid heart was observed (formation of two separate heart tubes). **(C')** Detection of c*Ccbe1* expression by WISH, demonstrating that pCAGGS-cCcbe1-IRES-GFP is overexpressing c*Ccbe1*. **(D)** Analysis of the defects caused by electroporated embryos with control vector pCAGGS-IRES-GFP or overexpression vector pCAGGS-cCcbe1-IRES-GFP. Bar charts showing the percentage of chick embryos presenting cardiac alterations after injection with control vector or overexpression vector. Only embryos at stage HH9 and later were considered to this analysis. The total of samples analyzed (n): 38 control vector and 38 overexpression vector embryos. The y-axis represents the percentage of embryos. The x-axis represents the defects: normal development, cardia bifida and other cardiac alterations. **(E-F)** Some embryos were subsequently analyzed immunohistochemistry staining for

MF20 (myocardium: red; Dapi: blue) in transverse sections (8µm). **(E-Ec')** Embryos injected with control vector showed no cardiac malformations. **(F-Fc')** embryos injected with overexpression vector showed *cardia bifida* defects. These images showed none alteration of cell expressing MF20.

We observed that, despite the development of *cardia bifida* in the c*Ccbe1* overexpression embryos, the expression of *Gata4* was also present in c*Ccbe1* overexpression embryos up to stage HH11 (Figure 3.7A-B'). This suggests that c*Ccbe1* may not be required for the specification and determination of the heart fields, but instead for proper morphogenetic patterning of the cardiogenic mesoderm.

3.3.6 c*Ccbe1* overexpression also affects cell proliferation

To determine if c*Ccbe1* overexpression also affects the proliferation of heart precursor cells, we analyzed cell proliferation through immunostaining for PHH3 on transverse section of c*Ccbe1* overexpression and control embryos.

Comparative analysis of proliferation in c*Ccbe1* overexpression embryos and control embryos revealed that the proliferation increases in both pharyngeal and splanchnic mesoderm of the c*Ccbe1* gain-of-function embryos (Figure 3.8A-B). c*Ccbe1* overexpression embryos showed an overall increase in proliferating cells. Quantification of proliferating cells in the cardiac region (splanchnic mesoderm and pharyngeal endoderm regions) and overall (cardiac plus non-cardiac regions) was consistent with increased proliferation in those regions. As for cardiac cells proliferation, we also observed an increase in c*Ccbe1* overexpression embryos when compared with the control embryos (Figure 3.8C). This data is consistent with a role of c*Ccbe1* in the control of SHF progenitors proliferation.

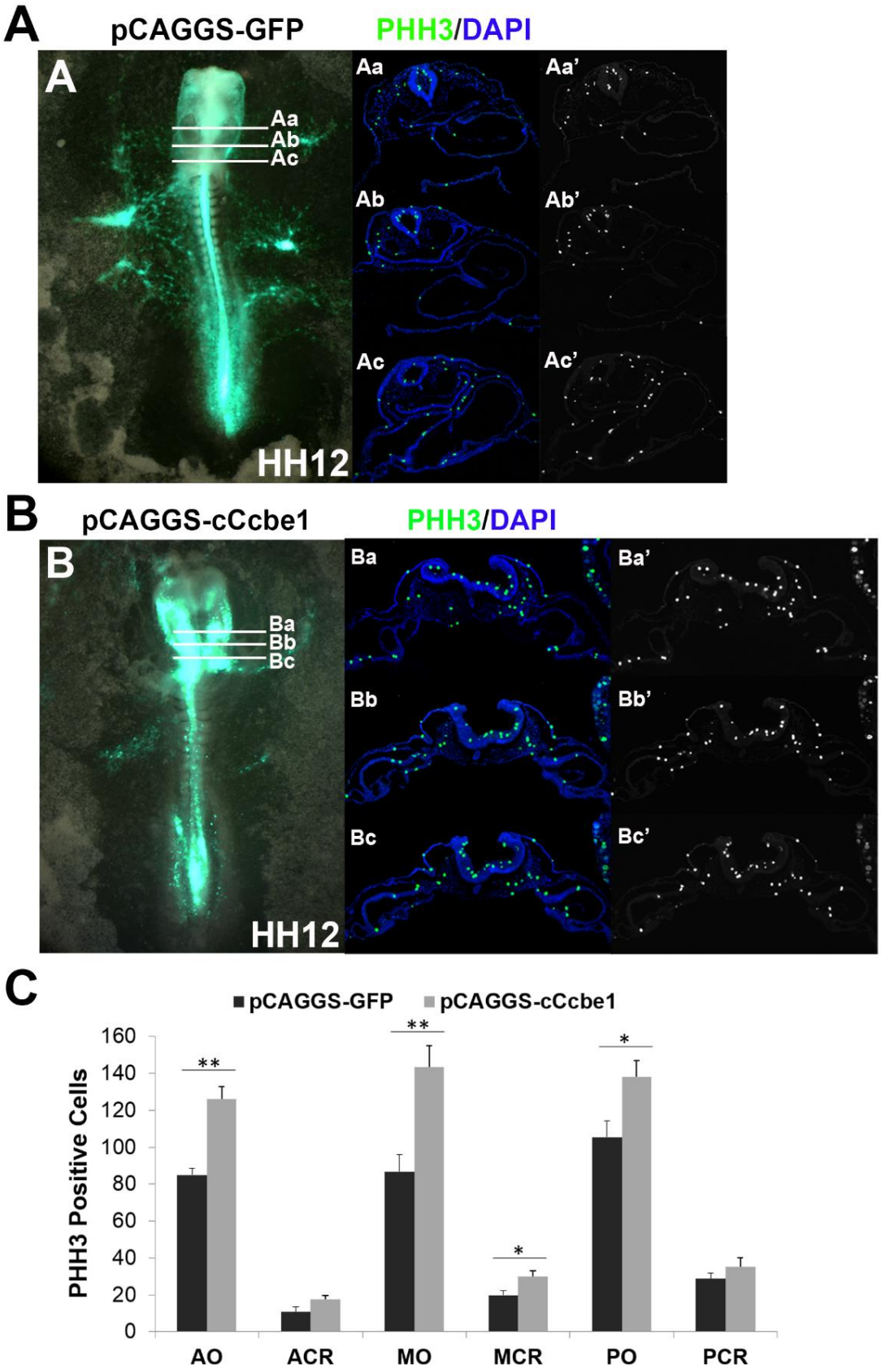

Figure 3.8 – c*Ccbe1* knockdown disturbs cell proliferation in chick embryos.
Embryos at stage HH3^{+}/HH4 were target with the control vector pCAGGS-IRES-GFP (A) or with the overexpression vector pCAGGS-cCcbe1-IRES-GFP (B) and developed until HH12. Embryos

were transverse sectioned and then immunohistochemistry staining was performed for PHH3 (green; Aa-Bc'). **(A-Ac')** Control treated embryos shows normal heart development and proliferation. **(B-Bb')** Overexpression-cCcbe1 treated embryos shows heart alterations and an increase in proliferating cells. Note that at this stage the heart is not proliferative, therefore the region of the pharyngeal and splanchnic mesoderm was taken in consideration (SHF contribution). Dapi: blue; PHH3: green.; **(C)** Analysis of the c*Ccbe1* overexpression in cardiac cells proliferation. Embryos were subsequently analyzed in transverse sections by immunohistochemistry staining for PHH3. Proliferating cells were counted in 2 distinct regions: cardiac region (pharyngeal and splanchnic mesoderm) and overall (all the regions in the embryo: cardiac and non-cardiac). The total of embryos analyzed (n): 4 pCAGGS-GFP and 4 pCAGGS-cCcbe1. The y-axis represents the PHH3 positive cells. The x-axis represents the regions of the counted PHH3 positive cells: anterior overall (AO), anterior cardiac region (ACR), medial overall (MO), medial cardiac region (MCR), posterior overall (PO) and posterior cardiac region (PCR). Error bars represent the S.E.M. from four replicates. *p<0.05; **p<0.01.

3.3.7 c*Ccbe1* loss and gain-of-function affects Hnk1 expression

Monoclonal antibody Hnk1 carbohydrate recognizes a subset of cell surface glycoproteins that mediate cell-cell or cell-substrate interactions (Kruse et al., 1984). During cardiogenesis, in various species (including the chick) Hnk1 epitope is present in migrating neural crest cells (Bronner-Fraser, 1987; Vincent and Thiery, 1984), in developing conduction cardiomyocytes, in cardiomyocytes expressing both MF20 and Hnk1 (not working cardiomyocytes), and in endocardial cushion mesenchymal cells (Nakajima et al., 2001). In addition, during chick early cardiogenesis, Hnk1 is scattered along the primitive heart tube, only later becoming restricted to the myocardium of the sinus venosus and atrium in which the central conduction system will be developed at a later stage (Nakajima et al., 2001). To determine if c*Ccbe1* loss- and gain-of-function influences Hnk1 expression in the chick embryo, we performed immunostaining with the Hnk1 antibody on transverse sections at the heart region of c*Ccbe1* knockdown, overexpression and respective control embryos (stage HH12).

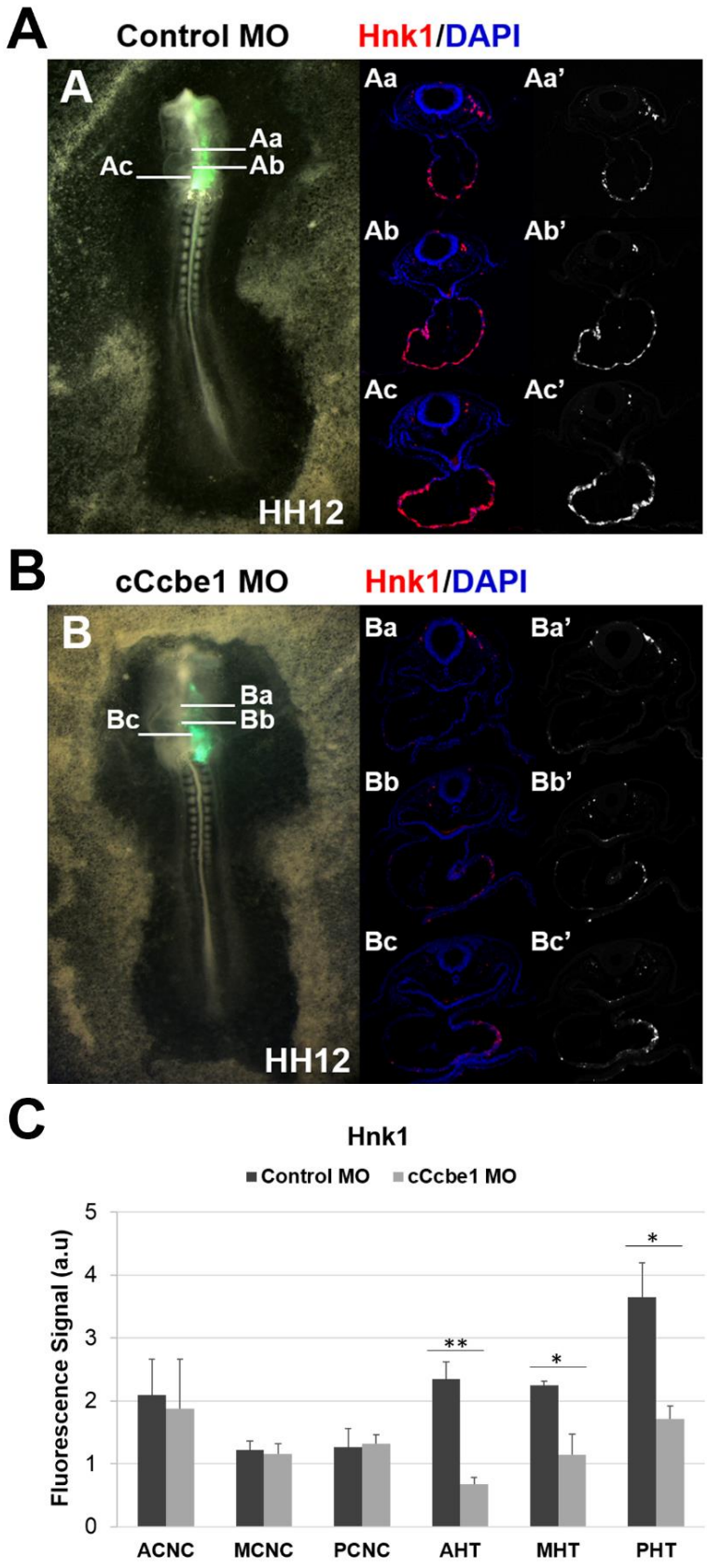

Figure 3.9 – Hnk1 immunofluorescence analysis of c*Ccbe1* loss-of-function in chick embryos.
Embryos were target at HH3^{+}/HH4 with cCcbe1 and Control morpholino and allowed to develop until stage HH12 (A and B). Embryos were subsequently analyzed transversal sections (Aa-Bc)

by immunostaining for Hnk1 (migrating CNC and conducting system marker: red; Dapi: blue). **(Aa-Ac')** Transverse sections (8µm) of embryos electroporated with CoMO at the level of the heart; Hnk1 expression is detected through the heart tube and CNC. **(Ba-Bc')** Transverse sections (8µm) of embryos electroporated with cCcbe1 MO at the level of the heart: these images highlight the lack of Hnk1 expression in the heart tube. **(C)** Quantitative analysis of Hnk1 immunostaining in two distinct regions: cardiac neural crest (CNC) cells and heart tube (HT). The total of embryos analyzed (n): 3 control MO and 3 cCcbe1 MO. The y-axis represents the Hnk1 fluorescence signal. The x-axis represents the regions of the Hnk1 measured signal: anterior CNC (ACNC), medial CNC (MCNC), posterior CNC (PCNC), anterior heart tube (AHT), medial heart tube (MHT), posterior heart tube (PHT). Error bars represent the S.E.M. from three replicates. *p<0.05; **p<0.01.

On the one hand, when comparing control and c*Ccbe1* knockdown embryos, while there were no significant differences in the cardiac neural crest (CNC) cells, the distribution of Hnk1 in the heart tube was substantially decreased (Figure 3.9A-B). Quantification of the level of Hnk1 signal in c*Ccbe1* morphants and control embryos in sections at the anterior, medial and posterior levels of the heart tube region showed that the level of Hnk1 was decreased in the c*Ccbe1* morphant embryos (Figure 3.9C). While the difference in the heart tube was consistent in all the analysed embryos, there were no obvious differences in most of the embryos at the level of the CNC cells. On the other hand, when comparing control and c*Ccbe1* overexpression embryos, the Hnk1 was increased in both CNC cells and heart tube regions in the c*Ccbe1* overexpression embryos (Figure 3.10A-B). Indeed, when we measured the Hnk1 signal the difference between the control and the c*Ccbe1* gain-of-function embryos was evident (Figure 3.10C), especially in the CNC cells where the intensity of Hnk1 staining was wider and stronger than in the control embryos. Taken together, altered Hnk1 levels caused by gain and loss-of-function of c*Ccbe1* suggest that the migration of CNC cells is affected, leading to an incorrect development of cardiomyocytes.

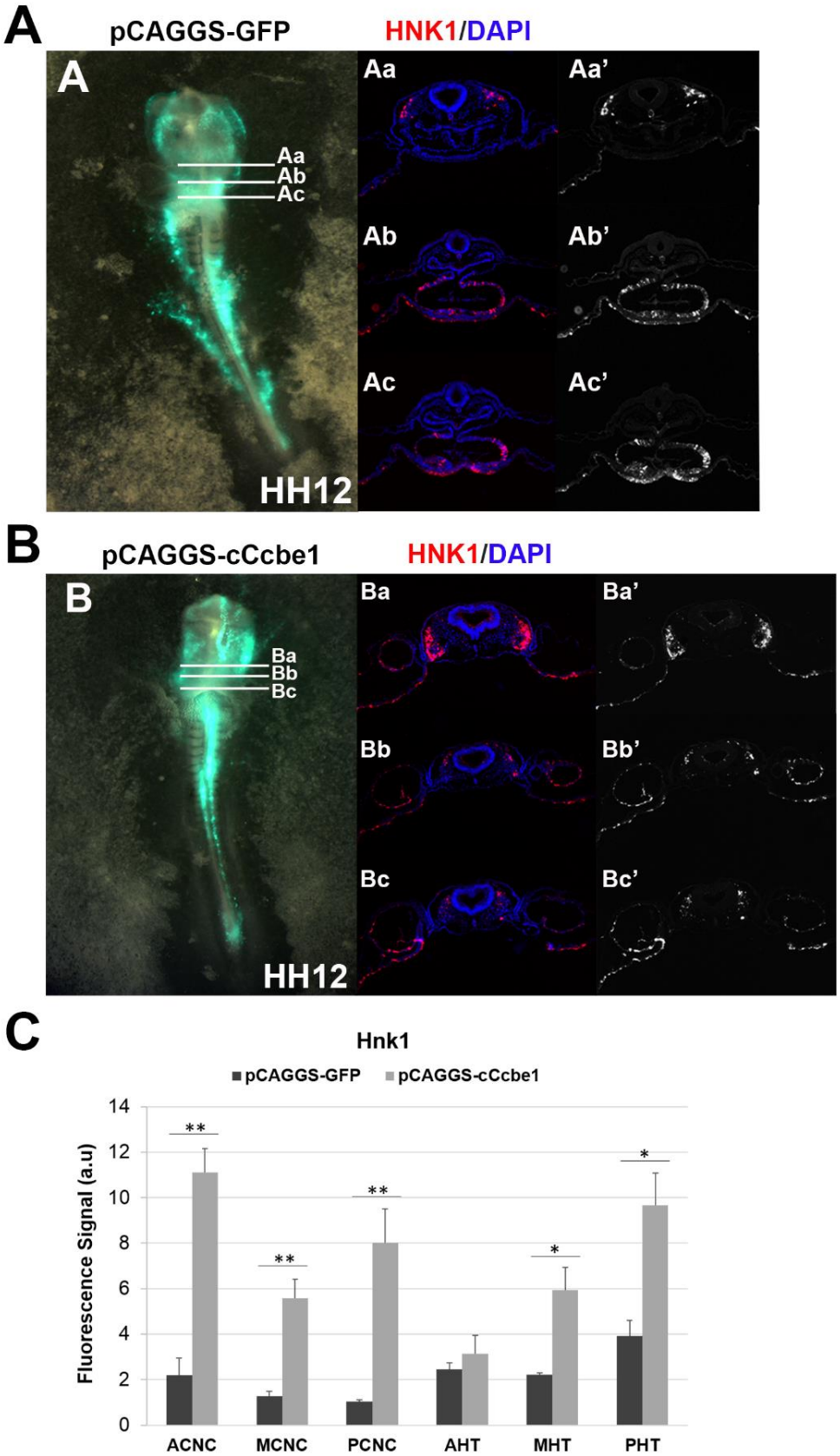

Figure 3.10 – Hnk1 immunofluorescence analysis of c*Ccbe1* gain-of-function in chick embryos.
Embryos were target at HH3⁺/HH4 with the overexpression vector pCAGGS-cCcbe1 and the control vector pCAGGS-GFP and allowed to develop until stage HH12 (A and B). Embryos were

subsequently analyzed transversal sections (Aa-Bc) by immunostaining for Hnk1 (migrating CNC and conducting system marker: red; Dapi: blue). **(Aa-Ac')** Transverse sections (8µm) of embryos electroporated with control vector at the level of the heart; Hnk1 expression is detected through the heart tube and CNC. **(Ba-Bc')** Transverse sections (8µm) of embryos electroporated with overexpression vector at the level of the heart: these images highlight increase of Hnk1 expression in the heart tube and CNC. **(C)** Quantitative analysis of Hnk1 immunostaining in two distinct regions: cardiac neural crest (CNC) cells and heart tube (HT). The total of embryos analyzed (n): 3 control vector and 3 overexpression vector. The y-axis represents the Hnk1 fluorescence signal. The x-axis represents the regions of the Hnk1 measured signal: anterior CNC (ACNC), medial CNC (MCNC), posterior CNC (PCNC), anterior heart tube (AHT), medial heart tube (MHT), posterior heart tube (PHT). Error bars represent the S.E.M. from three replicates. *p<0.05, **p<0.01.

3.4 Discussion

Expression analysis showed that c*Ccbe1* mRNA was initially detected very early in development in the cardiogenic region on either side of the primitive streak at stage HH4. c*Ccbe1* mRNA staining at this stage of development coincides with the mesodermal cells that emerge from the anterior two-thirds of the primitive streak to form two bilateral cardiogenic fields in the anterior lateral plate mesoderm. It is known that the precursor heart cells are restricted to the splanchnic mesoderm (Linask, 1992) and this region was where c*Ccbe1* expression was also visible. From stage HH5 to HH8, expression of c*Ccbe1* mRNA expands along the lateral plate mesoderm of the embryo resembling that observed in staining performed using markers of the FHF and SHF such as *Nkx2.5* and *Islet-1*, respectively. Indeed, histological sections showed that c*Ccbe1* is co-expressed with *Nkx2.5* and *Islet-1* in the splanchnic mesoderm, specifically in the ventrolateral aspect of the splanchnic mesoderm, where the differentiating myocardial cells (FHF) is known to be present, and also at the dorsomedially region, where is known to be a region of undifferentiated cells (SHF). Although, c*Ccbe1*-expressing cells could be detected in the myocardial tissue forming the primordial of the primitive heart tube at HH8, expression in the cardiac tissue in more advanced stages of heart morphogenesis (HH9^{+}-18) was undetectable. c*Ccbe1* expression is therefore continuous in the cardiogenic mesoderm and residual in the primordial myocardial tissues followed by absence of expression at later stages of heart development. This suggests that high levels of c*Ccbe1* expression are limited to multipotent and highly proliferative

progenitors at the inflow region of the heart tube and in the SHF, and downregulated upon cellular commitment towards cardiac lineages. Later in development (HH13-18) the c*Ccbe1* mRNA was found predominantly in the region of the *conus arteriosus* and in the SHF region. The latter coincided with the expression of *Islet-1*, which marks undifferentiated and highly proliferative cardiac progenitors (Cai et al., 2003). In fact, c*Ccbe1* once expressed in both heart fields population at early stages, progressively became restricted to the SHF population, as observed in *Islet-1* expression. Interestingly, in mice *Ccbe1* expression was shown in the three major populations of cardiac progenitors, namely the FHF, SHF and proepicardium (Facucho-Oliveira et al., 2011). This raises the possibility of a role of c*Ccbe1* in heart progenitors during cardiogenesis.

The Ccbe1 protein contains a collagen and calcium binding EGF-like domains, and may function in extracellular matrix remodeling and migration (Barton et al., 2010). The knockdown of c*Ccbe1* leads to incorrect formation of the heart tube. The bilateral cardiac progenitor populations seem to fail to migrate properly towards the midline in the *cCcbe1* knockdown embryos. It has been shown that in ovarian cancer cell lines silencing of CCBE1 is associated with increased cell migration and that, in contrast, CCBE1 overexpression inhibits it (Barton et al., 2010). Therefore, it is possible that avian c*Ccbe1* is required for the proper migration of the bilateral cardiac progenitor cells. Alternatively, and knowing that the heart precursor cells are highly proliferative, it is possible that this phenotype is also related to altered cell proliferation. Indeed, it has been shown that alterations in the proliferation of cardiac precursor cells affect the migration of the precursors towards the midline (Linask et al., 2005). Immunohistochemistry analysis of the proliferation marker PHH3 revealed that knockdown of c*Ccbe1* leads to decreased proliferation of the cardiac progenitor cells. These data indicate that in the absence of c*Ccbe1* the bilateral cardiac progenitor cells fail to fuse at the midline to form the heart tube due to, at least in part, defective cell proliferation.

On the other hand, the most severe phenotype of c*Ccbe1* overexpression is *cardia bifida*. A defect that develops in several loss-of-function models, including

Gata4 (Zhang et al., 2003); *N-cadherin* (Nakagawa and Takeichi, 1997), *Rho kinases* (Wei et al., 2001), *Furin* (Roebroek et al., 1998). Indeed, the defects observed in c*Ccbe1* overexpression embryos are strikingly similar to those seen in embryos lacking the transcription factor *Gata4*, in which the precardiac mesoderm fails to migrate properly hampering its fusing at the ventral midline (Zhang et al., 2003). Since it has been shown that overexpression of CCBE1 in cell culture leads to blockade of cell migration (Barton et al., 2010), it is possible that excess c*Ccbe1* in chick heart precursor cells may hamper their migration towards the midline to form the heart tube. Interestingly, c*Ccbe1* overexpression did not affect the expression of the cardiac transcription factor *Gata4*, despite the obvious morphological alterations. Similarly knockdown of c*Ccbe1* did not alter the expression of cardiac specification markers *Nkx2.5* (data not shown)*, Tbx5, Mhc, Fgf8* (data not shown) *and Isl1*. Taken together, these data suggest that c*Ccbe1* is not important for cardiomyocyte commitment, but instead it likely has a role in the proper proliferation and migration of the cardiac precursor cells to form the heart tube.

As mentioned above, the heart precursor cells proliferate and migrate as they travel towards their final destination at the midline to form the heart primordia and where they differentiate into cardiomyocytes. In the chick this happens around stage HH9 of development at the beginning of the fusion of the heart tube. Taking this into consideration, we analyzed the terminal cardiomyocyte differentiation in the c*Ccbe1* knockdown embryos. According to our data, the cells at the ventral midline in c*Ccbe1* knockdown embryos do not express the cardiomyocytes marker MF20. This suggests that the cells at the midline fail to initiate cardiac differentiation at the ventral midline. Alternatively and since the analyzed cardiac markers were unaffected in the gain- and loss-of-function experiments, it is also possible that defective proliferation and migration of the cardiac precursors cells hampers proper fusion at the midline and consequently non-cardiac fated cells occupy their place. In any of the cases, this affects the formation of a normal beating heart tube, indicating that c*Ccbe1* is involved in the coordination of early heart organogenesis in the avian embryo possibly through the regulation of proliferation and migration of cardiac precursors towards the ventral midline.

Furthermore, this is consistent with the c*Ccbe1* expression at the bilateral heart fields as they migrate to the midline.

It is known that Hnk1 is normally present in the cardiomyocyte precursor of the conduction system tissue and is involved in the development of mature His-Purkinje System architecture and consequently its function (Aoyama et al., 1995; Blom et al., 1999; Chuck and Watanabe, 1997; Nakajima et al., 2001). In addition, it is also known that Hnk1 is present in migrating CNC cells, and that the CNC cells are required for outflow septation (at later stages of development) and for the correct normal heart looping by addition of myocardium to the heart tube from the SHF (Yelbuz et al., 2002). Furthermore, CNC may not contribute directly to the His-Purkinje conduction system, but it may be required for its normal development (Bronner-Fraser, 1987). Following ablation of CNC cells in chick embryos, the conduction system bundles fail to compact leading to inhibition or delay in the maturation of the conduction system function (Gurjarpadhye et al., 2007). Furthermore, fate mapping studies CNC cells are found in close proximity with the developing conduction system (Nakamura et al., 2006; Poelmann et al., 2004; Poelmann and Gittenberger-de Groot, 1999), and deletion of Hf1b from CNC resulted in atrial and atrioventricular conduction dysfunction (St. Amand et al., 2006). According to our results, while increased c*Ccbe1* levels resulted in expansion of Hnk1-expressing domain in both CNC cells and heart tube region, loss of c*Ccbe1* decreased Hnk1 signal mostly in the heart tube region. This may affect the migration of CNC cells leading to an incorrect development of cardiomyocytes, and hence suggests that c*Ccbe1* may be also required during early heart development for the establishment of the heart conduction system.

In conclusion, here we presented that c*Ccbe1* is expressed in both FHF and SHF progenitor populations, and that later becomes restricted to the SHF. This suggested that c*Ccbe1* is downregulated as the progenitor cells differentiate towards more definitive cardiac phenotypes. Upon c*Ccbe1*-loss-of-function during early cardiogenesis the fusion of the heart fields was incomplete or failed to fuse correctly leading to the formation of an aberrant heart tube. On the other hand, c*Ccbe1*-gain-of-function led to severe heart tube defects, including marked *cardia bifida*. Furthermore, playing with the levels of c*Ccbe1* influences Hnk1

expression suggesting a possible role in the migration of the CNC cells leading to an incorrect development of cardiomyocytes. Taken together, these data support the view that c*Ccbe1* plays an important role during early heart development and, therefore, is a candidate gene for cardiomyopathy. The relevance of Ccbe1 in mammalian cardiogenesis and the possible significance of Ccbe1 alterations in cardiac syndromes should deserve further attention.

CHAPTER 4 – GENERAL DISCUSSION

Congenital heart defects represent almost 1% of newborn children and in the human population 30% of cardiac malformations leads to the loss of the embryo before birth (Bruneau, 2008). This suggests that many of the congenital heart malformations arise from defects at early stages of heart development. Driven by curiosity and in the way to discover new treatments for heart diseases, scientists have been trying to reveal unknown processes required for cardiovascular development. While various model organisms such as mouse, *Xenopus* or zebrafish embryos are often studied to gain insights about the complex processes driving normal as well as abnormal development of the vertebrate heart, the chicken embryo has centered itself as the longstanding classic system used by embryologists and cardiovascular scientists to illustrate the principles of basic vertebrate embryology and cardiovascular development. The avian embryo offers distinct advantages as an embryonic model system to study cardiovascular disease. Unlike mammals, it is easy to obtain and direct observation of a living embryo is possible at early stages of embryogenesis, allowing *ex ovo* culture and the direct observation of the cellular movements comprising heart formation. Furthermore, chick and human heart development share similar morphological mechanisms and many cardiovascular defects found in the avian embryo are similar to those found in humans (Abu-Issa and Kirby, 2008; Tutarel et al., 2005).

In this thesis, the main focus was to study and characterize the role of c*Ccbe1* during early heart development in the chick.

This novel gene, c*Ccbe1*, is first detected at stage HH4-4+ in the cardiogenic mesoderm of the HFR on either side of the primitive. c*Ccbe1* expression in the bilateral HFR could be observed until the beginning of their fusion to form the linear heart tube at stage HH9. Double WISH analysis revealed that c*Ccbe1* is co-expressed with *Nkx2.5* and *Islet-1* in these regions, which is consistent with c*Ccbe1* expression in the HFR since very early during cardiac development. Furthermore, transverse sections of double WISH analysis demonstrated that c*Ccbe1* co-labels with *Nkx2.5* in the ventrolateral aspect of the splanchnic mesoderm (FHF) and with *Nkx2.5* and *Islet-1* a stronger co-expression in the dorsomedially region of the splanchnic mesoderm, which corresponds to the SHF, extending towards the cranial paraxial mesoderm. At stage HH9 to HH12,

c*Ccbe1* transcripts were observed near the posterior part of the heart (inflow), which could mean the beginning of the restriction of c*Ccbe1* to the SHF population in the caudal dorsal pericardial wall, known as the center of proliferation, where proliferate rapidly contributing with progenitors to the correct cardiac morphogenesis in both poles of the heart (van den Berg et al., 2009). More cranially c*Ccbe1* expression was detected lateral to the pharynx progressing to the anterior part of the heart (outflow) near the region of the *conus arteriosus*, which is consistent with the contribution of proliferating progenitors to the poles of the heart tube. At stage HH13 to HH18, c*Ccbe1* expression was found in the anterior part of the embryo that surrounds the pharynx, known to represent the SHF (pharyngeal mesoderm). Double WISH analysis revealed that c*Ccbe1* is co-expressed with *Nkx2.5* and *Islet-1* in this region, indicating that c*Ccbe1* is indeed expressed in the SHF. Furthermore, c*Ccbe1* was also found in the caudal part of the distal outflow tract of the heart tube, coinciding with the expression of *Islet-1*, which is known to be a region where SHF contribute with cells to the elongation of the heart tube. Taken together, c*Ccbe1* exhibits an interesting expression pattern during early heart development, being initially expressed since very early in the FHF and SHF of the heart forming regions and later is highly specific of the SHF region during early heart development in the chick. Furthermore, due to the overlapping expression of c*Ccbe1* and *Islet-1* in the SHF, specifically in the center of rapid proliferation, c*Ccbe1* might play a general role in the proliferation rather than having a specific function in delineating fields of heart precursors.

The c*Ccbe1* functional studies presented in this thesis demonstrate that c*Ccbe1* is required during early heart development. The knockdown of c*Ccbe1* leads to incorrect formation of the heart tube, in which the bilateral fields seem to fail to migrate properly towards the midline, fuse and close to develop a proper heart tube. Knowing that the heart precursor cells are highly proliferative, it is likely that this phenotype is related to the observed altered cell proliferation. In addition, studies performed in our lab support these findings. Accordingly, mouse embryonic fibroblast isolated from mCcbe1 KO proliferate less when compared with the WT cells (Perestrelo et al, *unpublished*). Furthermore, in *Islet-1* knockout mice have also been shown to have reduced cell proliferation, which resulted in

reduce proliferative cells in the region of the pharyngeal endoderm and much lower in the splanchnic mesoderm leading to a deficient migration of the SHF progenitors into the heart tube, and consequently leads to absence of the OFT, right ventricle and must of the atria (Cai et al., 2003). Therefore, reduced cell proliferation in the absence of c*Ccbe1* in the avian embryo may be the underlying mechanism causing improper movement of the bilateral cardiac fields towards the midline. Furthermore, it is known that the cardiac tube formation is closely associated with the morphogenesis of the foregut. The medial region of the foregut walls approach each other at the midline commencing the ventral closure where the two separated myocardial sheets facing the midline continue to proliferate and approach each other to fuse shortly into a linear heart tube, beneath the ventral foregut (Linask et al., 2005). We found that the fusion of the opposing foregut endodermal tissue might be blocked or partially blocked by knockdown of c*Ccbe1*, first, due to the expression that this gene presents in the SHF region, then for the phenotype that the morphants embryos showed, and last for the decreased in cardiac proliferation. In addition, knockdown of c*Ccbe1* activity could arrest the fusion of the two cardiac sheets at the midline remaining as two separate or partially separated epithelial compartments. Therefore, the remodeling events leading to closure of the foregut and fusion of the cardiac primordia into a single heart tube seem to require c*Ccbe1* activity.

On the other hand, the most severe phenotype of c*Ccbe1* overexpression is *cardia bifida*. Indeed, the defects observed in c*Ccbe1* overexpression embryos are strikingly similar to those seen in embryos lacking the transcription factor *Gata4*, in which the precardiac mesoderm fails to migrate properly hampering its fusing at the ventral midline (Zhang et al., 2003). Since it has been shown that overexpression of CCBE1 in cell culture leads to blockade of cell migration (Barton et al., 2010), it is possible that excess c*Ccbe1* in chick heart precursor cells may hamper their migration towards the midline to form the heart tube. c*Ccbe1* overexpression did however not affect the expression of the cardiac transcription factor *Gata4*, despite the obvious morphological alterations. In addition, it has been shown that MMP2, which like c*Ccbe1* is detected in regions similar to *Islet-1*, mediates cell migration and proliferation of cardiac progenitors, and is implicated as well in (cardiac) neural crest. Indeed, MMP2 is known to be

required for the degradation of extracellular matrix allowing cellular movement/migration. Loss of MMP2 in avian embryos leads to severe heart tube defects including cardia bifida, which is consistent with blockade of cellular migration. According to this report and like with c*Ccbe1* overexpression, MMP2 loss of function leads to defects associated with ventral closure of the heart tube (Linask et al., 2005). This suggests that altering the levels c*Ccbe1* may interfere with the migration of cardiac progenitor cells. Taken together, these data indicate that c*Ccbe1* may not be required for cardiomyocyte commitment, but instead it likely has a role in proper proliferation and migration of the cardiac precursor cells to form the heart tube.

The presence of c*Ccbe1* in the SHF, overlapping with the expression of *Islet-1* and the role in the cardiac proliferation, led us to consider if c*Ccbe1* would also interact with the CNC, since it is known that CNC are involved in cardiovascular development being a major component in the tissue interactions in the caudal pharynx and OFT (SHF regions) (Keyte and Hutson, 2012). To achieve this, we performed immunostaining for Hnk1 on transverse sections at the heart region of c*Ccbe1* overexpressed, knockdown and respective control embryos. According to our results, while increased c*Ccbe1* levels resulted in expansion of Hnk1-expressing domain in both CNC cells and heart tube region, loss of c*Ccbe1* decreased Hnk1 signal mostly in the heart tube region. This may affect the migration of CNC cells leading to myocardial dysfunction, and thus suggests that c*Ccbe1* may be also required during early heart development for the establishment of the heart conduction system.

In conclusion, the data presented here demonstrates that c*Ccbe1* is present in both FHF and SHF progenitor populations, and that later becomes restricted to the SHF being located at the rapid proliferation center, which is known to be a driving force of cardiac morphogenesis. The functional studies of c*Ccbe1* revealed that, altering c*Ccbe1* expression causes cardiac abnormalities, being most probably triggered by the arrest of the fusion of the precardiac cells at the midline. c*Ccbe1* activity seem to be involved in the remodeling events that lead to the closure of the foregut and fusion of the cardiac primordia into a linear heart tube. Furthermore, disturbing the levels of c*Ccbe1* causes alterations in the Hnk1

expression suggesting a possible role in the migration of the CNC cells leading to an incorrect development of cardiomyocytes. Together, our results reveal a crucial role for c*Ccbe1* during early heart development, which may be a crucial piece of evidence towards the understanding of the molecular genetics of cardiomyopathy disorders.

CHAPTER 5 – FUTURE PERSPECTIVES

This PhD project focused on the study and characterization of the potential role of c*Ccbe1* in early heart development, where some questions have been answered while others remained unanswered. To address some of these issues several experiments may be undertaken.

First it should be further analyze the functional role of c*Ccbe1* by overexpression and knockdown experiments in chick embryos, specifically:

- WISH with other markers to better characterize the phenotypes observed (i.e. *aMhc*, *vMhc*, *Shh*, *Fgf10*).

- WISH and immunostaining for MMP2, at key stages of early heart development, to access any interactions between this gene and c*Ccbe1*. MMP2 is involved in the extracellular matrix (ECM), mediates cell migration, and is implicated in neural crest and cardiac development. Studies carried out by Linask, K. et al 2005, showed that neutralizing MMP2 produced severe heart tube defects (ex: cardia bifida). This occurs due to the arrest of heart tube bending by inhibiting the breakdown of the dorsal mesocardial ECM. Furthermore, alterations in cell proliferation within the dorsal mesocardium and mesoderm of the anterior heart field occurred.

- Observe the effect of the functional experiments of cCcbe1 in the high proliferative SHF cells from stage HH13 to HH22, through electroporation *in ovo* experiments. At these stages of development the SHF cells have already start the contribution to the formation of the outflow tract and right ventricle. The phenotype will be evaluated by the presence or absence of structures corresponding to the SHF progenitor population contribution. Furthermore, WISH will be performed using different cardiac markers for the posterior regions (i.e. *Tbx5*, *aMhc*) and anterior regions (i.e. *vMhc*, *Fgf10*, *Wnt11*) of the heart.

- Isolate second heart fields explants of knockdown and overexpression injected embryos in order to perform migration, proliferation (BrdU) and differentiation (MF20) assays as described by Dyer and Kirby, 2009.

- Ascertain the role of cCcbe1 in cardiac neural crest cells using specific markers, like *Hnk1*, *Wnt1*, *Pitx2*, *Pax3*, in embryos from stage HH14 to HH24, through *in ovo* electroporation.

- Determination of apoptosis will be analyzed in knockdown embryos by TUNEL assays.

- Determine if c*Ccbe1* functions in a tissue-autonomous fashion, will be assessed through components of the extracellular matrix such as Fibronectin and Fibrillin, in which are involved the HFR fusion.

Determine the cCcbe1 signaling pathway, by accessing the type of proteins that might be transcriptionally activating or downregulating cCcbe1 and access the requirement of the gene to promote cardiac differentiation by beads implantation experiments. Beads are coated with proteins (i.e. Fgf8, Fgf10, Bmp4, Gata4, Shh, Nkx2.5, MMP2, Pax3, Islet-1) and placed in the developing embryo to provide sustained exposure. Moreover, the method allows for continued development so that embryos can be analyzed at a more mature stage to detect changes in anatomy and in the expression pattern of the gene of interest.

REFERENCES

Abu-Issa, R., Kirby, M.L., 2007. Heart field: From Mesoderm to Heart Tube. Cell Dev. Biol., 23:45-68.

Abu-Issa, R., Kirby, M.L., 2008. Patterning of the heart field in the chick. . Developmental biology 319, 223-333.

Abu-Issa, R., Waldo, K., Kirby, M.L., 2004. Heart fields: one, two or more? Developmental Biology 272, 281-285.

Alders, M., Hogan, B.M., Gjini, E., Salehi, F., Al-Gazali, L., Hennekam, E.A., Holmberg, E.E., Mannens, M.M.A.M., Mulder, M.F., Offerhaus, G.J.A., Prescott, T.E., Schroor, E.J., Verheij, J.B.G.M., Witte, M., Zwijnenburg, P.J., Vikkula, M., Schulte-Merker, S., Hennekam, R.C., 2009. Mutations in CCBE1 cause generalized lymph vessel dysplasia in humans. Nat Genet 41, 1272-1274.

Alsan, B.H., Schultheiss, T.M., 2002. Regulation of avian cardiogenesis by Fgf8 signaling. Development 129, 1935-1943.

Andree, B., Duprez, D., Vorbusch, B., Arnold, H.H., Brand, T., 1998. BMP-2 induces ectopic expression of cardiac lineage markers and interferes with somite formation in chicken embryos. Mech Dev., 70:119 –131.

Aoyama, N., Tamaki, H., Kikawada, R., Yamashina, S., 1995. Development of the conduction system in the rat heart as determined by Leu-7 (HNK-1) immunohistochemistry and computer graphics reconstruction. Lab. Invest., 72:355–366.

Baldini, A., 2005. Dissecting contiguous gene defects: TBX1. Current Opinion in Genetics & Development 15, 279-284.

Barth, J.L., Clark, C.D., Fresco, V.M., Knoll, E.P., Lee, B., Argraves, W.S., Lee, K.-H., 2010. Jarid2 is among a set of genes differentially regulated by Nkx2.5 during outflow tract morphogenesis. Developmental Dynamics 239, 2024-2033.

Barton, C.a., Gloss, B.S., Qu, W., Statham, a.L., Hacker, N.F., Sutherland, R.L., Clark, S.J., O'Brien, P.M., 2010. Collagen and calcium-binding EGF domains 1 is frequently inactivated in ovarian cancer by aberrant promoter hypermethylation and modulates cell migration and survival. British journal of cancer 102, 87–96.

Bejsovec, A., 2005. Wnt Pathway Activation: New Relations and Locations. Cell 120, 11-14.

Bento, M., Correia, E., Tavares, A.T., Becker, J.D., Belo, J.A., 2011. Identification of differentially expressed genes in the heart precursor cells of the chick embryo. Gene Expression Patterns 11, 437-447.

Bertrand, N., Roux, M., Ryckebüsch, L., Niederreither, K., Dollé, P., Moon, A., Capecchi, M., Zaffran, S., 2011. Hox genes define distinct progenitor sub-domains within the second heart field. Developmental Biology 353, 266-274.

Blokzijl, A., Dahlqvist, C., Reissmann, E., Falk, A., Moliner, A., Lendahl, U., Ibáñez, C.F., 2003. Cross-talk between the Notch and TGF-β signaling pathways mediated by interaction of the Notch intracellular domain with Smad3. The Journal of Cell Biology 163, 723-728.

Blom, N.A., Gittenberger-de Groot, A.C., DeRuiter, M.C., Poelmann, R.E., Mentink, M.M.T., Ottenkamp, J., 1999. Development of the Cardiac Conduction Tissue in Human Embryos Using HNK-1 Antigen Expression: Possible Relevance for Understanding of Abnormal Atrial Automaticity. Circulation 99, 800-806.

Boettger, T., Knoetgen, H., Wittler, L., Kessel, M., 2001. The avian organizer. Int. J. Dev. Biol., 45, 281-287.

Bos, F.L., Caunt, M., Peterson-Maduro, J., Planas-Paz, L., Kowalski, J., Karpanen, T., van Impel, A., Tong, R., Ernst, J.A., Korving, J., van Es, J.H., Lammert, E., Duckers, H.J., Schulte-Merker, S., 2011. CCBE1 Is Essential for Mammalian Lymphatic Vascular Development and Enhances the Lymphangiogenic Effect of Vascular Endothelial Growth Factor-C In Vivo. Circulation Research 109, 486-491.

Böttcher, R.T., Niehrs, C., 2005. Fibroblast Growth Factor Signaling during Early Vertebrate Development. Endocrine Reviews 26, 63-77.

Brade, T., Männer, J., Kühl, M., 2006. The role of Wnt signalling in cardiac development and tissue remodelling in the mature heart. Cardiovascular Research 72, 198-209.

Brand, T., 2003. Heart development: molecular insights into cardiac specification and early morphogenesis. Dev. Biol. , 258, 251-219.

Bray, S.J., 2006. Notch signalling: a simple pathway becomes complex. Nat Rev Mol Cell Biol., 7:678–689.

Bronner-Fraser, M., 1987. Perturbation of cranial neural crest migration by the HNK-1 antibody. Developmental Biology 123, 321-331.

Bruneau, B.G., 2008. The developmental genetics of congenital heart disease. . Nature, 451, 943-458.

Buckingham, M., Meilhac, S., Zaffran, S., 2005. Building the mammalian heart from two sources of myocardial cells. Nature reviews. Genetics 6, 826–835.

Cai, C.L., Liang, X., Shi, Y., Chu, P.H., Pfaff, S.L., Chen, J., Evans, S., 2003. Isl1 identifies a cardiac progenitor population that proliferates prior to differentiation and contributes a majority of cells to the heart. Dev. Cell 5 (6), 877–889.

Chau, M.D.L., Tuft, R., Fogarty, K., Bao, Z.-Z., 2006. Notch signaling plays a key role in cardiac cell differentiation. Mechanisms of Development 123, 626-640.

Chen, L., Fulcoli, F.G., Tang, S., Baldini, A., 2009. Tbx1 Regulates Proliferation and Differentiation of Multipotent Heart Progenitors. Circulation Research 105, 842-851.

Chu, J., Shen, M.M., 2010. Functional redundancy of EGF-CFC genes in epiblast and extraembryonic patterning during early mouse embryogenesis. Developmental Biology 342, 63-73.

Chuck, E.T., Watanabe, M., 1997. Differential expression of PSA-NCAM and HNK-1 epitopes in the developing cardiac conduction system of the chick. Developmental Dynamics 209, 182-195.

Cohen, E.D., Miller, M.F., Wang, Z., Moon, R.T., Morrisey, E.E., 2012. Wnt5a and Wnt11 are essential for second heart field progenitor development. Development 139, 1931-1940.

Cohen, E.D., Wang, Z., Lepore, J.J., Lu, M.M., Taketo, M.M., Epstein, D.J., Morrisey, E.E., 2007. Wnt/beta-catenin signaling promotes expansion of Isl-1-positive cardiac progenitor cells through regulation of FGF signaling. J. Clin. Invest. , 117:1794–1804.

Colas, J.F., Lawson, A., Schoenwolf, G.C., 2000. Evidence that translation of smooth muscle alpha-actin mRNA is delayed in the chick promyocardium until fusion of the bilateral heart-forming regions. . Dev. Dyn., 218, 316–330.

Connell, F., Kalidas, K., Ostergaard, P., Brice, G., Homfray, T., Roberts, L., Bunyan, D., Mitton, S., Mansour, S., Mortimer, P., Jeffery, S., 2010. Linkage and sequence analysis indicate that CCBE1 is mutated in recessively inherited generalised lymphatic dysplasia. Hum Genet 127, 231-241.

Dailey, L., Ambrosetti, D., Mansukhani, A., Basilico, C., 2005. Mechanisms underlying differential responses to FGF signaling. Cytokine & growth factor reviews 16, 233-247.

Darnell, D.K., Stark, M.R., Schoenwolf, G.C., 1999. Timing and cell interactions underlying neural induction in the chick embryo. Development, 126(111):2505-2514.

Davis, R.L., Turner, D.L., 2001. Vertebrate hairy and Enhancer of split related proteins: transcriptional repressors regulating cellular differentiation and embryonic patterning. Oncogene 20, 8342-8357.

de Boer, B.A., van den Berg, G., de Boer, P.A.J., Moorman, A.F.M., Ruijter, J.M., 2012. Growth of the developing mouse heart: An interactive qualitative and quantitative 3D atlas. Developmental Biology 368, 203-213.

de la Cruz, M.V., Sánchez Gómez, C., Arteaga, M.M., 1977. Experimental study of the development of the truncus and the conus in the chick embryo. J Anat, 123: 661–686.

DeHaan, R.L., 1963. Organization of the cardiogenic plate in the early chick embryo. Acta Embryol. Morphol. Exp., 6, 26–38.

Dodou, E., Verzi, M.P., Anderson, J.P., Xu, S.M., Black, B.L., 2004. Mef2c is a direct transcriptional target of ISL1 and GATA factors in the anterior heart field during mouse embryonic development. Development 131, 3931-3942.

Dyer, L.A., Kirby, M.L., 2009. The role of secondary heart field in cardiac development. Developmental Biology 336, 137-144.

Eisenberg, C.A., Eisenberg, L.M., 1999. WNT11 promotes cardiac tissue formation of early mesoderm. Developmental Dynamics 216, 45-58.

Eisenberg, C.A., Gourdie, R.G., Eisenberg, L.M., 1997. Wnt-11 is expressed in early avian mesoderm and required for the differentiation of the quail mesoderm cell line QCE-6. Development 124, 525-536.

Evans, S.M., Yelon, D., Conlon, F.L., Kirby, M.L., 2010. Myocardial Lineage Development. Circulation Research 107, 1428-1444.

Eyal-Giladi, 1997. Establishment of the axis in chordates: facts and speculations. Development, 124, 2285-2296.

Eyal-Giladi, H., Debby, H., Harel, N., 1992. The posterior section of the chick area pellucida and its involvement in hypoblast and primitive streak formation. Development, 116: 819-830.

Eyal-Giladi, H., Kochav, S., Menashi, M.K., 1976. On the origin of primordial germ cells in the chick embryo. Differentiation research in biological diversity 6, 13–16.

Facucho-Oliveira, J., Bento, M., Belo, J.A., 2011. Ccbe1 expression marks the cardiac and lymphatic progenitor lineages during early stages of mouse development. The International journal of developmental biology 55, 1007-1014.

Galli, D., Domínguez, J.N., Zaffran, S., Munk, A., Brown, N.A., Buckingham, M.E., 2008. Atrial myocardium derives from the posterior region of the second heart field, which acquires left-right identity as Pitx2c is expressed. Development 135, 1157-1167.

Garcia-Martinez, V., Schoenwolf, G.C., 1993. Primitive-streak origin of the cardiovascular system in avian embryos. Dev. Biol., 159, 706– 719.

Gessert, S., Kühl, M., 2010. The Multiple Phases and Faces of Wnt Signaling During Cardiac Differentiation and Development. Circulation Research 107, 186-199.

Gilbert, S.F., 2003. Developmental Biology. Sinauer Associates.

Gurjarpadhye, A., Hewett, K.W., Justus, C., Wen, X., Stadt, H., Kirby, M.L., Sedmera, D., Gourdie, R.G., 2007. Cardiac neural crest ablation inhibits compaction and electrical function of conduction system bundles. American Journal of Physiology - Heart and Circulatory Physiology 292, H1291-H1300.

Hamburger, V., Hamilton, H.L., 1951. A series of normal stages in the development of the chick embryo. . Journal of Morphology 88, 49–92.

Harvey, R.P., 2002. Patterning the vertebrate heart. Nat Rev Genet, 544–556.

Harvey, R.P., Rosenthal, N., 1999. Heart Development. Academic Press, San Diego.

Hoffmann, A.D., Peterson, M.A., Friedland-Little, J.M., Anderson, S.A., Moskowitz, I.P., 2009. sonic hedgehog is required in pulmonary endoderm for atrial septation. Development 136, 1761-1770.

Hogan, B.M., Bos, F.L., Bussmann, J., Witte, M., Chi, N.C., Duckers, H.J., Schulte-Merker, S., 2009. ccbe1 is required for embryonic lymphangiogenesis and venous sprouting. Nat Genet 41, 396-398.

Hurle, J.M., Icardo, J.M., Ojeda, J.L., 1980. Compositional and structural heterogenicity of the cardiac jelly of the chick embryo tubular heart: a TEM, SEM and histochemical study. Journal of Embryology and Experimental Morphology 56, 211-223.

Hutson, M.R., Zeng, X.L., Kim, A.J., Antoon, E., Harward, S., Kirby, M.L., 2010. Arterial pole progenitors interpret opposing FGF/BMP signals to proliferate or differentiate. Development 137, 3001-3011.

Hutson, M.R., Zhang, P., Stadt, H.A., Sato, A.K., Li, Y.-X., Burch, J., Creazzo, T.L., Kirby, M.L., 2006. Cardiac arterial pole alignment is sensitive to FGF8 signaling in the pharynx. Developmental Biology 295, 486-497.

Ilagan, R., Abu-Issa, R., Brown, D., Yang, Y.-P., Jiao, K., Schwartz, R.J., Klingensmith, J., Meyers, E.N., 2006. Fgf8 is required for anterior heart field development. Development 133, 2435-2445.

Iso, T., Kedes, L., Hamamori, Y., 2003. HES and HERP families: Multiple effectors of the notch signaling pathway. Journal of Cellular Physiology 194, 237-255.

Itoh, N., Ornitz, D.M., 2004. Evolution of the Fgf and Fgfr gene families. Trends in genetics : TIG 20, 563-569.

Kelly, R.G., 2012. The Second Heart Field. Developmental Biology 100, 33-65.

Kelly, R.G., Brown, N.A., Buckingham, M.E., 2001. The Arterial Pole of the Mouse Heart Forms from Fgf10-Expressing Cells in Pharyngeal Mesoderm. Developmental cell 1, 435-440.

Kelly, R.G., Papaioannou, V.E., 2007. Visualization of outflow tract development in the absence of Tbx1 using an FgF10 enhancer trap transgene. Developmental Dynamics 236, 821-828.

Keyte, A., Hutson, M.R., 2012. The neural crest in cardiac congenital anomalies. Differentiation 84, 25-40.

Kirby, M.L., 2002. Molecular embryogenesis of the heart. Pediatr Dev Path 5, 516-543.

Kishigami, S., Mishina, Y., 2005. BMP signaling and early embryonic patterning. Cytokine & growth factor reviews 16, 265-278.

Kitisin, K., Saha, T., Blake, T., Golestaneh, N., Deng, M., Kim, C., Tang, Y., Shetty, K., Mishra, B., Mishra, L., 2007. TGF-beta Signaling in Development. Sci. STKE 2007, cm1.

Klaus, A., Müller, M., Schulz, H., Saga, Y., Martin, J.F., Birchmeier, W., 2012. Wnt/β-catenin and Bmp signals control distinct sets of transcription factors in cardiac progenitor cells. Proceedings of the National Academy of Sciences 109, 10921-10926.

Klaus, A., Saga, Y., Taketo, M.M., Tzahor, E., Birchmeier, W., 2007. Distinct roles of Wnt/β-catenin and Bmp signaling during early cardiogenesis. Proceedings of the National Academy of Sciences 104, 18531-18536.

Kohn, A.D., Moon, R.T., 2005. Wnt and calcium signaling: beta-catenin-independent pathways. Cell calcium, 38, 439–446.

Kruse, J., Mailhammer, R., Wernecke, H., Faissner, A., Sommer, I., Goridis, C., Schachner, M., 1984. Neural cell adhesion molecules and myelin-associated glycoprotein share a common carbohydrate moiety recognized by monoclonal antibodies L2 and HNK-1. Nature 311, 153-155.

Kuo, C.T., Morrisey, E.E., Anandappa, R., Sigrist, K., Lu, M.M., Parmacek, M.S., Soudais, C., Leiden, J.M., 1997. GATA4 transcription factor is required for ventral morphogenesis and heart tube formation. Genes & Development 11, 1048-1060.

Kwon, C., Qian, L., Cheng, P., Nigam, V., Arnold, J., Srivastava, D., 2009. A regulatory pathway involving Notch1/[beta]-catenin/Isl1 determines cardiac progenitor cell fate. Nat Cell Biol 11, 951-957.

Laugwitz, K.-L., Moretti, A., Caron, L., Nakano, A., Chien, K.R., 2008. Islet1 cardiovascular progenitors: a single source for heart lineages? Development 135, 193-205.

Laugwitz, K.L., Moretti, A., Lam, J., Gruber, P., Chen, Y., Woodard, S., Lin, L.Z., Cai, C.L., Lu, M.M., Reth, M., Platoshyn, O., Yuan, J.X., Evans, S., Chien, K.R., 2005. Postnatal isl1+ cardioblasts enter fully differentiated cardiomyocyte lineages. Nature, 433:647– 653.

Liao, J., Aggarwal, V.S., Nowotschin, S., Bondarev, A., Lipner, S., Morrow, B.E., 2008. Identification of downstream genetic pathways of Tbx1 in the second heart field. Developmental Biology 316, 524-537.

Linask, K.K., 1992. N-Cadherin localization in early heart development and polar expression of Na+, K+-ATPase, and integrin during pericardial coelom formation and epithelialization of the differentiating myocardium. Dev. Biol., 151, 213– 224.

Linask, K.K., Han, M., Cai, D.H., Brauer, P.R., Maisastry, S.M., 2005. Cardiac morphogenesis: Matrix metalloproteinase coordination of cellular mechanisms underlying heart tube formation and directionality of looping. Developmental Dynamics 233, 739-753.

Lints, T.J., Parsons, L.M., Hartley, L., Lyons, I., Harvey, R.P., 1993. Nkx2.5: a novel murine homeobox gene expressed in early heart progenitor cells and their myogenic descendants. Development, 119: 419-431.

Logan, C.Y., Nusse, R., 2004. THE WNT SIGNALING PATHWAY IN DEVELOPMENT AND DISEASE. Annual Review of Cell and Developmental Biology 20, 781-810.

López-Sánchez, C., García-Martínez, V., 2011. Molecular determinants of cardiac specification. Cardiovascular Research 91, 185-195.

Lopez-Sanchez, C., Garcia-Martinez, V., Schoenwolf, G.C., 2001. Localization of cells of the prospective neural plate, heart and somites within the primitive streak and epiblast of avian embryos at intermediate primitive-streak stages. Cells Tissues Organs, 169:334-346.

Lopez-Sanchez, C., Garcia-Masa, N., Gañan, C.M., Garcia-Martinez, V., 2009. Movement and commitment of primitive streak precardiac cells during cardiogenesis. . The International journal of developmental biology, 53, 1445–1455.

MacDonald, B.T., Tamai, K., He, X., 2009. Wnt/²-Catenin Signaling: Components, Mechanisms, and Diseases. Developmental cell 17, 9-26.

Marvin, M.J., Di Rocco, G., Gardiner, A., Bush, S.M., Lassar, A.B., 2001. Inhibition of Wnt activity induces heart formation from posterior mesoderm. Genes & Development 15, 316-327.

Massagué, J., Chen, Y.-G., 2000. Controlling TGF-β signaling. Genes & Development 14, 627-644.

Meilhac, S.M., Esner, M., Kelly, R.G., Nicolas, J.F., Buckingham, M.E., 2004. The clonal origin of myocardial cells in different regions of the embryonic mouse heart. . Dev. Cell 6(5):685–698.

Mesbah, K., Rana, M.S., Francou, A., van Duijvenboden, K., Papaioannou, V.E., Moorman, A.F., Kelly, R.G., Christoffels, V.M., 2012. Identification of a Tbx1/Tbx2/Tbx3 genetic pathway governing pharyngeal and arterial pole morphogenesis. Human Molecular Genetics 21, 1217-1229.

Miazga, C.M., McLaughlin, K.A., 2009. Coordinating the timing of cardiac precursor development during gastrulation: A new role for Notch signaling. Developmental Biology 333, 285-296.

Miquerol, L., Kelly, R.G., 2013. Organogenesis of the vertebrate heart. Wiley Interdisciplinary Reviews: Developmental Biology 2, 17-29.

Mjaatvedt, C.H., Nakaoka, T.M.-R., R., Norris, R.A., Kern, M.J., Eisenberg, C.A., Turner, D., Markwald, R.R., 2001. The outflow tract of the heart is recruited from a novel heart-forming field. Dev Biol 238, 297-109.

Molkentin, J.D., Lin, Q., Duncan, S.A., Olson, E.N., 1997. Requirement of the transcription factor GATA4 for heart tube formation and ventral morphogenesis. Genes & Development 11, 1061-1072.

Momose, T., Tonegawa, A., Takeuchi, J., Ogawa, H., Umesono, K., Yasuda, K., 1999. Efficient targeting of gene expression in chick embryos by microelectroporation. Development, Growth & Differentiation 41, 335-344.

Moretti, A., Caron, L., Nakano, A., Lam, J.T., Bernshausen, A., Chen, Y., Qyang, Y., Bu, L., Sasaki, M., Martin-Puig, S., Sun, Y., Evans, S.M., Laugwitz, K.-L., Chien, K.R., 2006. Multipotent Embryonic Isl1+ Progenitor Cells Lead to Cardiac, Smooth Muscle, and Endothelial Cell Diversification. Cell 127, 1151-1165.

Mosimann, C., Hausmann, G., Basler, K., 2009. Beta-Catenin hits chromatin: regulation of Wnt target gene activation. Nat Rev Mol Cell Biol 10, 276-286.

Münsterberg, A., Yue, Q., 2008. Cardiac progenitor migration and specification: The dual function of Wnts. . Cell adhesion migration 2, 74–76.

Nakagawa, S., Takeichi, M., 1997. N-cadherin is crucial for heart formation in the chick embryo. Development, growth & differentiation 39, 451-455.

Nakajima, Y., 2010. Second lineage of heart forming region provides new understanding of conotruncal heart defects. Congenital Anomalies 50, 8-14.

Nakajima, Y., Yoshimura, K., Nomura, M., Nakamura, H., 2001. Expression of HNK1 epitope by the cardiomyocytes of the early embryonic chick: In situ and in vitro studies. The Anatomical Record 263, 326-333.

Nakamura, T., Colbert, M.C., Robbins, J., 2006. Neural Crest Cells Retain Multipotential Characteristics in the Developing Valves and Label the Cardiac Conduction System. Circulation Research 98, 1547-1554.

Nakamura, T., Saito, D., Kawasumi, A., Shinohara, K., Asai, Y., Takaoka, K., Dong, F., Takamatsu, A., Belo, J.A., Mochizuki, A., Hamada, H., 2012. Fluid flow and interlinked feedback loops establish left/right asymmetric decay of Cerl2 mRNA. Nat Commun 3.

New, D.A.T., 1955. A new technique for the cultivation of the chick embryo in vitro. Embryol. Exp. Morphol., 3, 326-331.

Niessen, K., Karsan, A., 2008. Notch Signaling in Cardiac Development. Circulation Research 102, 1169-1181.

Noden, D.M., 1991. Origins and patterning of avian outflow tract endocardium. Development 111, 867-876.

Noseda, M., Peterkin, T., Simões, F.C., Patient, R., Schneider, M.D., 2011. Cardiopoietic Factors: Extracellular Signals for Cardiac Lineage Commitment. Circulation Research 108, 129-152.

Nusse, R., 2005. Wnt signaling in disease and in development. Cell Research, 15, 28–32.

Nusse, R., Varmus, H., 2012. Three decades of Wnts: a personal perspective on how a scientific field developed. The EMBO Journal 31, 2670-2684.

Nusse, R., Varmus, H.E., 1992. Wnt genes. Cell 69, 1073-1087.

Pane, L.S., Zhang, Z., Ferrentino, R., Huynh, T., Cutillo, L., Baldini, A., 2012. Tbx1 is a negative modulator of Mef2c. Hum Mol Geneti 21, 2485-2496.

Park, E.J., Ogden, L.A., Talbot, A., Evans, S., Cai, C.-L., Black, B.L., Frank, D.U., Moon, A.M., 2006. Required, tissue-specific roles for Fgf8 in outflow tract formation and remodeling. Development 133, 2419-2433.

Park, E.J., Watanabe, Y., Smyth, G., Miyagawa-Tomita, S., Meyers, E., Klingensmith, J., Camenisch, T., Buckingham, M., Moon, A.M., 2008. An FGF autocrine loop initiated in second heart field mesoderm regulates morphogenesis at the arterial pole of the heart. Development 135, 3599-3610.

Parlow, M.H., Bolender, D.L., Kokan-Moore, N.P., Lough, J., 1991. Localization of bFGF-like proteins as punctate inclusions in the preseptation myocardium of the chicken embryo. Developmental Biology 146, 139-147.

Poelmann, R., Jongbloed, M.M., Molin, D.M., Fekkes, M., Wang, Z., Fishman, G., Doetschman, T., Azhar, M., Gittenberger-de Groot, A., 2004. The neural crest is contiguous with the cardiac conduction system in the mouse embryo: a role in induction? Anat Embryol 208, 389-393.

Poelmann, R.E., Gittenberger-de Groot, A.C., 1999. A Subpopulation of Apoptosis-Prone Cardiac Neural Crest Cells Targets to the Venous Pole: Multiple Functions in Heart Development? Developmental Biology 207, 271-286.

Prall, O.W., Menon, M.K., Solloway, M.J., Watanabe, Y., Zaffran, S., Bajolle, F., Biben, C., McBride, J.J., Robertson, B.R., Chaulet, H., 2007. An Nkx2-5/Bmp2/Smad1 negative feedback loop controls heart progenitor specification and proliferation. Cell, 128: 947–959.

Rochais, F., Dandonneau, M., Mesbah, K., Jarry, T., Mattei, M.-G., Kelly, R.G., 2009a. <italic>Hes1</italic> Is Expressed in the Second Heart Field and Is Required for Outflow Tract Development. PLoS ONE 4, e6267.

Rochais, F., Mesbah, K., Kelly, R.G., 2009b. Signaling Pathways Controlling Second Heart Field Development. Circulation Research 104, 933-942.

Rodríguez Esteban, C., Capdevila, J., Economides, A.N., Pascual, J., Ortiz, A., Izpisúa Belmonte, J.C., 1999. The novel Cer-like protein Caronte mediates the establishment of embryonic left-right asymmetry. . Nature 401, 243–451.

Roebroek, A.J., Umans, L., Pauli, I.G., Robertson, E.J., van Leuven, F., Van de Ven, W.J., Constam, D.B., 1998. Failure of ventral closure and axial rotation in embryos lacking the proprotein convertase Furin. Development 125, 4863-4876.

Rosenquist, C.G., 1966. A radioautographic study of labelled grafts in the chick blastoderm: development from primitive streak to stage 12. Contr. Embryol. Carneg. Inst., 38, 71-110.

Ruijtenbeek, K., De Mey, J.G.R., Blanco, C.E., 2002. The Chicken Embryo in Developmental Physiology of the Cardiovascular System: A Traditional Model with New Possibilities. American Journal of Physiology - Regulatory, Integrative and Comparative Physiology 283, R549-R551.

Rutenberg, J.B., Fischer, A., Jia, H., Gessler, M., Zhong, T.P., Mercola, M., 2006. Developmental patterning of the cardiac atrioventricular canal by Notch and Hairy-related transcription factors. Development 133, 4381-4390.

Sanders, E.J., Varedi, M., French, A.S., 1993. Cell proliferation in the gastrulating chick embryo: a study using BrdU incorporation and PCNA localization. . Development, 118, 389-199.

Schier, A.F., 2003. NODAL SIGNALING IN VERTEBRATE DEVELOPMENT. Annual Review of Cell and Developmental Biology 19, 589-621.

Schlessinger, J., 2000. Cell Signaling by Receptor Tyrosine Kinases. Cell 103, 211-225.

Schoenwolf, G.C., Garcia-Martinez, V., Diaz, M.S., 1992. Mesoderm movement and fate during amphibian gastrulation and neurulation. Development Dynamics, 193: 235-248.

Schultheiss, T.M., J.B., B., Lassar, A.B., 1997. A role for bone morphogenetic proteins in the induction of early cardiac myogenesis. Genes Dev., 11, 451-462.

Schultheiss, T.M., Xydas, S., Lassar, A.B., 1995. Induction of avian cardiac myogenesis by anterior endoderm. . Development 121, 4203–4214.

Sheldahl, L.C., Slusarski, D.C., Pandur, P., Miller, J.R., Kühl, M., Moon, R.T., 2003. Dishevelled activates Ca2+ flux, PKC, and CamKII in vertebrate embryos. The Journal of Cell Biology 161, 769-777.

Sissman, J., 1966. Cell multiplication rates during development of the primitive cardiac tube in the chick embryo. Nature, 504-507.

Solnica-Krezel, L., 2005. Conserved Patterns of Cell Movements during Vertebrate Gastrulation. Current Biology 15, R213-R228.

Srivastava, D., 2006. Making or breaking the heart: From lineage determination to morphogenesis. Cell, 126: 1037-1048.

Srivastava, D., Olson, E.N., 2000. A genetic blueprint for cardiac development. Nature, 407:221–226.

St. Amand, T.R., Lu, J.T., Zamora, M., Gu, Y., Stricker, J., Hoshijima, M., Epstein, J.A., Ross Jr, J.J., Ruiz-Lozano, P., Chien, K.R., 2006. Distinct roles of HF-1b/Sp4 in ventricular and neural crest cells lineages affect cardiac conduction system development. Developmental Biology 291, 208-217.

Stalsberg, H., DeHaan, R.L., 1969. The precardiac areas and formation of the tubular heart in the chick embryo. Dev. Biol. , 19, 128.

Stern, C.D., 2004. The chick embryo – past, present and future as a model system in developmental biology. Mechanisms of Development 121, 1011-1013.

Sugi, Y., Lough, J., 1995. Activin-A and FGF-2 Mimic the Inductive Effects of Anterior Endoderm on Terminal Cardiac Myogenesis in Vitro. Developmental Biology 168, 567-574.

Sugi, Y., Sasse, J., Barron, M., Lough, J., 1995. Developmental expression of fibroblast growth factor receptor-1 (cek-1; flg) during heart development. Developmental Dynamics 202, 115-125.

Sugi, Y., Sasse, J., Lough, J., 1993. Inhibition of Precardiac Mesoderm Cell Proliferation by Antisense Oligodeoxynucleotide Complementary to Fibroblast Growth Factor-2 (FGF-2). Developmental Biology 157, 28-37.

Sun, Y., Liang, X., Najafi, N., Cass, M., Lin, L., Cai, C.-L., Chen, J., Evans, S.M., 2007. Islet 1 is expressed in distinct cardiovascular lineages, including pacemaker and coronary vascular cells. Developmental Biology 304, 286-296.

Taber, L.A., 1998. Mechanical aspects of cardiac development. Prog. Biophys. Mol. Biol., 69, 237-255.

Tada, M., Concha, M.L., Heisenberg, C.-P., 2002. Non-canonical Wnt signalling and regulation of gastrulation movements. Seminars in Cell & Developmental Biology 13, 251-260.

Tavares, A.T., Andrade, S., Silva, A.C., Belo, J.A., 2007. Cerberus is a feedback inhibitor of Nodal asymmetric signaling in the chick embryo. Development 134, 2051-2060.

Théveniau-Ruissy, M., Dandonneau, M., Mesbah, K., Ghez, O., Mattei, M.-G., Miquerol, L., Kelly, R.G., 2008. The del22q11.2 Candidate Gene Tbx1 Controls Regional Outflow Tract Identity and Coronary Artery Patterning. Circulation Research 103, 142-148.

Tirosh-Finkel, L., Zeisel, A., Brodt-Ivenshitz, M., Shamai, A., Yao, Z., Seger, R., Domany, E., Tzahor, E., 2010. BMP-mediated inhibition of FGF signaling promotes cardiomyocyte differentiation of anterior heart field progenitors. Development 137, 2989-3000.

Tsuchihashi, T., Maeda, J., Shin, C.H., Ivey, K.N., Black, L., Olson, E.N., Yamagishi, H., Srivastava, D., 2011. Hand2 function in second heart field progenitors is essential for cardiogenesis. Developmental Biology 351, 62-69.

Turner, N., Grose, R., 2010. Fibroblast growth factor signalling: from development to cancer. Nat Rev Cancer 10, 116-129.

Tutarel, O., Norozi, K., Hornung, O., Orhan, G., Wübbolt-Lehmann, P., Wessel, A., Yelbuz, T.M., 2005. Cardiac Failure in the Chick Embryo Resembles Heart Failure in Humans. Circulation 112, e352-e353.

Tzahor, E., Lassar, A.B., 2001. Wnt signals from the neural tube block ectopic cardiogenesis. Genes & Development 15, 255-260.

Urness, L.D., Bleyl, S.B., Wright, T.J., Moon, A.M., Mansour, S.L., 2011. Redundant and dosage sensitive requirements for Fgf3 and Fgf10 in cardiovascular development. Developmental Biology 356, 383-397.

van den Berg, G., Abu-Issa, R., de Boer, B.A., Hutson, M.R., de Boer, P.A.J., Soufan, A.T., Ruijter, J.M., Kirby, M.L., van den Hoff, M.J.B., Moorman, A.F.M., 2009. A Caudal Proliferating Growth Center Contributes to Both Poles of the Forming Heart Tube. Circulation Research 104, 179-188.

Vincent, M., Thiery, J.P., 1984. A cell surface marker for neural crest and placodal cells: further evolution of the peripheral and central nervous system. Dev Biol 103, 468-481.

Vincent, S.D., Buckingham, M.E., 2010. Chapter One - How to Make a Heart: The Origin and Regulation of Cardiac Progenitor Cells, in: Peter, K. (Ed.), Current Topics in Developmental Biology. Academic Press, pp. 1-41.

Virágh, S., Challice, C.E., 1973. Origin and differentiation of cardiac muscle cells in the mouse. . Journal of Ultrastructure Research 42, 41–24.

Vitelli, F., Taddei, I., Morishima, M., Meyers, E.N., Lindsay, E.A., Baldini, A., 2002. A genetic link between Tbx1 and fibroblast growth factor signaling. Development 129, 4605-4611.

Waldo, K.L., Hutson, M.R., Ward, C.C., Zdanowicz, M., Stadt, H.A., Kumiski, D., Abu-Issa, R., Kirby, M.L., 2005. Secondary heart field contributes myocardium and smooth muscle to the arterial pole of the developing heart. Developmental Biology 281, 78-90.

Waldo, K.L., Kumiski, D.H., Wallis, K.T., Stadt, H.A.H., M.R., Platt, D.H., Kirby, M.L., 2001. Conotruncal myocardium arises from a secondary heart field. Development 128, 3179-3188.

Wang, J., Greene, S.B., Bonilla-Claudio, M., Tao, Y., Zhang, J., Bai, Y., Huang, Z., Black, B.L., Wang, F., Martin, J.F., 2010. Bmp Signaling Regulates Myocardial Differentiation from Cardiac Progenitors Through a MicroRNA-Mediated Mechanism. Developmental cell 19, 903-912.

Watanabe, Y., Kokubo, H., Miyagawa-Tomita, S., Endo, M., Igarashi, K., Aisaki, K.i., Kanno, J., Saga, Y., 2006. Activation of Notch1 signaling in cardiogenic mesoderm induces abnormal heart morphogenesis in mouse. Development 133, 1625-1634.

Watanabe, Y., Miyagawa-Tomita, S., Vincent, S.D., Kelly, R.G., Moon, A.M., Buckingham, M.E., 2010. Role of Mesodermal FGF8 and FGF10 Overlaps in the Development of the Arterial Pole of the Heart and Pharyngeal Arch Arteries. Circulation Research 106, 495-503.

Wei, L., Roberts, W., Wang, L., Yamada, M., Zhang, S., Zhao, Z., Rivkees, S.A., Schwartz, R.J., Imanaka-Yoshida, K., 2001. Rho kinases play an obligatory role in vertebrate embryonic organogenesis. Development 128, 2953-2962.

Xie, L., Hoffmann, Andrew D., Burnicka-Turek, O., Friedland-Little, Joshua M., Zhang, K., Moskowitz, Ivan P., 2012. Tbx5-Hedgehog Molecular Networks Are Essential in the Second Heart Field for Atrial Septation. Developmental cell 23, 280-291.

Xu, H., Morishima, M., Wylie, J.N., Schwartz, R.J., Bruneau, B.G., Lindsay, E.A., Baldini, A., 2004. Tbx1 has a dual role in the morphogenesis of the cardiac outflow tract. Development 131, 3217-3227.

Yang, X., Dormann, D., Munsterberg, A., Weijer, C.J., 2002. Cell movement patterns during gastrulation in the chick are controlled by positive and negative chemotaxis mediated by FGF4 and FGF8. Dev. Cell 3:425–437.

Yelbuz, T.M., Waldo, K.L., Kumiski, D.H., Stadt, H.A., Wolfe, R.R., Leatherbury, L., Kirby, M.L., 2002. Shortened Outflow Tract Leads to Altered Cardiac Looping After Neural Crest Ablation. Circulation 106, 504-510.

Zhang, H., Toyofuku, T., Kamei, J., Hori, M., 2003. GATA-4 regulates cardiac morphogenesis through transactivation of the N-cadherin gene. Biochemical and Biophysical Research Communications 312, 1033-1038.

Zhang, Z., Huynh, T., Baldini, A., 2006. Mesodermal expression of Tbx1 is necessary and sufficient for pharyngeal arch and cardiac outflow tract development. Development 133, 3587-3595.

APPENDIX

Appendix 1

Hamburger and Hamilton stage table

Appendix 2

List of Solutions

Solution	Composition
Hybridization buffer	50% formamide; 5x SSC (pH7.5); 0.1% Tween20; 50µg/ml tRNA; 100µg/ml Heparin; 0.01% DEPC
MABT	0.1M maleic acid buffer; 0.15M NaCl; 0.1% Tween-20 (pH7.5)
NTMT	0.1M NaCl; 0.1M Tris-HCl (pH9.5); 0.5M MgCl2; 0.1% tween-20
PBS	13,6mM NaCl; 0.27mM KCl; 0.8mM Na2HPO42H2O; 0.01 mM CaCl2.2H2O; 0.05mM MgCl2.6H2O (pH7.5)
Solution I	50% Formamide; 4xSSC (pH4.5); H2O MilQ; 0.1% Tween-20
Solution III	50% Formamide; 2xSSC (pH4.5); H2O MilQ
SSC 20X	3M NaCl; 0.3M Sodium Citrate
TAE Buffer	40mM Tris-acetate; 2mM EDTA (pH8)